"THE EFFECT OF HIGH PRESSURE ON THE RATES OF ELECTRON EXCHANGE REACTIONS"

William Harry Jolley

B.Sc. (Hons.) University of Sydney

Thesis submitted for the degree of

Doctor of Philosophy

Department of Physical and Inorganic Chemistry

University of Adelaide

March, 1970

This thesis contains no material which has been accepted for the award of any other degree or diploma in any University, and to the best of my knowledge and belief, contains no material previously published or written by another person, except when due reference is made in the text.

William H. Jolley

ACKNOWLEDGEMENTS

I wish to thank sincerely my supervisor, Professor D.R. Stranks, for his constant encouragement, inspiration and guidance throughout the course of this work. Also to Professor D.O. Jordan, Head of Department of Physical and Inorganic Chemistry, University of Adelaide, I express my thanks for making laboratory facilities and equipment available to me within the Department.

I wish also to thank the other members of staff and research students for many invaluable discussions throughout this project.

I express sincere gratitude to Mrs. D.L. Hewish for the typing of this manuscript.

Finally, I acknowledge the financial assistance of a Commonwealth Postgraduate Scholarship, which enabled me to undertake and complete this work.

SUMMARY

Three electron exchange reactions have been studied under high pressure, using radioisotope tracers to follow the reactions. The high pressure apparatus developed for these studies has been reported in some detail. The reactions chosen for study were the $Co^{II}(EDTA)$ - $Co^{III}(EDTA)$ exchange, the $Co(en)_3^{2+}$ - $Co(en)_3^{3+}$ exchange and the Fe^{II}_{aq} - Fe^{III}_{aq} exchange.

The $Co^{II}(EDTA)$ - $Co^{III}(EDTA)$ electron exchange reaction was studied in aqueous solution in the range 1 to 2300 bar at 85°C. From the variation of the rate of exchange with pressure, the volume of activation, $\Delta V^{\ddagger}$, for the reaction was found to be -4.5 ± 0.5 c.c. mole^{-1}. Using the Marcus-Hush theory for outer-sphere electron transfer reactions in solution, an expression has been derived for the volume of activation. This has been used to give a predicted value of $\Delta V^{\ddagger} = -7.6$ c.c. mole^{-1} for the $Co^{II}(EDTA)$ - $Co^{III}(EDTA)$ exchange. When the uncertainties in both the measured and predicted values were considered, the two values were seen to be in quite reasonable agreement.

A subsidiary study of the effect of pressure on the equilibrium existing between the two forms of the Co(III)-EDTA complex in acid solution, was also undertaken. This yielded the value of $\Delta\bar{V} = -5.5 \pm 1.4$ c.c. mole^{-1} for the overall volume change of the reaction, with increasing pressure favouring the formation of the protonated complex, in which the EDTA ligand was pentacoordinate. From a study

of the kinetics of this equilibrium under pressure, a likely mechanism has been proposed for both the forward and back reactions.

The $Co(en)_3^{2+}$ - $Co(en)_3^{3+}$ electron exchange reaction was studied at 65°C and at pressures between 1 and 2100 bar. The volume of activation, obtained from the variation of rate with pressure, was found to be -21.1 ± 1.5 c.c. $mole^{-1}$. The predicted value, obtained from the Marcus-Hush theory, was -18.6 c.c. $mole^{-1}$. Again, satisfactory agreement between the measured and calculated values was observed.

Both the $Co^{II}(EDTA)$ - $Co^{III}(EDTA)$ reaction and the $Co(en)_3^{2+}$ - $Co(en)_3^{3+}$ reaction were believed to proceed by an outer-sphere mechanism. The substantial agreement between the measured and predicted $\Delta V^{\neq}$ values for both these reactions, was taken to indicate the adequacy of the Marcus-Hush theory in predicting correctly the volumes of activation for outer-sphere electron transfers. A comparison of the measured and predicted values of $\Delta V^{\neq}$ for the Fe^{II}_{aq} - Fe^{III}_{aq} reaction was then made, as a means of determining the mechanism involved for this reaction.

The Fe^{II}_{aq} - Fe^{III}_{aq} exchange was studied at 2.0°C, in the pressure range 1 to 1400 bar. By studying the reaction as a function of $[H^+]$ at each pressure, the volume of activation for the hexaquo path was obtained, and an estimate made of the volume of activation for the hydroxo path. The measured volume of activation for the hexaquo path was -12.2 ± 1.5 c.c. $mole^{-1}$, while the predicted value, based on an

outer-sphere model, was -14.9 c.c. mole^{-1}. The value predicted from the Marcus-Hush theory, was thus in substantial agreement with the measured value, and this was taken to imply that an outer-sphere mechanism was operative. On the estimate made for the hydroxo path, it appeared that an outer-sphere mechanism was involved here also.

CONTENTS

Introduction

Electron exchange reactions, which formally involve the process of electron transfer between metal ions, are of fundamental importance in the understanding of the general category of oxidation-reduction reactions. It is for this reason that considerable effort is being spent in attempting to gain insight into the mechanisms involved in this type of reaction.

The effect of pressure on chemical reactions has been long known, but a detailed knowledge is only emerging in present times. The first quantitative statement was made in 1884 by Le Chatelier[1] who said that when a reversible chemical reaction was subjected to pressure, it tended to proceed in such a direction as to reduce the volume of the system. This has found application, for instance, in the well-known Haber process, where 3 molecules of hydrogen combine with 1 molecule of nitrogen to produce only 2 molecules of ammonia; the production of ammonia is thus favoured by increased pressure.

In liquid phase reactions the application of the principle is less straightforward. An increase of pressure favours a reaction leading to the production of ions, even though the number of particles is increased. This effect arises from the solvation of the charged species because the electrostriction of the solvent reduces the total volume of the system. Ostwald[2] in 1878 first became aware that the ionisation of weak electrolytes would be enhanced by increased pressure,

through measurements of the volume changes accompanying neutralisation reactions.

Le Chatelier's principle applies only to equilibrium processes and pressure effects are thus characterised by the overall volume changes, ΔV, for the reactions. The effect of pressure on rate processes was first noticed by Röutgen[3] in 1892 when he found, during experiments on the known increase in conductivity of aqueous HCl under pressure, that the rate of inversion of sucrose was decreased by the application of pressure. However it was not until comparatively recent years that investigators began applying pressure to rate processes as a means to probe the intimate nature of the reaction process.

Essentially the same ideas concerning pressure effects on equilibrium processes can be applied to rate processes, when we consider that rates are controlled by the transition state which can be considered in equilibrium with the reactants. The effect of pressure now will be characterised by $\Delta V^{\ddagger}$, the so-called "volume of activation", which measures the effective difference in volume between the separated reactants and the reactants when in the transition state. This quantity, then, will furnish information about the intermediate transition state. For example, a bimolecular reaction would be expected to be accelerated by pressure, since the reactants would be more compact in the transition state as they react. However a unimolecular decomposition into free radicals would be retarded by

pressure as the transition state must involve a certain degree of bond expansion. On the other hand, the rate of a unimolecular ionisation should increase with pressure because electrostriction in the transition state would decrease the volume of the system.

Another useful principle in the interpretation of pressure effects is the microscopic principle which postulates that, at constant temperature, an increase of pressure tends to increase the degree of order in the system. This, for instance, helps to explain why liquid phase polymerisations are accelerated under pressure. It would be expected that there would be a relation between $\Delta V^{\ddagger}$ and $\Delta S^{\ddagger}$, the entropy of activation, and an attempt has been made at formulating this.[4] However no general correlation between the two quantities has been found. This may be because this microscopic principle is based merely on a molecular model and not on any thermodynamic relation.

The volume of activation is probably easier to interpret on the molecular scale than the other activation parameters, viz. the free energy, enthalpy and entropy of activation.[5] This is because nuclear positions alone tell us much about molecular volumes, but for the other activation parameters a knowledge of molecular energies as well as nuclear positions is required. For this reason it might be considered surprising that, in reaction kinetics, the temperature dependence of rates has been studied to the almost complete exclusion of the pressure dependence. A major factor in this preference has

probably been the experimental convenience of temperature variation.

Nevertheless, over recent years the rates of a considerable number of reactions in the liquid phase have been studied under pressure. Unfortunately these have been almost exclusively in the field of physical organic chemistry, using organic substrates. This is to be expected, though, since the study of inorganic solution kinetics has always lagged well behind the study of organic mechanisms.

A sufficient number of organic systems has now been studied to allow predictions concerning the effects of pressure on a particular class of reaction,[6] and even to generalise about the contribution to $\Delta V^{\ddagger}$ of each mechanistic feature e.g. bond cleavage, cyclisation, charge dispersal etc.[7]

These generalisations are of great value in interpreting the measured $\Delta V^{\ddagger}$ for a given reaction in terms of the nature of the transition state, provided the reaction belongs to a known class. When it comes to inorganic reactions, however, these generalisations are of only limited value, since these reactions have additional features of their own. It is obviously highly desirable to have a bank of measured $\Delta V^{\ddagger}$'s for reactions from all classes of inorganic reactions in solution, and it might then be possible to impute certain mechanistic features to a given reaction from a consideration of its measured $\Delta V^{\ddagger}$. One of the reasons for these present studies is to help

offset this dearth of information.

A number of inorganic systems in the solid state has been investigated under ultra-high pressure, especially with regard to phase changes. One solid state study under ultra-high pressure is of interest. This is the racemisation of the salts $K_3Co(C_2O_4)_3.xH_2O$, $Fe(phen)_3(ClO_4)_2.xH_2O$ and $Ni(phen)_3(ClO_4)_2.xH_2O$, studied by Dachille and coworkers.[8,9,10] Pressures up to 40 kbar accelerated the racemisation in each case, with a volume of activation of about -1 c.c. mole^{-1}. The racemisations almost certainly occur by an intramolecular process and on the basis of the sign of $\Delta V^{\ddagger}$, dissociation of a ligand leading to a trigonal bipyramidal activated complex was excluded as a possible mechanism. This is in contrast to the solution phase racemisation where it has been shown[10] that for $Cr(C_2O_4)_3^{3-}$ and $Co(C_2O_4)_3^{3-}$ a one-ended dissociation of an oxalate ligand is involved. The authors proposed a trigonal prismatic structure for the transition state. The interpretation of $\Delta V^{\ddagger}$ in these systems is complicated by possible contributions to $\Delta V^{\ddagger}$ from unknown effects of pressure on the crystal lattice.

The first significant pressure study of an inorganic reaction in solution was the base hydrolysis of the bromopentaamminecobalt(III) ion,

$$Co(NH_3)_5Br^{2+} + OH^- \rightarrow Co(NH_3)_5OH^{2+} + Br^-,$$

reported in 1955 by Burris and Laidler.[4] They found $\Delta V^{\ddagger} = +8.5$ c.c. mole^{-1} for the reaction. No detailed analysis of the transition state in terms of $\Delta V^{\ddagger}$ was attempted. In this and a subsequent paper,[11] where several other ionic reactions were discussed, their primary purpose was to show that the predominant contribution to $\Delta V^{\ddagger}$ came from the electrostriction of the solvent around the ions. A correlation of $\Delta S^{\ddagger}$ with $\Delta V^{\ddagger}$ was also attempted, with partial success.

In 1958 Hunt and Taube[12] employed pressure as a variable in the study of water exchange between the aquopentaamminecobalt(III) ion and solvent,

$$(NH_3)_5CoOH_2^{3+} + H_2\overset{*}{O} \rightleftarrows (NH_3)_5Co\overset{*}{O}H_2^{3+} + H_2O,$$

in an effort to distinguish the mechanism. The measured $\Delta V^{\ddagger}$ was +1.2 c.c. mole^{-1}. On the basis of this they argued that an extreme S_N2 mechanism was not operative since this would have led to a negative $\Delta V^{\ddagger}$; on the other hand a true S_N1 mechanism would have led to a more positive $\Delta V^{\ddagger}$. On this and other evidence, then, it appeared that in the transition state the Co-O bond was stretched slightly to some critical value, but it was not clear whether a true intermediate was formed on decomposition of the activated complex nor whether the entering water molecule was involved to any extent in the activation process.

Several other substitution reactions have since been studied

under pressure. In 1966 Brower et al.[13] examined the following reactions:

$$Pt(NH_3)Cl_3^- + H_2O \rightleftarrows Pt(NH_3)Cl_2(H_2O) + Cl^-$$

$$PtCl_4^{2-} + H_2O \rightleftarrows PtCl_3(H_2O)^- + Cl^-.$$

A simplifying feature of the first reaction was that the charge type was the same for both reactants and products; in the second reaction there was a charge separation in the products. The values of $\Delta V^{\ddagger}$ found were -14 c.c. mole^{-1} and -17 c.c. mole^{-1} respectively. As a basis for the interpretation of these figures, they measured the "volumes of hydration" for the maleate and malate ions and thus obtained the value of -8.3 c.c. mole^{-1} for the hydration of an unsaturated divalent ion. For the contribution from the leaving Cl^-, they took the value of +16 c.c. mole^{-1} which was the activation volume for the unimolecular decomposition of CCl_3^- in the base catalysed hydrolysis of chloroform:[14]

$$CHCl_3 + OH^- \rightleftarrows H_2O + CCl_3^- \xrightarrow{\text{slow}} Cl^- + CCl_2 \xrightarrow{\text{fast}} \text{products}.$$

The mechanism was then postulated to consist of the following processes:

(i) one or two water molecules moved inwards in the axial positions, forming to some degree the Pt-OH_2 bond found in the product;

(ii) a Pt-Cl bond elongated;

(iii) these rate determining processes were followed by the rapid loss of Cl^- and then relaxation to the square planar

configuration with the $Pt-OH_2$ bond firmly intact.

A more recent system studied by Brower[15] was the formation of the ferric thiocyanate complex:

$$Fe(H_2O)_6^{3+} + SCN^- \rightarrow Fe(H_2O)_5SCN^{2+} + H_2O.$$

This study is of more interest from a technical point of view, since a pressure-jump method was used to follow the reaction. The measured $\Delta V^{\ddagger}$ of +5 c.c. $mole^{-1}$ could be interpreted in terms of either an S_N1 or S_N2 mechanism.

In 1969 Jones and Swaddle[16] reported the volumes of activation for a series of hydrolysis reactions represented by the equation:

$$Co(NH_3)_5X^{(3-n)+} + H_2O \rightarrow Co(NH_3)_5H_2O^{3+} + X^{n-}$$

where $X^{n-} = NO_3^-$, Br^-, Cl^-, SO_4^{2-}. Values of $\Delta V^{\ddagger}$ ranged from -6 to -17 c.c. $mole^{-1}$. In each case the value for $\Delta V^{\ddagger}$ was virtually equal to ΔV, the volume change for the overall reaction. This implied that the transition state resembled the products very closely. Hence these reactions appeared to proceed by an S_N1 type mechanism.

The volume of activation has recently been measured by Taylor and Hathaway[17] for the bromide substitution of trans-dichlorobis(triethylphosphine)platinum(II):

$$trans\text{-}Pt(P(C_2H_5)_3)_2Cl_2 + Br^- \rightarrow trans\text{-}Pt(P(C_2H_5)_3)_2BrCl + Cl^-.$$

The substitution follows a 2-term rate law, corresponding to a solvolytic path and a bimolecular nucleophilic substitution path. The

volumes of activation for each path were found to be -28 c.c. mole^{-1} and -27 c.c. mole^{-1} respectively. Employing similar arguments to Brower et al.,[13] the authors proposed for both paths a mechanism similar to that for the $Pt(NH_3)Cl_3^-$ and $PtCl_4^{2-}$ hydrolyses, where the solvent plays an important role in the formation of the transition state.

Volumes of activation are especially useful in substitution reactions to determine whether the solvent takes an active part in the activation process. The determination of the kinetic rate order for a given reaction will not normally indicate this, whereas in most cases the measured volume of activation should.

Apart from the substitution reactions described above, there has been only one other pressure study carried out on inorganic systems in solution. This study was made by Candlin and Halpern[18] on a series of electron transfer reactions between cobalt(III) complexes and Fe_{aq}^{2+}. The Co(III) complexes were $Co(NH_3)_5X^{2+}$ with $X^- = F^-$, Cl^-, Br^-, N_3^-, cis- and trans-$Co(NH_3)_4(N_3)_2^+$, and $Co(HY)Cl^-$ (Y^{4-} = ethylenediaminetetraacetate). The rationale for this study was to provide a means for distinguishing between inner-sphere and outer-sphere mechanisms. According to the following scheme, the liberation of a water molecule from the first coordination shell to the solvent, in the case of an inner-sphere mechanism, should lead to a significant difference in the $\Delta V^{\ddagger}$ for each mechanism.

$$Co(NH_3)_5Cl^{2+} + Fe(H_2O)_6^{2+} \begin{cases} \xrightarrow{\text{inner-sphere}} [(NH_3)_5Co\text{-}Cl\text{-}Fe(H_2O)_5]^{\ddagger,4+} + H_2O \\ \xrightarrow{\text{outer-sphere}} [(NH_3)_5CoCl(H_2O)Fe(H_2O)_5]^{\ddagger,4+} \end{cases}$$

The values of $\Delta V^{\ddagger}$ ranged from +2.2 to +14 c.c. mole^{-1}. For all of the reactions studied, other indirect evidence indicated an inner-sphere mechanism. The observed values of $\Delta V^{\ddagger}$ were consistent with this. As the authors pointed out, measured $\Delta V^{\ddagger}$'s provide a potentially useful criterion for distinguishing between inner- and outer-sphere electron-transfer mechanisms, and it would be desirable to calibrate the method by examining some reactions of known mechanism.

For this reason we have chosen for these present studies electron exchange systems which are believed to proceed via an outer-sphere mechanism. Further, there has been a considerable advance over recent years in the theoretical treatment of electron transfer reactions The theories are not yet capable of handling reactions of the inner-sphere type, which involve the breaking and formation of bonds, but are restricted to outer-sphere reactions. Most success has been met with the simplest class of electron transfer reactions, viz. thermoneutral electron exchange reactions, where reactants and products are identical.

A large contribution to the exchange barrier arises from the rearrangement of the ligands and of the surrounding solvent in the activation process. This rearrangement should be measured most directly

by the volume of activation, $\Delta V^{\ddagger}$. Hence measured $\Delta V^{\ddagger}$'s should provide a good and alternative test of the electron-transfer theory.

In these laboratories a start has already been made on the measurements of volumes of activation for suitable electron exchange systems. $\Delta V^{\ddagger}$ for the exchange between Tl(I) and Tl(III),

$$Tl^{3+}_{aq} + \overset{*}{Tl}^{+}_{aq} \rightleftarrows \overset{*}{Tl}^{+}_{aq} + Tl^{3+}_{aq},$$

has already been reported[19a] as -13.2 c.c. mole^{-1}. This value is consistent with an outer-sphere one-electron mechanism.[19b]

In these present studies, the volumes of activation for the following electron exchange systems are examined:

$$\overset{*}{Co}(HEDTA)H_2O^{-} + Co(EDTA)^{-} \rightleftarrows \overset{*}{Co}(EDTA)^{-} + Co(HEDTA)H_2O^{-}$$

$$\overset{*}{Co}(en)_3^{2+} + Co(en)_3^{3+} \rightleftarrows \overset{*}{Co}(en)_3^{3+} + Co(en)_3^{2+}$$

$$Fe(H_2O)_6^{2+} + \overset{*}{Fe}(H_2O)_6^{3+} \rightleftarrows Fe(H_2O)_6^{3+} + \overset{*}{Fe}(H_2O)_6^{2+}$$

The first two of these reactions are believed to be outer-sphere reactions, by virtue of the substitution inert character of Co(III). The Fe^{2+}_{aq}-Fe^{3+}_{aq} exchange is generally assumed to be an outer-sphere reaction but there still exists some doubt, and these studies were designed to clarify this.

Chapter 1

Electron Exchange Reactions

1.1 Oxidation-Reduction Reactions

Oxidation-reduction reactions (or redox reactions) are an important and large class of chemical reactions. In the last two decades their study has been one of the major fields of activity in inorganic chemical research. As a result, considerable insight has been gained into the mechanisms of these reactions and a stage has been reached where quantitative theories have been formulated, with a fair deal of success, to predict the rates of the simpler types of redox reaction.

A number of reviews on redox reactions have appeared over the last few years. Among the most recent and important are those by Taube (1959),[20] Halpern (1961),[21] Sutin (1962),[22] Reynolds and Lumry (1966)[23] and Basolo and Pearson (1967).[24]

A modern definition of oxidation is "electron loss" and of reduction "electron gain". As the two processes are necessarily concomitant, the reactions are referred to as "oxidation-reduction reactions" or simply "redox reactions". Whether the mechanism of a redox reaction involves the actual transfer of an electron (or electrons) from reductant to oxidant, or whether simply atom transfer occurs in the particular reaction, is still the object of much research, since the formal effect can be the same. For example, in the reaction

$$Fe(H_2O)_6^{2+} + \overset{*}{Fe}(H_2O)_5OH^{2+} \rightleftharpoons Fe(H_2O)_5OH^{2+} + \overset{*}{Fe}(H_2O)_6^{2+}$$

where the asterisk merely serves to label a given nucleus, the net result is the same whether an electron or a hydrogen atom is transferred from the original Fe(II) species.

1.2 Electron-Exchange Reactions

Two main types of redox reaction have been distinguished, depending on whether the reaction occurs between nuclei of the same element or different elements.

The first type can be illustrated by the reaction:

$$\overset{*}{Co}(H_2O)_6^{2+} + Co(H_2O)_6^{3+} \rightleftharpoons \overset{*}{Co}(H_2O)_6^{3+} + Co(H_2O)_6^{2+}.$$

These reactions have the important feature that the standard free energy change for reaction ΔG^o is zero (except in some special cases where the two oxidation states of the element are in different chemical forms, such as $Co(H_2O)_5Cl^{2+}$ - $Co(H_2O)_6^{2+}$). This type of reaction is normally called an "electron exchange reaction".

The second type can be illustrated by the reaction:

$$Co(H_2O)_6^{3+} + Fe(H_2O)_6^{2+} \rightarrow Co(H_2O)_6^{2+} + Fe(H_2O)_6^{3+}.$$

These reactions, involving two different elements, always have a net standard free energy change. This class of reaction is usually termed merely an "electron transfer reaction".

Because the term "electron transfer reaction" could apply equally

well to all redox reactions, since they all formally involve the transfer of an electron, there is some merit in the recent suggestion of Reynolds and Lumry[23] that the first type be called "homonuclear electron transfer" and the second "heteronuclear electron transfer", but there has been no general acceptance of this terminology.

In these studies we shall be concerned with the type of reaction exemplified by the $Co^{2+}_{aq} - Co^{3+}_{aq}$ system, and which we shall refer to as an "electron exchange reaction".

1.2.1 Kinetics of Electron Exchange Reactions

The most common method of measuring electron exchange rates is by labelling one of the species with a radioactive tracer, since the reactants and products are otherwise indistinguishable. In some cases, though, other methods can be used, such as optical rotation, nuclear magnetic resonance and electron paramagnetic resonance.

An electron exchange reaction is a particular case of an isotopic exchange reaction which can be represented by the general equation

$$AX + BX^* \rightleftarrows AX^* + BX$$

where X* is a distinguishable isotope that can exchange with a normal isotope, X. The isotope, X*, is only introduced as an analytical tool to detect and measure the continuous exchange process which

occurs whether X* is present or not.

The rate of disappearance of the isotopic species (present in negligible concentration compared to AX and BX) from the initially labelled reactant, BX*, is described by a first order rate law. This rate law, equation (1.1), was first derived by McKay[25] in 1938 and is usually referred to as the McKay equation. The derivation is given in standard texts.[26] The rate, R, at which X atoms, both labelled and unlabelled, exchange between AX and BX is given by

$$R = -\frac{2.303}{t}\ \frac{ab}{a+b}\log\,(1-F) \qquad (1.1)$$

where $a = [AX] + [AX^*]$, $b = [BX] + [BX^*]$ and F, the fraction of exchange at time t, is given by

$$F = \frac{x_t - x_o}{x_\infty - x_o}. \qquad (1.2)$$

x is a quantity, usually specific activity, proportional to the concentration of X* in AX. The subscripts refer to reaction times zero, t and infinity.

It is assumed that R is independent of the different isotopic masses. This is really an approximation, but except for the hydrogen isotopes, the error is negligible.[27]

This first order rate law is applicable to all exchange reactions irrespective of the actual exchange mechanism and independent of the order of the reaction with respect to its chemical constituents.

The rate of exchange, R, is obtained from the slope of the linear plot of log (1 - F) against time, or more conveniently by determining the half-time of exchange, $t_{1/2}$, from this plot (when F = 0.5) and substituting in the expression:

$$R = \frac{0.693}{t_{1/2}} \frac{ab}{a + b} \qquad (1.3)$$

This requires the determination of F at various time intervals after labelling one of the reactants. In turn this requires some appropriate analytical procedure for separating AX and BX at these times and also at a time when the exchange has essentially reached equilibrium (after at least eight half-times).

If some exchange is induced during the separation procedure, or if the separation is incomplete, then provided these sources of error are reproducible, this leads to a modified equation:[28]

$$R = -\frac{2.303}{t} \frac{ab}{a + b} \{\log (1 - F') - \log (1 - F_o)\} \qquad (1.4)$$

where F' and F_o are the observed fractions of exchange at times t and zero respectively. Again, R is obtained from the slope of the plot of log (1 - F') against time.

1.3 Mechanisms of Redox Reactions

There are two main mechanisms by which redox reactions involving metal complexes occur. These are the outer-sphere and inner-sphere

mechanisms. Apart from the question as to whether electron or atom transfer occurs in a given reaction, it is also usually a major problem to decide whether it occurs via an inner-sphere or outer-sphere mechanism and most research is directed towards the resolution of this problem first.

1.3.1 The Inner-Sphere Mechanism

A reaction occurs by an inner-sphere mechanism when the two metal ions in the transition state are connected by a bridging ligand common to both coordination spheres.

The inner-sphere mechanism was first clearly demonstrated by Taube et al.[29] with reactions of the type:

$$Co(NH_3)_5Cl^{2+} + Cr(H_2O)_6^{2+} + 5H_3O^+ \rightarrow Co(H_2O)_6^{2+} + (H_2O)_5CrCl^{2+} + 5NH_4^+.$$

All of the chloride in the product was found to be bound to the Cr(III) ion. Because of the substitution-inert character of both Co(III) and Cr(III) complexes, and the substitution-labile character of Cr(II), this implied that in the transition state the chloride ligand was bound directly to both the Co and Cr ions.

In this type of mechanism it is considered that electron transfer is facilitated by the bridging group providing orbitals of proper symmetry, giving good overlap with the appropriate metal-ion orbitals and hence delocalising the metal-ion electrons.[21] Where the energies

of the orbitals of the two metal ions involved differ significantly, then the bridging group reduces the energy difference and enhances the rate of electron transfer.[30] The bridging group might also serve to reduce the coulombic repulsion between ionic reactants of like charge, either because of its opposite charge or by keeping the reactant ions separated.[23]

It should be noted, too, that the bridging ligand can be monatomic or polyatomic.

1.3.2 The Outer-Sphere Mechanism

In the outer-sphere mechanism the first coordination shells of the metal ions remain intact in the transition state. An outer-sphere mechanism is indicated when rapid electron transfer occurs between two substitution-inert complexes, as for example in the reaction

$$Fe(CN)_6^{4-} + \overset{*}{Fe}(CN)_6^{3-} \rightleftarrows Fe(CN)_6^{3-} + \overset{*}{Fe}(CN)_6^{4-}.$$

Where only one reactant is inert, outer-sphere transition states are again likely if possible bridging ligands are missing, as for example with $Co(NH_3)_6^{3+}$.

In a qualitative sense, it might at first appear that electron transfer through an outer-sphere transition state would be extremely unlikely, since the ligands of the first coordination spheres (and perhaps also solvent molecules) effectively insulate the electrons and orbitals of the central metal ions. However electron transfer does occur and there are two main theories which account for it.

The first is the electron tunnelling theory developed by Weiss,[31] by Marcus, Zwolinski and Eyring[32] and by Laidler and Sacher,[33,34] whereby the electron leaks through a potential energy barrier. This is a well-known quantum mechanical phenomenon. The electron tunnelling theory is a non-adiabatic one, in that the electron jumps from one potential energy surface to another. The second theory is an adiabatic one due to Marcus[35] and Hush,[36] in which the state of the system at any stage of the reaction is described by a single eigen-function and the electrons are able to adjust themselves to changing nuclear configurations throughout the reaction path. The majority of chemical reactions can be adequately described by an essentially adiabatic process. This theory will be discussed in more detail in a later section.

It is generally assumed that in outer-sphere activated complexes the first coordination shells of the reactants are in Van der Waal's contact. However, outer-sphere activated complexes may also be bridged. It appears, for example, that in the $Fe(CN)_6^{4-}$ - $Fe(CN)_6^{3-}$ exchange, which is greatly catalysed by cations, the cation plays a bridging role between the inner coordination shells,[23,37] and the transition state can be represented, for instance, by

$$[Fe(CN)_6^{3-}...K^{+}...Fe(CN)_6^{4-}]^{\neq}.$$

There may also be cases where solvent remains between the reactants,

but unless an especially good pathway is thus provided for electron transfer it is more probable that Van der Waal's distances are the optimum distances of approach.

The hydrogen-atom transfer mechanism is often discussed as a separate mechanism, but it can be treated just as well as a hydrogen-bridged outer-sphere mechanism. For example the Fe^{2+}_{aq} - $FeOH^{2+}_{aq}$ exchange can be represented by

$$Fe(H_2O)_6^{2+} + \overset{*}{Fe}(H_2O)_5OH^{2+} \rightleftharpoons [(H_2O)_5Fe - \overset{H}{\underset{|}{O}} \cdots H \cdots \underset{|}{\overset{}{O}}\overset{H}{} - \overset{*}{Fe}(H_2O)_5]$$

$$\rightleftharpoons Fe(H_2O)_6OH^{2+} + \overset{*}{Fe}(H_2O)_6^{2+}$$

where, in the transition state, the hydrogen atom functions as a bridge between the two symmetrical exchanging centres, both with their first coordination shell intact.

It is important to realise that although the inner-sphere and outer-sphere mechanisms are distinct, they are not mutually exclusive. This has been demonstrated by Sutin and co-workers[38,39] in several systems. For example, in the chloride catalysed $Fe(H_2O)_6^{3+}$ - $Fe(H_2O)_6^{2+}$ exchange reaction, using the fact that the uncatalysed dissociation of $FeCl^{2+}$ proceeds considerably more slowly than the electron exchange, they showed that two paths were involved. The exchange proceeded about 70% by an inner-sphere chloride-bridged

mechanism and about 30% by an outer-sphere mechanism.

Hence, any given reaction may proceed by one or the other, or both, of these two mechanisms.

Other possible mechanisms have been proposed from time to time. For example, if the Fe^{2+}_{aq} - $FeOH^{2+}_{aq}$ exchange occurs by hydrogen atom transfer, instead of direct electron transfer, it is possible that the bridge may consist of a chain of water molecules, all hydrogen-bonded to provide a path for hydrogen atom transfer in a manner analogous to the Grotthus conduction mechanism.

In some solvents, such as ammonia, the electron is stabilised sufficiently by solvation to make electron migration through the solvent possible. The hydrated electron is well characterised,[40] but because of its high energies of formation it would not be expected to be of importance in any but photochemical reactions.

1.4 The Marcus-Hush Theory of Electron Transfer

No satisfactory theory yet exists for predicting *a priori* the rate constants for reactions where bonds are broken and formed, and this includes electron transfer reactions of the inner-sphere type. However for outer-sphere electron transfer reactions, which are inherently much simpler, the Marcus-Hush theory predicts rate constants with a fair degree of success.

Both Marcus[35] and Hush[36] have independently developed adiabatic theories of outer-sphere electron transfer rates in solution. Both theories are essentially equivalent in that they make the same basic assumptions, the different parameters in each treatment can mostly be correlated and the conclusions from each are similar.[36c,41] Hush's treatment is more mechanistic in approach and is conceptually easier to visualise. For this reason, in the outline that follows, we will follow Hush's treatment and, in the main, the symbols used are his.

This theory is applicable only to outer-sphere reactions and a basic assumption is that the orbital overlap is small and hence the overlap integral can be set equal to zero. For an electron transfer process

$$a + b(e) \rightarrow a(e) + b$$

the probability density function for the transferring electron is then

$$\psi^2 = \lambda\phi_a^{\,2} + (1 - \lambda)\phi_b^{\,2}$$

where ψ is the time-independent wave function of the transferring electr and ϕ_a, ϕ_b are its wave functions in the ground state when associated with kernels a and b, which can be monatomic or polyatomic. The parameter, λ, then represents the average fraction of the electron that has transferred, and in terms of the transition state theory is a convenient reaction coordinate, which varies smoothly from 0 to 1 durin the electron transfer process. For electron exchange reactions

$\lambda = \frac{1}{2}$ at the transition state, as would be expected for a symmetrical activated complex.

This interpretation of $\lambda^{\ddagger}$ representing the actual charge distribution of the reactants in the activated complex has been criticised by Marcus[41] on theoretical grounds. Nevertheless it forms a useful concept in the understanding of these reactions.

The rate constant is calculated from transition state theory, according to which the rate constant, k, for an infinitely dilute solution, is given by

$$k = \kappa \frac{RT}{Nh} e^{-\Delta G^{\ddagger}/RT} \qquad (1.5)$$

where $\Delta G^{\ddagger}$ here represents the standard free energy of activation. For convenience, the usual superscript zero to designate a standard free energy is omitted, and to the end of this chapter it is to be understood that all free energies are standard free energies.

Although the electronic interaction is considered weak enough to neglect in calculating the energy of a state, it is at the same time assumed large enough to allow the reaction to proceed with a transmission coefficient, κ, which is essentially unity.

The free energy of activation, $\Delta G^{\ddagger}$, is calculated by separating the energy of the a...(e)...b system into the binding energy of the electron and the environmental energy of the system with respect to its surroundings, and then writing explicit expressions for each term.

For an outer-sphere one-electron transfer in solution, represented by the equation

$$a^{Z_1} + b^{Z_2} \rightarrow a^{Z_1 - 1} + b^{Z_2 + 1} \qquad (1.6)$$

the free energy of activation is given by the expression

$$\Delta G^{\ddagger} = {}^{i}\Delta^{p}\mu + \theta_a(\lambda^{\ddagger}) + \theta_b(1 - \lambda^{\ddagger}) + {}^{p}\Delta^{t}\mu_{int} + \lambda^{\ddagger}\, {}^{i}\Delta^{f}\mu. \qquad (1.7)$$

p denotes a state where the ions are at a separation σ, the internuclear distance in the activated complex, but where the system has the charge distribution of the reactants; i and f denote the initial and final states, with a and b far apart; and t denotes the transition state.

The first term of equation (1.7) represents the free energy change in bringing the reactants to the separation σ just prior to the electron transfer. The next two terms correspond to the energy changes for each ion due to the rearrangement of the ligands in the first coordination shell and of the surrounding solvent. ${}^{p}\Delta^{t}\mu_{int}$ is an interaction term, giving the change in interionic energy at the separation σ as the charges on the kernels a and b change from the initial to the transition state distribution. The final term depends on the overall free energy change for the reaction.

To obtain an expression for ${}^{i}\Delta^{p}\mu$, only the coulomb energy of repulsion is considered and other potential energy terms are assumed very small. It is also assumed that, provided the reactant

concentrations are expressed in moles cm^{-3}, the entropy change is also small. If the reactant concentrations are expressed in moles $(V\ cm^3)^{-1}$, this gives

$$i_{\Delta}p_{\mu} = \frac{Z_1 Z_2 e}{\varepsilon\sigma} - \frac{RT}{N} \ln V. \qquad (1.8)$$

Z_1 and Z_2 are the charges on the reactant ions, e the electronic charge, and ε the bulk dielectric constant of the medium which is assumed homogeneous.

The exchange barrier results from the superposition of two single-ion exchange barriers plus interaction terms. The environmental-energy part of the exchange barrier for each ion is obtained in the form

$$\theta(\lambda) = {}^{p}\Delta^{t}\mu_{env} - \lambda\,{}^{i}\Delta^{f}\mu_{env} \qquad (1.9)$$

This function is then calculated in the same way as ionic solvation energies. These consist of three terms (assuming any other terms are unimportant):

(i) $\theta(\lambda)_{cavity}$, the energy of "cavity" formation in the solvent;

(ii) $\theta(\lambda)_{complex}$, the cohesive energy of the complex ion;

(iii) $\theta(\lambda)_{diel}$, the dielectric charging energy of the complex ion.

$\theta(\lambda)_{diel}$ is the dominant term. Because of the assumed weak electronic interaction between the ions, the time period of motion of the transferring electron will be less than those of the firmly-bound solvent electrons. Hence in going from the initial to the transition

state charge distribution, while at separation σ, the electronic polarisation of the solvent will be determined by the instantaneous charge distribution on each ion; but the atomic and orientational polarisations (due to nuclear motion) will be determined by only the average charge on each ion. For the ion a, then, this results in the replacement of the usual Born equation for the charging energy of a spherical particle by the expression

$$\mu_{diel}\ (Z_1 - \lambda) = \frac{[(1 - \lambda)Z_1^{\,2} + \lambda(Z_1 - 1)^2]e^2}{2r_1}\left(\frac{1}{\varepsilon_o} - 1\right)$$

$$- \frac{(Z_1 - \lambda)^2 e^2}{2r_1}\left(\frac{1}{\varepsilon_o} - \frac{1}{\varepsilon}\right) \qquad (1.10)$$

Hence the dielectric charging term for ion a, in going from state p to the transition state, is given by

$$\theta_a(\lambda)_{diel} = \frac{\lambda(1 - \lambda)e^2}{2r_1}\left(\frac{1}{\varepsilon_o} - \frac{1}{\varepsilon}\right) \qquad (1.11)$$

ε_o is the dielectric constant at optical frequencies, measuring the electronic polarisability of the solvent. r_1 is the radius of the complex ion, a, including its first coordination shell. If r_1 varies significantly with charge (e.g. contractions due to crystal field effects) then this can be taken into account.

The cohesive energy of the complex ion, $\theta(\lambda)_{complex}$, is estimated from a suitable potential function or, if data are available, from force constants for the metal-ligand stretching. In the common case

where the ligand is a water molecule, a simple potential function, using an ion-dipole model for the attractive forces and an inverse power term for the repulsion, is suitable. Such a function for the symmetrical vibration of a shell of n_a water molecules in the field of an ion of charge q is

$$U(d,q) = \frac{-n_a|q|e\mu}{d^2} + \frac{A}{d^m} \qquad (1.12)$$

where μ is the dipole moment of a water molecule at a distance, d, from the metal ion, and A and m are arbitrary parameters. m can be estimated from the variation of d_e, the metal-ligand equilibrium distance, with charge. This leads to the following expression for the cohesive energy of the ion a:

$$\theta_a(\lambda)_{complex} = \frac{\lambda(1 - \lambda)n_a e\mu}{d_e^2|Z_1|(m_a - 2)} \qquad (1.13)$$

For transition metal ions, where crystal field effects are important, an additional term has to be added to the potential function to allow for the extra crystal field stabilisation energy. It is not then possible to obtain a simple expression for $\theta(\lambda)_{complex}$ analogous to (1.13), but it can be estimated.

The energy of "cavity" formation, $\theta(\lambda)_{cavity}$, is assumed constant for all states and so can be neglected here.

The interionic interaction energy, $^{p}\Delta^{t}\mu_{int}$, is calculated by

again considering only the electrical contribution. With the same assumptions made in calculating $\theta(\lambda)_{diel}$, the interaction energy is given by

$$p_{\Delta}t_{\mu_{int}} = -\frac{\lambda^{\mp}(1-\lambda^{\mp})e^2}{\sigma}\left(\frac{1}{\varepsilon_o}-\frac{1}{\varepsilon}\right)+\frac{\lambda^{\mp}e^2}{\sigma\varepsilon}(Z_1-Z_2-1) \qquad (1.14)$$

For ions not subject to crystal field effects and for which the inner-shell potential energy is adequately described by a function of the form given in equation (1.12), the free energy of activation for electron transfer can be written explicitly as

$$\Delta G^{\mp} = \frac{Z_1Z_2e^2}{\sigma\varepsilon}+\frac{\lambda^{\mp}e^2}{\sigma\varepsilon}(Z_1-Z_2-1)+\lambda^{\mp}\,{}^{i}\Delta f_{\mu}-\frac{RT}{N}\ln V$$

$$+\lambda^{\mp}(1-\lambda^{\mp})\left[\left\{\frac{1}{2r_1}+\frac{1}{2r_2}-\frac{1}{\sigma}\right\}\left\{\frac{1}{\varepsilon_o}-\frac{1}{\varepsilon}\right\}e^2\right.$$

$$\left.+\left\{\frac{n_a}{d_{ea}^{\,2}|Z_1|(m_a-2)}+\frac{n_b}{d_{eb}^{\,2}|Z_2|(m_b-2)}\right\}e\mu\right] \qquad (1.15)$$

This is of the form

$$\Delta G^{\mp} = \zeta+\lambda^{\mp}\xi+\lambda^{\mp}(1-\lambda^{\mp})\chi \qquad (1.16)$$

By minimising this expression with respect to $\lambda^{\mp}$, the value of $\lambda^{\mp}$ is given by

$$\lambda^{\mp} = \frac{1}{2}\left(1+\frac{\xi}{\chi}\right) \qquad (1.17)$$

where $\xi = \frac{e^2}{\sigma\varepsilon}(Z_1-Z_2-1)+{}^{i}\Delta f_{\mu}$ (1.18)

$$\text{and } \chi = \left(\frac{1}{2r_1} + \frac{1}{2r_2} - \frac{1}{\sigma}\right)\left(\frac{1}{\varepsilon_o} - \frac{1}{\varepsilon}\right)e^2 + \left\{\frac{n_a}{d_{ea}^{\,2}|Z_1|(m_a - 2)}\right.$$

$$\left. + \frac{n_b}{d_{eb}^{\,2}|Z_2|(m_b - 2)}\right\}e\mu \qquad (1.19)$$

Thus for a one-electron exchange reaction, for which $i_\Delta f_\mu$ is zero, $\lambda^{\ddagger} = \frac{1}{2}$ as expected.

Expressions for the enthalpy of activation, $\Delta H^{\ddagger}$, and the entropy of activation, $\Delta S^{\ddagger}$, can also be readily obtained from equation (1.15) by differentiation of $\Delta G^{\ddagger}$ with respect to temperature.

The comparison of theoretical predictions with experimental data on electron exchange reactions is encouraging. There is good agreement in a number of cases, and where there is a major discrepancy this can often be attributed to a special factor. Some representative data[36c] is given in Table 1.1.

Table 1.1

Calculated and Experimental Data for Some Electron Exchange Reactions in Aqueous Solution at 25°C

System	$\Delta H^{\ddagger}_{calc}$	$\Delta S^{\ddagger}_{calc}$	$\Delta H^{\ddagger}_{expt}$	$\Delta S^{\ddagger}_{expt}$
Fe^{3+}/Fe^{2+}	10.8	-32	9.9	-25
V^{3+}/V^{2+}	7.5	-31	13.2	-25
Ce^{4+}/Ce^{3+}	6.8	-45	7.7	-40

(Energies in kcal. $mole^{-1}$, entropies in cal. $deg.^{-1}$ $mole^{-1}$.)

The low enthalpy of activation predicted for the V^{3+}/V^{2+} system might be attributed to the crystal field radius contraction of $V(H_2O)_6^{2+}$.

For a series of similar reactions without crystal field effects, $\Delta H^{\ddagger}$ and $\Delta S^{\ddagger}$ are predicted to vary smoothly with changing ionic radii, and the predicted rates do not change very much (cf. the exchange reactions of the actinide ions).[36c] This is not the case with transition metal ions, where the crystal field effects give rise to large variations in predicted rates.

It is interesting to compare the magnitudes of the various contributions to the overall enthalpy of activation, $\Delta H^{\ddagger}$. For the exchange reactions, M^{4+}/M^{3+}, of actinide ions in aqueous solution at 25°C and zero ionic strength, the contributions are nearly constant and are as follows:[36c]

$\Delta H^{\ddagger}_{\text{dielectric}}$ = 6.4 kcal. mole^{-1} (includes $^{p}\Delta^{t}H_{\text{interaction}}$)

$\Delta H^{\ddagger}_{\text{repulsion}}$ = -2.5 kcal. mole^{-1}

$\Delta H^{\ddagger}_{\text{complex}}$ = 4.2 kcal. mole^{-1}

This gives $\Delta H^{\ddagger}$ = 8.1 kcal. mole^{-1}

For the exchange reactions, M^{3+}/M^{2+}, of the ions of the first transition series, the terms $\Delta H^{\ddagger}_{\text{dielectric}}$ and $\Delta H^{\ddagger}_{\text{repulsion}}$ are similar within the series, with values of about 7 kcal. mole^{-1} and -1.5 kcal. mole^{-1} respectively. However, the values of $\Delta H^{\ddagger}_{\text{complex}}$ vary from 2 to 11 kcal. mole^{-1}, as a result of the different crystal field contractions for each metal ion. This gives rise to widely

differing values of $\Delta H^{\ddagger}$, from 7.5 to 18 kcal. $mole^{-1}$, and hence of predicted rates, for the transition metal ions.

A major part of the barrier for electron transfer arises from the reorganisation energy, involving both the inner coordination shell and the surrounding solvent. It is the contributions to this term which prove most elusive, especially that for the inner coordination shell, and the various theoretical treatments differ most in their methods of estimating this term. Hush uses a specific molecular model to estimate it. Independent tests of some of his assumptions could be made from a knowledge of bond lengths and force constants for the inner coordination shell[41] and from the examination of $\Delta S^{\ddagger}$ values for a number of reactions.[22] A further test should be provided by the examination of $\Delta V^{\ddagger}$ values for a number of reactions, since this quantity is directly related to the reorganisation that occurs in the activation process.

Chapter 2

Theory of Pressure Effects on Reaction Rates

2.1 Introduction

The primary purpose of all kinetic studies is to elucidate the mechanism by which a reaction occurs. Since the volume of activation, $\Delta V^{\ddagger}$, obtained by pressure studies, can be interpreted on the molecular scale, it complements the other activation parameters, $\Delta H^{\ddagger}$ and $\Delta S^{\ddagger}$, and so is a useful quantity to the kineticist.

Pressure studies of homogeneous liquid-phase reactions are more fruitful than gas-phase pressure studies, because in solution the concentrations of the reactants do not change grossly with pressure. Several reviews have appeared over the last few years discussing the mechanistic implications of the results of such liquid-phase pressure studies, the most important reviews being those by Whalley,[42,43] le Noble[7] and Hamann.[6,44,45]

In order to develop the theory of pressure effects on reaction rates, it will be necessary first to review briefly the transition state theory of reaction rates, since the description of pressure effects is best described in terms of this theory.

2.2 Transition State Theory of Reaction Rates

There are two main theories of reaction rates, the collision theory and the transition state theory. The former describes chemical

reactions in terms of molecular collision events, while transition state theory employs the concept of potential energy surfaces in its description. Although their methods of approach to the problem are different, the two theories are essentially equivalent if their different parameters are correlated.[26] For instance, for a bimolecular reaction it can be shown that the expressions obtained from each theory for the rate constant of the reaction are identical if the steric factor, from the collision theory, is related to the partition functions from transition state theory. For present purposes the description in terms of transition state theory is more suitable.

The transition state theory formulates the process of a chemical reaction as the coming together of the reactant species to form an activated complex, $X^{\ddagger}$, which then decomposes into products. The activated complex is regarded as a definite molecular species which exists at the top of an energy barrier lying between the initial and final states. The rate of the reaction is determined by the rate at which this activated complex passes over this barrier. Such a general reaction could be represented as

$$aA + bB + \ldots \rightleftarrows X^{\ddagger} \rightarrow lL + mM + \ldots$$

The activated complexes, $X^{\ddagger}$, are assumed to be in equilibrium with the reactants. This equilibrium can be characterised by the relation

$$\frac{[X^{\ddagger}]}{[A]^a[B]^b\ldots} = K^{\ddagger} \qquad (2.1)$$

where $K^{\ddagger}$ is the equilibrium constant (more strictly the equilibrium product, since [A], [B], ... denote the concentrations of A, B, ..., not their activities). $K^{\ddagger}$ can be written in terms of the appropriate partition functions, and then, for an infinitely dilute solution, the transition state rate expression is deduced as

$$k = \kappa \frac{RT}{Nh} (K^{\ddagger})' \qquad (2.2)$$

where k is the rate constant, κ the transmission coefficient, R the universal gas constant, T the absolute temperature, N Avogadro's number, h Planck's constant and $(K^{\ddagger})'$ is given by

$$K^{\ddagger} = (2\pi m^{\ddagger} \frac{RT}{N})^{1/2} \frac{\delta}{h} (K^{\ddagger})' \qquad (2.3)$$

The term $(2\pi m^{\ddagger} RT/N)^{1/2} \delta/h$ is the contribution from the degree of freedom along the reaction coordinate towards the total partition function per unit volume for the activated complex. $m^{\ddagger}$ is the effective mass of the activated complex for motion along the reaction coordinate and δ is the length of the reaction coordinate defining the transition state.

The transmission coefficient, κ, is a parameter introduced into the rate expression to allow for the possibility that not every activated complex reaching the top of the potential energy barrier will

be converted into a reaction product. κ represents the probability that the activated complex will decompose into products. Normally κ is considered to be equal to, or very close to, unity. Further it is customary to assume that κ is independent of both temperature and pressure.[45]

2.3 Thermodynamic Description of Pressure Effects

For a homogeneous liquid-phase in which the following chemical equilibrium exists

$$aA + bB + \ldots \rightleftarrows lL + mM + \ldots$$

the chemical potential of the component J may be written as

$$\mu_J = \mu_J^o + RT \ln a_J \qquad (2.4)$$

where μ_J^o is the chemical potential of J in its standard state, and a_J is the activity of J.

The condition for thermodynamic equilibrium is

$$a\mu_A + b\mu_B + \ldots = l\mu_L + m\mu_M + \ldots \qquad (2.5)$$

From (2.4) we may then write

$$RT \ln \frac{(a_L)^l (a_M)^m \ldots}{(a_A)^a (a_B)^b \ldots} = a\mu_A^o + b\mu_B^o + \ldots - l\mu_L^o - m\mu_M^o - \ldots \qquad (2.6)$$

Defining an equilibrium constant, K, by

$$K = \frac{(a_L)^l (a_M)^m \ldots}{(a_A)^a (a_B)^b \ldots} \tag{2.7}$$

we may write (2.6) as

$$RT \ln K = a\mu_A^o + b\mu_B^o + \ldots - l\mu_L^o - m\mu_M^o - \ldots \tag{2.8}$$

Further, we have that

$$\left(\frac{\partial \mu_J}{\partial p}\right)_T = \bar{V}_J \tag{2.9}$$

where $\bar{V}_J$ is the partial molar volume of J and p the pressure. Hence we have

$$\left(\frac{\partial RT \ln K}{\partial p}\right) = a\bar{V}_A^o + b\bar{V}_B^o + \ldots - l\bar{V}_L^o - m\bar{V}_M^o - \ldots$$

$$= -\Delta\bar{V}^o \tag{2.10}$$

where $\Delta\bar{V}^o$ is the excess of the partial molar volumes of the products over those of the reactants, all in their standard states. Equation (2.10) provides the fundamental account of the effect of pressure upon any chemical equilibrium.

In reaction kinetics, the concentrations of the species in solution are normally expressed in terms of their molar concentrations, given by

$$c_J = n_J/V \tag{2.11}$$

where n_J is the number of moles of component J, and V is the volume of thesolution expressed in litres.

An activity coefficient, y_J, can now be defined as

$$y_J = a_J/c_J. \tag{2.12}$$

For dilute solutions, y_J, for a solute component J, is defined to approach unity as the concentrations of all solute species approach zero, i.e. the standard state is at infinite dilution.

We may now rewrite (2.7) as

$$K = K_c \times \frac{(y_L)^l (y_M)^m \ldots}{(y_A)^a (y_B)^b \ldots} \tag{2.13}$$

$$\text{where } K_c = \frac{(c_L)^l (c_M)^m \ldots}{(c_A)^a (c_B)^b \ldots} \tag{2.14}$$

Hence,

$$\left(\frac{\partial RT \ln K}{\partial p}\right)_T = \left(\frac{\partial RT \ln K_c}{\partial p}\right)_T + \frac{\partial}{\partial p} \left\{RT \ln \frac{(y_L)^l (y_M)^m \ldots}{(y_A)^a (y_B)^b \ldots}\right\}_T \tag{2.15}$$

and from (2.4),

$$\left(\frac{RT \ln y_J}{p}\right)_T = \bar{V}_J - \bar{V}_J^o - RT\beta \tag{2.16}$$

where β, the compressibility coefficient of the solution, is given by

$$\beta = -\frac{1}{V}\left(\frac{\partial V}{\partial p}\right)_T. \tag{2.17}$$

Thus we obtain

$$\left(\frac{\partial RT \ln K_c}{\partial p}\right)_T = -\Delta\bar{V} + (1 + m + \ldots - a - b - \ldots)RT\beta \tag{2.18}$$

where $\Delta\bar{V}$ is the excess of the partial molar volumes of the products over those of the reactants under the concentration conditions employed. Equation (2.18) shows how the equilibrium constant (more strictly the equilibrium product), K_c, depends on the effective volumes of the reactants and products. In the limit of infinitely dilute solutions, β is equal to the compressibility coefficient of the pure solvent and $\Delta\bar{V}$ becomes $\Delta\bar{V}^o$, referring to the standard states of reactants and products. In dilute solutions the differences between these will be small.

Now, in the transition state theory, $K^{\ddagger}$ represents an equilibrium product, and from equations (2.2) and (2.3) we have that

$$\ln k = \ln K^{\ddagger} + \text{constant.} \qquad (2.19)$$

Hence the pressure dependence of the rate constant, k, is obtained as

$$\left(\frac{\partial RT \ln k}{\partial p}\right)_T = \left(\frac{\partial RT \ln K^{\ddagger}}{\partial p}\right)_T = -\Delta\bar{V}^{\ddagger} + (1 - a - b - \ldots)RT\beta \qquad (2.20)$$

where $\Delta\bar{V}^{\ddagger} = \bar{V}_X{}^{\ddagger} - a\bar{V}_A - b\bar{V}_B - \ldots$ (2.21)

That is, the effect of pressure on the rate constant, k, is governed by the excess partial molar volume of the activated complex over those of the reactants.

In deriving equation (2.20) it has been assumed, following normal

practice,[43] that $m^{\ddagger}$ and δ (equation (2.3)) are independent of pressure. Inasmuch as this assumption is correct, we can identify $\Delta\bar{V}^{\ddagger}$ with the true volume change on activation.

Furthermore, equation (2.20) is strictly only correct for reactants in their standard states, which for the present considerations is at infinite dilution. Hence the $\Delta\bar{V}^{\ddagger}$ of equation (2.20) refers to reactants at infinite dilution.

It has been frequent practice in the literature to treat experimental data according to the approximate relation

$$\left(\frac{\partial RT \ln k}{\partial p}\right)_T = -\Delta V^{\ddagger}_{exp} \qquad (2.22)$$

where $\Delta V^{\ddagger}_{exp}$ is conventionally called the "volume of activation". Clearly $\Delta V^{\ddagger}_{exp}$ is a composite function and cannot be equated to $\Delta\bar{V}^{\ddagger}$. The value of $\Delta V^{\ddagger}_{exp}$, deduced from experimental measurements, should be corrected for the term in $RT\beta$ and for finite ionic strength effects to approximate more closely to the more fundamental quantity, $\Delta\bar{V}^{\ddagger}$. For solvent water at 25°C and 1 bar, the term in $RT\beta$, for a bimolecular reaction, amounts to about 1.1 c.c. $mole^{-1}$. With the improved experiment techniques of the present day it is normally possible to measure activation volumes to better than $\pm$ 1 c.c. $mole^{-1}$. Since there will be only small differences between the quantities $\Delta\bar{V}^{\ddagger}$ and $\{\Delta V^{\ddagger}_{exp} + (1 - a - b - \ldots)RT\beta\}$, both now referring to the conditions of the prevailing medium, we shall hereafter call them both the "volume

of activation" and designate this quantity by $\Delta V^{\ddagger}$.

The correction for ionic strength effects is made by a term involving the pressure dependence of the activity coefficients.[42] For the purpose of comparing calculated and experimental values of $\Delta V^{\ddagger}$, the ionic strength correction could be made to either the measured $\Delta V^{\ddagger}$, i.e. to $\{\Delta V^{\ddagger}_{exp} + (1 - a - b \ldots) RT\beta\}$, or to the calculated $\Delta V^{\ddagger}$. Because the latter is more convenient, this is the procedure that has been adopted in these studies.

Unfortunately, $\Delta V^{\ddagger}$ is not independent of pressure and frequently plots of ln k vs. pressure are distinctly curved, especially where the volume changes are caused by electrostriction.[6] An example of this emerges in the present studies. The most useful value of $\Delta V^{\ddagger}$ is obviously the limiting value at atmospheric pressure, $\Delta V^{\ddagger}_1$. Various authors[42-45] have discussed the methods whereby $\Delta V^{\ddagger}_1$ may be estimated, but there is no general agreement as to which procedure yields the most accurate value of $\Delta V^{\ddagger}_1$.

There are two main methods that are used. The first is to assume that $\Delta V^{\ddagger}$ is independent of pressure over a small pressure range and to calculate the average $\Delta V^{\ddagger}$ over this range, using an expression of the form:

$$\ln \frac{k_{n+1}}{k_n} = - \frac{\Delta V^{\ddagger}}{RT} (P_{n+1} - P_n). \qquad (2.23)$$

Then by plotting the average $\Delta V^{\ddagger}$ values so obtained (or their reciprocals) against the mean pressure of each interval and extrapolating to 1 bar (effectively zero) a value of $\Delta V_1^{\ddagger}$ can be obtained. This procedure seems to be most satisfactory when the curvature of the plot of ln k against pressure is not small or when there are too few points to fit an equation numerically.

The fitting of an equation is the second main method. Because the theoretical relation between k and p is not known, an assumed empirical equation is used. Normally this is a power series in p of the form

$$\ln k = a + bp + cp^2 \qquad (2.24)$$

The value of $\Delta V^{\ddagger}$ at any pressure, including 1 bar, can then be obtained from the slope. This procedure seems to be best when the curvature of the ln k against p plot is only slight.

Le Noble[7] has pointed out that, although the value of $\Delta V^{\ddagger}$ at 1 bar is the most useful value, it is also the least accurate, since measurements can be made on only one side of it. Furthermore, if through some quirk of nature these graphs have some unusually large curvature just above zero pressure, then the value normally calculated for $\Delta V_1^{\ddagger}$ will bear little resemblance to the true value of $\Delta V_1^{\ddagger}$. It seems, however, on present evidence that this is not the case and the curvature in the ln k vs. p plots usually becomes evident only above 1kbar.

This curvature of the ln k vs. p plots arises from the compressibility of the transition state and is to be expected both because the initial and transition states usually have different compressibilities and because a change of pressure affects the interaction between the transition state and the solvent and therefore changes the nature of the transition state itself. This variation of $\Delta V^{\ddagger}$ with pressure is especially important for reactions with large values of $|\Delta V^{\ddagger}|$ because a large difference in volume between the transition state and the reactants is generally paralleled by a large difference in compressibility.[42]

A significant and controversial paper on this topic, published by Benson and Berson,[46] evoked a lively discussion in the literature. They assumed that for non-ionic reactions an activated complex could be represented by Tait's equation of state, which implied that $\Delta V^{\ddagger}$ must always vary with pressure (contrary to some experimental results). In a subsequent discussion by Walling and Tanner,[47] these authors conclude that usually transition states cannot be treated as having the compressibility properties of ordinary stable molecules.

Hyne and coworkers[48] showed, in a careful analysis of one system, that the quantity $(\partial \Delta V^{\ddagger}/\partial p)_T$ is a real, additional activation parameter and its investigation could very well provide information about the structure and properties of the transition state. For ionic reactions it is probable that the main contribution to the

compressibility of the transition state arises from the interaction of the activated complex with the solvent, depending on the second derivative of the dielectric constant of the solvent with respect to pressure, in the same way that the major contribution to $\Delta V^{\ddagger}$ arises from the electrostriction of the solvent, depending on the first derivative of ε with respect to p.

2.4 Volumes of Activation of Electron Exchange Reactions

The pressure dependence of $\Delta G^{\ddagger}$, the free energy of activation, is given by the relation

$$\left(\frac{\partial \Delta G^{\ddagger}}{\partial p}\right)_T = \Delta \bar{V}^{\ddagger}. \qquad (2.25)$$

In this expression, $\Delta \bar{V}^{\ddagger}$ is the excess partial molar volume of the transition state over those of the reactants under the prevailing conditions.

As Whalley[43] has pointed out, $\Delta G^{\ddagger}$ suffers from the same defect as $(K^{\ddagger})'$ (equation (2.3)), in that it is an incomplete quantity, with the part due to motion along the reaction coordinate being absent. Hence the derivative $(\partial \Delta G^{\ddagger}/\partial p)_T$ is not a true volume. However, as before, it is commonly assumed that this does not lead to any significant error and $(\partial \Delta G^{\ddagger}/\partial p)_T$ is identified as the volume of activation.

An explicit expression for the volume of activation of an

outer-sphere electron transfer reaction could thus be obtained by differentiating equation (1.15) with respect to pressure.

For the case of a one-electron exchange reaction, where the overall free energy change is zero and $\lambda^{\ddagger} = \frac{1}{2}$, we can differentiate equation (1.15) to obtain the expression:

$$\Delta\bar{V}^{\ddagger} = \frac{Z_1 Z_2 e^2}{\sigma} \frac{\partial}{\partial p}\left(\frac{1}{\varepsilon}\right)_T + \frac{1}{4}\{e^2\left(\frac{1}{2r_1} + \frac{1}{2r_2} - \frac{1}{\sigma}\right) \frac{\partial}{\partial p}\left(\frac{1}{\varepsilon_o} - \frac{1}{\varepsilon}\right)_T\} \quad (2.26)$$

Since equation (1.15) refers to the standard free energy change for electron transfer, $\Delta\bar{V}^{\ddagger}$ in equation (2.26) refers to the volume change for reactants in their standard states, i.e. at infinite dilution. As mentioned previously, a correction to this value can be made for ionic strength effects.

It is assumed in deriving equation (2.26) that the quantities σ, r_1, r_2, m and d_e are independent of pressure. There is no compelling reason to believe that σ will change with pressure unless there is solvent between the reactant ions in the transition state.[49] In the present outer-sphere theory, a "close contact" model is employed and it is assumed that σ is equal to the sum of the estimated radii of the reactant complex ions, calculated from Van der Waal's radii. Under these conditions, the reason for the assumed pressure independence of σ is the same as for the quantities r_1, r_2, m and d_e. These all relate to the metal-ligand bond which is assumed incompressible, except under ultra-high pressures. This can be

shown to be a good approximation for simple ions and will be even better for transition metal ions which have extra crystal field stabilisation energies.[49] If this crystal field stabilisation energy for transition metal ions is explicitly taken into account in the expression for $\Delta G^{\ddagger}$, as it should be, then on differentiating with respect to pressure this extra term will also disappear, since its component terms are assumed pressure invariant for the same reason given above.

Since $\Delta V^{\ddagger}$ thus obtained can be equated to the measured volume of activation, equation (2.26) provides another test of the Marcus-Hush theory in that it evaluates the pressure dependence of the basic theoretical expression in an analogous way to $\Delta S^{\ddagger}$, which evaluates the temperature dependence of the same expression.

2.5 The Molecular Interpretation of Volumes of Activation

In discussing the volume changes brought about by increased pressure in the process of activation, it is convenient, as first suggested by Evans and Polanyi[50] in 1935, to separate $\Delta V^{\ddagger}$ into two terms, $\Delta V_r^{\ddagger}$ and $\Delta V_s^{\ddagger}$. $\Delta V_r^{\ddagger}$ represents the contribution to $\Delta V^{\ddagger}$ arising from the change in volumes of the reactant species themselves, and $\Delta V_s^{\ddagger}$ corresponds to the contribution due to the change in volume of the surrounding solvent. It is assumed that these effects may be separated such that

$$\Delta V^{\ddagger} = \Delta V_r^{\ddagger} + \Delta V_s^{\ddagger}. \qquad (2.27)$$

2.5.1 The Term $\Delta V_r^{\ddagger}$

$\Delta V_r^{\ddagger}$, which represents the change in partial molar volumes of the reactant species is forming the transition state, can be estimated from assumed changes in the interatomic distances and Van der Waal's radii of the reactants.

The contributions to $\Delta V_r^{\ddagger}$ will arise almost entirely from the partial formation and/or partial breaking of bonds in the activated complex.

(i) The Breaking of Chemical Bonds

If a reaction involves the breaking of a bond, almost certainly this bond will be stretched in the transition state. The degree of stretching has frequently been quoted as being about 10% of the original bond length, following Ri and Eyring.[51] This now appears to be a considerable underestimate and Hamann[45] has argued that there is no justification for this general rule, nor in fact for any general rule since the degree of stretching probably varies widely for different reactions.

However, an order of magnitude calculation can be made for the contribution of bond breaking to $\Delta V_r^{\ddagger}$ by assuming that a given elongation, δl, of a bond of initial length l, occurs along the axis of a cylinder of constant cross-section. If the Van der Waal's radii

of the two atoms are r_A and r_B, we can put the cross-sectional area of the cylinder equal to the mean of these values. It follows that

$$(\Delta V_r^{\ddagger})_b = \pi(r_A^2 + r_B^2)\delta 1/2 \qquad (2.28)$$

where the subscript b refers to a bond breaking term. For example, consider the reaction

$$N_2O \rightarrow N_2 + O.$$

The Van der Waal's radii of the N and O atoms are 1.5 Å and 1.40 Å respectively, while the N-O bond length is initially 1.19 Å and at the transition state has been calculated as 1.73 Å.[45] This gives $(\Delta V_r^{\ddagger})_b = +2.2$ c.c. mole^{-1}.

The more complex the reactant species are, the more approximate this calculation will be, since it is then more difficult to select an appropriate cross-sectional area.

It is evident that the term $(\Delta V_r^{\ddagger})_b$ for bond breaking must always be positive, since there will always be an expansion in forming the transition state.

(ii) The Formation of Chemical Bonds

In a reaction involving the formation of a new bond, the considerations are just the reverse of those outlined above. We can assume the initial internuclear distance to be equal to the sum of the

Van der Waal's radii, $r_A + r_B$, of the two reactant species. The internuclear separation in the transition state will be $1 + \delta 1$, where 1 is the bond length in the product, and hence the contribution to $\Delta V_1^{\ddagger}$ will be

$$(\Delta V_r^{\ddagger})_f = -\pi(r_A^2 + r_B^2)(r_A + r_B - 1 - \delta 1)/2 \qquad (2.29)$$

where the subscript f denotes a bond forming term.

For example, in the reaction

$$O + N_2 \rightarrow N_2O$$

the initial O...N separation will be 2.9 Å while in the transition state it will be the same as for the reaction in the other direction, 1.73 Å. This gives $(\Delta V_r^{\ddagger})_f = -4.8$ c.c. mole^{-1}.

Again it is evident that the term for bond formation, $(\Delta V_r^{\ddagger})_f$, must be negative, since the formation of the transition state must always involve a contraction.

(iii) Combination of Bond Formation and Bond Breaking

Since a $(\Delta V_r^{\ddagger})_b$ term is always positive and a $(\Delta V_r^{\ddagger})_f$ term always negative, in a reaction involving the simultaneous formation of one bond and breaking of another, the sign of $\Delta V_r^{\ddagger}$ will be determined by whichever one is predominant. From the study of a number of reactions, it appears that almost invariably $(\Delta V_r^{\ddagger})_f$ is substantially greater numerically than $(\Delta V_r^{\ddagger})_b$.[45] Hence for a reaction involving the

simultaneous formation of one bond and breaking of another, $\Delta V_r^{\ddagger}$ will be negative. For example, the reaction

$$H_2 + I_2 \rightarrow 2HI$$

which has been assumed until recently to involve the simultaneous formation of two bonds and breaking of two others, would have a calculated net $\Delta V_r^{\ddagger}$ of -15 c.c. mole^{-1}.

2.5.2 The Term $\Delta V_s^{\ddagger}$

$\Delta V_s^{\ddagger}$ represents the change in volume due to the rearrangement of solvent molecules accompanying the activation process. This rearrangement can be due to a steric factor, which affects the packing of the solvent molecules, and/or it can be due to electrostatic effects which cause the surrounding solvent to either contract or dilate around the activated complex.

In liquid systems, the first factor appears unimportant. However the second factor can be of major importance, especially where electrical charges are developed or neutralised in the activation process.

If an electric charge is fully or partially formed in the activated complex, it will exert an attractive force on the permanent or induced dipoles of the solvent molecules and cause them to contract around it. Obviously, the larger the charge and the more polar the solvent, the larger will be this effect, which is termed electrostriction.

An expression for estimating the degree of electrostriction of a solvent around an ion can be obtained by differentiating Born's equation[52] for the free energy of solvation of an ion with respect to pressure. This gives

$$\Delta V_{el} = -\frac{Z^2 e^2}{2r\varepsilon^2}\frac{\partial \varepsilon}{\partial p} \qquad (2.30)$$

where ΔV_{el} is the contraction (electrostriction) of a medium of dielectric constant ε around a sphere of radius r and charge Ze. Although Born's model assumes spherical particles and a homogeneous dielectric medium, experimental evidence indicates that it gives a reasonably good description of the thermodynamic properties of electrolyte solutions.[53] Applied to monatomic singly-charged ions in water, equation (2.30) yields a value of $\Delta V_{el} \simeq -10$ c.c. mole^{-1}.

The question as to whether $\Delta V_r^{\ddagger}$ or $\Delta V_s^{\ddagger}$ is the predominant term for any given reaction cannot really be answered, since there is no way of knowing the charge that is developed in the transition state. Of course for a reaction where $\Delta V_r^{\ddagger}$ and $\Delta V_s^{\ddagger}$ are of opposite sign the experimental $\Delta V^{\ddagger}$ will indicate which term is the larger. But for reactions where $\Delta V_r^{\ddagger}$ and $\Delta V_s^{\ddagger}$ have the same sign, no unambiguous answer can be given. Nevertheless, Buchanan and Hamann[54] have proposed that, as a working hypothesis, $\Delta V_s^{\ddagger}$ will always be the dominant term in reactions which produce or remove ionic charges, and a larger range of reactions seems to bear this out.[6]

For the special class of outer-sphere electron exchange reactions considered earlier, the term $\Delta V_r^{\ddagger}$ will be effectively zero, since if there is any small change in the radius of one of the reactant species in the transition state, required by the Franck-Condon principle, this will be almost exactly compensated by a similar change in the other. Hence, for these reactions, the measured $\Delta V^{\ddagger}$ can be attributed almost entirely to changes in the solvent surrounding the ions.

The first two systems chosen for the present studies, viz. the $Co(EDTA)^-$ - $Co(HEDTA)^-$ and $Co(en)_3^{3+}$ - $Co(en)_3^{2+}$ systems, are believed to proceed by an outer-sphere mechanism. The adequacy of the Marcus-Hush theory in predicting $\Delta V^{\ddagger}$ values for this type of reaction can be gauged by a comparison of the calculated and measured values of $\Delta V^{\ddagger}$ for these two systems. For the third system in these present studies, the Fe_{aq}^{2+} - Fe_{aq}^{3+} exchange, the mechanism is not so clear, and a comparison of the calculated and measured values for this reaction should assist in determining its mechanism.

Chapter 3

High Pressure Apparatus and Techniques

3.1 Introduction

For the present purpose of studying the effect of pressure on the reaction rates of inorganic reactions in solution, pressures up to 2 or 3 kbar only are required, as the major effect occurs in this range. Although this is at the low end of the high pressure spectrum for high pressure studies, nevertheless the design of the high pressure vessels is basically the same as for those to be used at higher pressures.

A considerable amount of technical knowledge concerning pressure seals, pressure connections, pressure intensifiers and the like has been acquired by workers in the field over the last few decades and there are now several excellent reviews covering all these aspects of high pressure apparatus - see, for example, Hamann,[6] C.C. Bradley[55] and R.S. Bradley.[56]

The basic problem in the design of high pressure equipment is to know what internal pressure a vessel of given material and known wall thickness will support. Almost invariably these vessels are hollow cylinders, both for reasons of convenience in manufacture and for even distribution of stress over the vessel. There has been a number of theoretical and empirical relations proposed to give the bursting pressure of a cylinder in terms of the tensile strength of the wall material and the thickness of the wall.

For a thin-walled cylinder of internal and external radii r_1 and r_2 respectively, it can be shown[6] that the cylinder will start to yield with permanent deformation when

$$p = \frac{r_2 - r_1}{r_1} f = (K - 1)f \qquad (3.1)$$

and it will burst when

$$p = (K - 1)\sigma \qquad (3.2)$$

where f and σ are the yield stress and ultimate tensile stress of the wall material. K is the ratio of external to internal radius. This equation is strictly valid only for very thin cylinders but it is very useful in that it gives good estimates of the yield and bursting pressures for values of K up to 1.1.[6] For moderately high pressures this is usually sufficient.

For thick cylinders, Manning[57] has derived an equation relating the bursting pressure to the results of torsion tests. However, although this formula has been shown to agree well with experiment,[58] it is inconvenient to apply due to the more difficult nature of torsion tests and the lengthy calculations involved. More recently, Leinss[59] has proposed an empirical relation,

$$p = \frac{\sigma}{1/(K - 1) + \beta} \qquad (3.3)$$

where β is an empirical parameter which is characteristic of the

material used. The results of a number of experiments have been shown to conform to this equation and for most purposes it is probably the most useful of all the relations that have been proposed.

A general requirement for the study of the kinetics of any reaction is that the reaction mixture must be sampled for analysis at various known times in the course of the reaction. For high pressure kinetic studies this poses an additional design problem. Not only must the design allow for sampling of the reaction mixture at given times, but also the reactant solution must not come in contact with the pressure vessel material, because of possible chemical interaction. This last requirement is particularly important for aqueous solutions, because of their greater reactivity with metals.

3.2 High Pressure Vessels

Since the present studies were among the first high pressure studies to be carried out in these laboratories, new high pressure vessels were developed and modified during the course of this work. The different vessels will be described in the order in which they were designed.

3.2.1 Individual Pressure Vessels

The first high pressure vessels used consisted of a set of six identical vessels, shown in Figure 3.1. They were designed in these

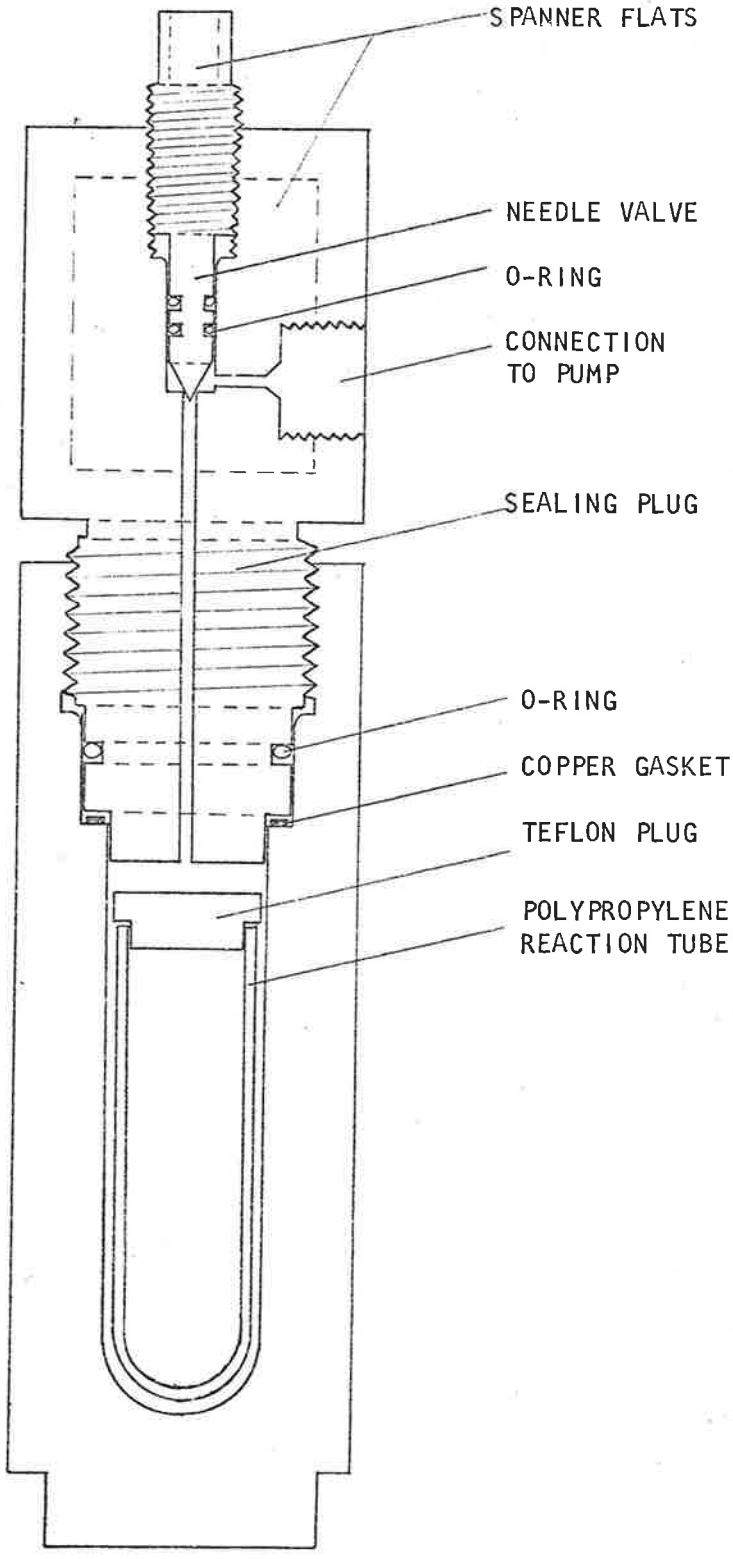

Figure 3.1 Individual Pressure Vessel

laboratories and were constructed from 65 Ton SD50 stainless steel, with a rating of 6000 bar. The reaction vessel itself consisted of a polypropylene tube of about 9 ml. capacity, with a tight-fitting Teflon plug. This was completely surrounded inside the pressure vessel by Ondina 17 oil, which was the pressure medium for transmitting the pressure to the reaction solution.

The pressure seal for the main body of the vessel was effected by a Neoprene or Viton-A O-ring at lower temperatures (up to 30°C), but for higher temperatures a copper gasket, seated below the sealing plug, was used. It was found that the O-rings failed after a matter of a few hours under pressure at the higher temperatures.

The pressure was generated by a manual hydraulic pump, which was connected by a standard Aminco pressure connector to the side outlet of the pressure vessel, and the pressure raised to the desired value with the needle valve open. This was then closed, and with the pressure vesse now completely sealed, the connection to the pump was removed.

The set of six pressure vessels was used for each kinetic run, since the reaction solution within each vessel could provide only one aliquot to give one point on a kinetic plot. To carry out a run, then, the reaction solution was prepared and immediately divided into six parts to fill each of the six reaction vessels, one for each pressure vessel. Due allowance was made for the time interval between loading and pressurizing each vessel.

When each vessel was to be sampled, it was placed on the pressure line, as shown below (Figure 3.2).

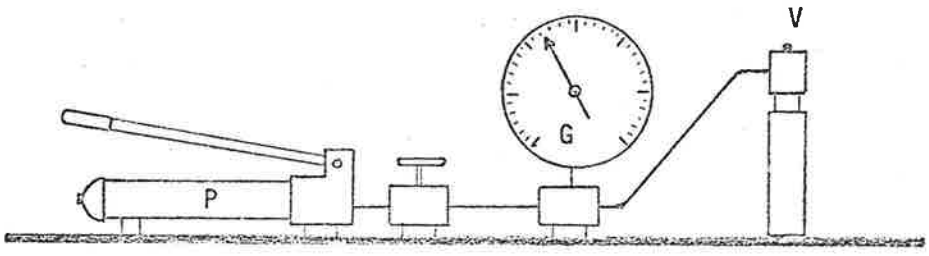

Figure 3.2 Pressure Line Assembly.

With the needle valve (V) still closed, the pressure in the line was raised by the pump (P) to the expected value inside the pressure vessel. The needle valve was then opened, and if the pressure in the vessel had dropped from its initial value due to a leakage, it was immediately evident from the pressure gauge (G) and the solution was rejected. Such leakages rarely occurred however. If no drop in pressure had occurred, the pressure was released back through the pump and then the vessel was dismantled and the reaction solution withdrawn for sampling.

These pressure vessels suffered from two major difficulties. The first and most obvious is that each point on a kinetic plot came from a separate determination from an individual pressure vessel, and not from a bulk solution in a single reaction vessel. The second is that,

when working at higher temperatures, the final pressure could not be accurately predicted beforehand, since the vessels had to be pressurized at room temperature and subsequently raised to the required working temperature. This of course raised the pressure inside the vessel, and the final pressure had to be measured when opening the vessel for sampling by balancing its pressure against the pressure in the line.

3.2.2 High Pressure Sampling Vessel

The second model of pressure vessel obviated the difficulties just mentioned, by allowing aliquots to be withdrawn from the one reaction solution and by being continuously on the pressure line, thus permitting the pressure to be registered on the gauge throughout a run. This model consisted of a single pressure vessel, which is shown in Figure 3.3.

The vessel was designed in these laboratories with the aid of data supplied by Dr. A. Ewald (University of Sydney). The main body and screw plug were made from 75 Ton SD50 steel, with 316 stainless steel used for the other parts. This vessel was similarly sealed with either an O-ring or copper gasket, depending on the working temperature.

The reaction vessel, shown in Figure 3.4(a), was made of Perspex with a Teflon plunger. It was found convenient to lubricate the barrel of the reaction vessel with a very thin film of Apiezon N grease.

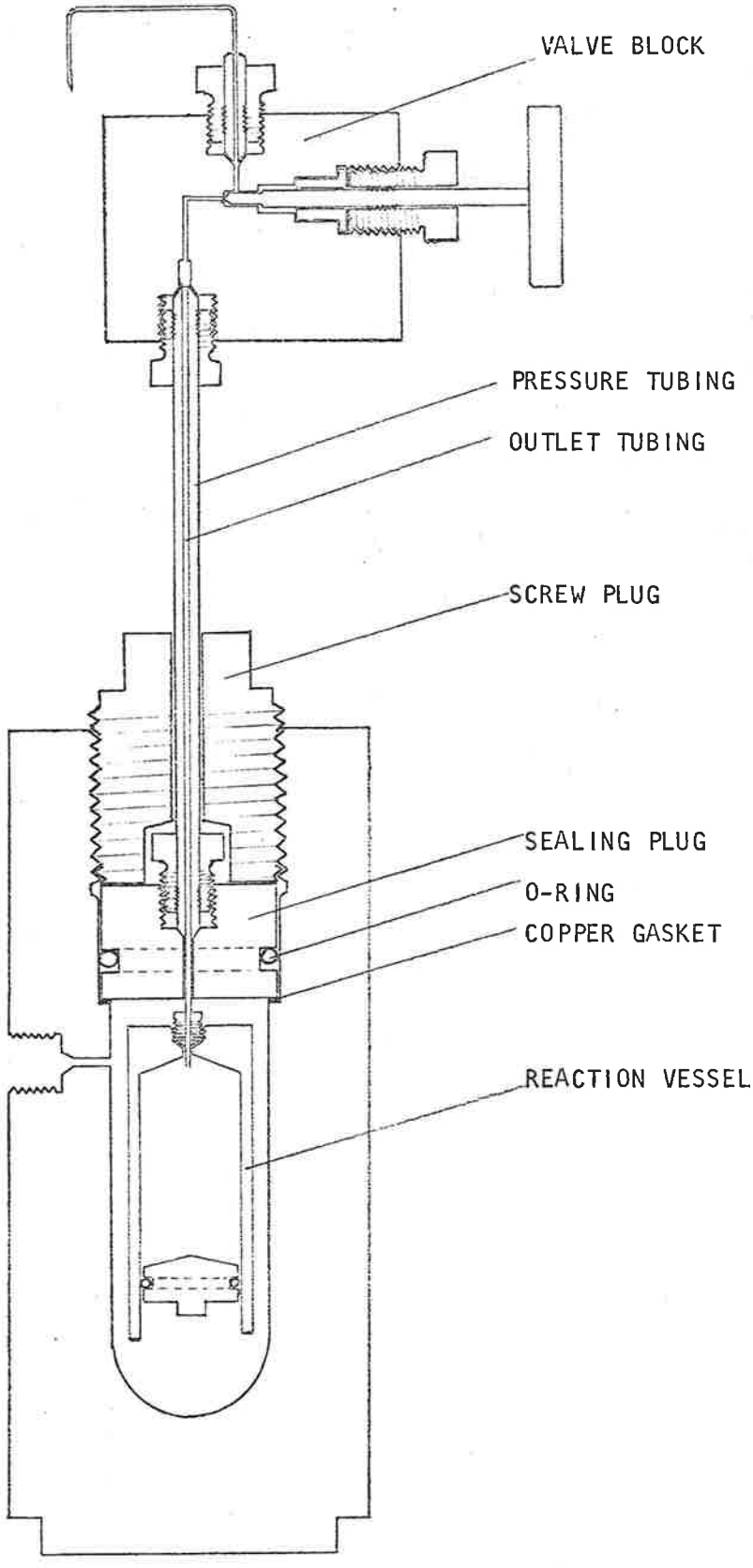

Figure 3.3 High Pressure Sampling Vessel

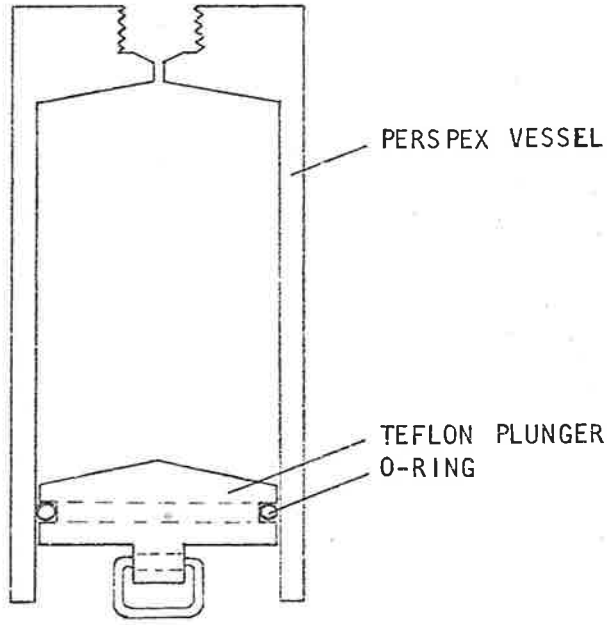

Figure 3.4(a) Reaction Vessel

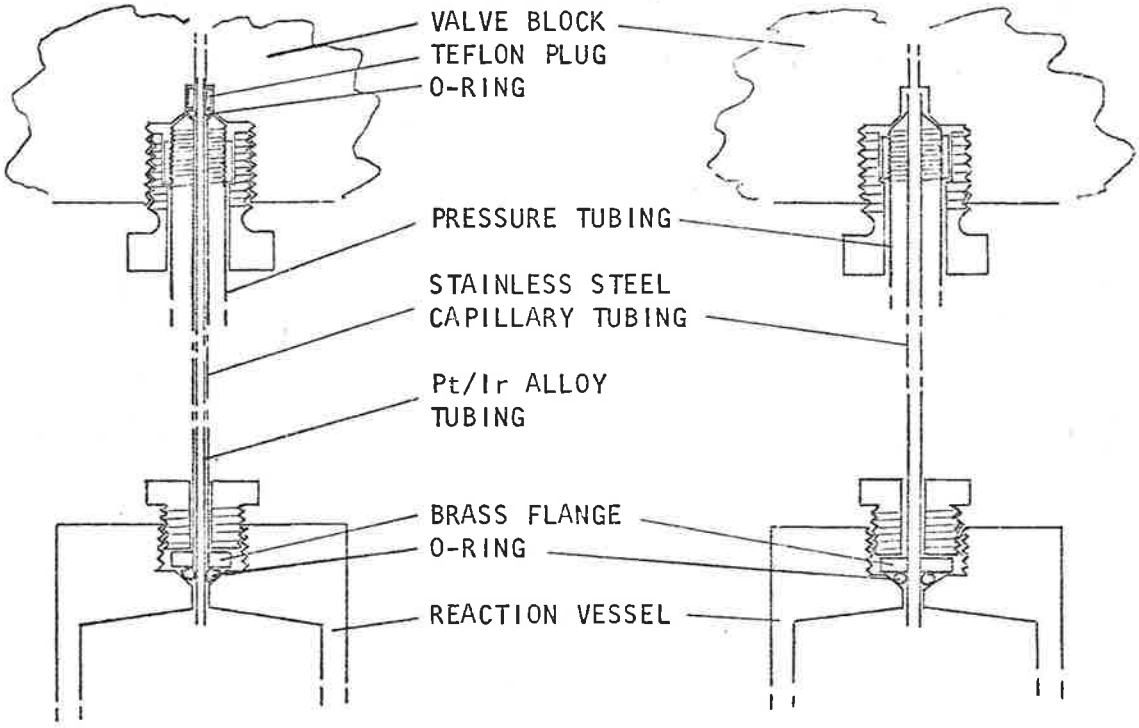

Fig. 3.4(b) Connections between Reaction Vessel and Valve Block

This was an inert hydrocarbon-based lubricant and tests showed that it did not interfere with any reaction studied. There were several interchangeable vessels, with capacities varying from 30 ml. to 100 ml. To remove an aliquot of reaction solution for sampling, the needle valve was opened and the pressure forced the solution out as the plunger moved up the reaction vessel. The pressure was then quickly readjusted with the pump.

Several modifications had to be made to achieve a satisfactory connection between the reaction vessel and the sample valve block, due to attack of the metal connection fittings by the various reaction solutions. A simple Luer lock connection was first tried. This was later replaced by a screw-in connection with the end gold-plated. This was finally replaced by the connection shown in Figure 3.4(b). In some cases, a stainless steel capillary tube was found satisfactory for the outlet tube connecting the reaction solution to the valve block. However, for the more reactive solutions, the stainless steel capillary had to be replaced by a platinum-iridium alloy tubing, which was inert. The extremely small diameter of this tubing, 0.022", made it difficult to seal, and so it was less convenient to use than the stainless steel tubing. The methods of sealing these two tubes are indicated in Figure 3.4(b).

3.2.3 Optical Pressure Vessel

For the study of reactions which can be followed spectrophotometrically, a third pressure vessel was designed. This is shown in Figures 3.5(a) and (b). The reaction cell was mounted centrally inside the pressure vessel, intercepting the light path between the two windows. The reaction cell was made of silica, with a 1 cm. square lower section and a cylindrical neck, as shown in Figure 3.5(a). The cap consisted of a small Teflon plunger with a Neoprene O-ring. This served to separate the reactant solution from the surrounding pressure medium and allowed pressure to be applied to the reactant solution without strain on the silica cell.

The pressure medium used in the present studies was again Ondina 17 oil. This is transparent in the visible wavelength region but absorbs in the U.V. If it were desirable to work in the U.V. region, another suitable pressure medium, such as n-hexane could be used, with a phase separator between the pressure vessel and the pump.

The windows of the pressure vessel were constructed of clear sapphire discs, supplied by Linde Crystal Products, U.S.A. The crystals were cut with an orientation of 90° and the faces of the discs were optically flat to five wavelengths, with a parallelism to 0.0005-0.001 inches. They transmitted down to 140 nm and so were suitable for studies in the U.V. region.

The aperture of the windows was not of critical dimensions. From

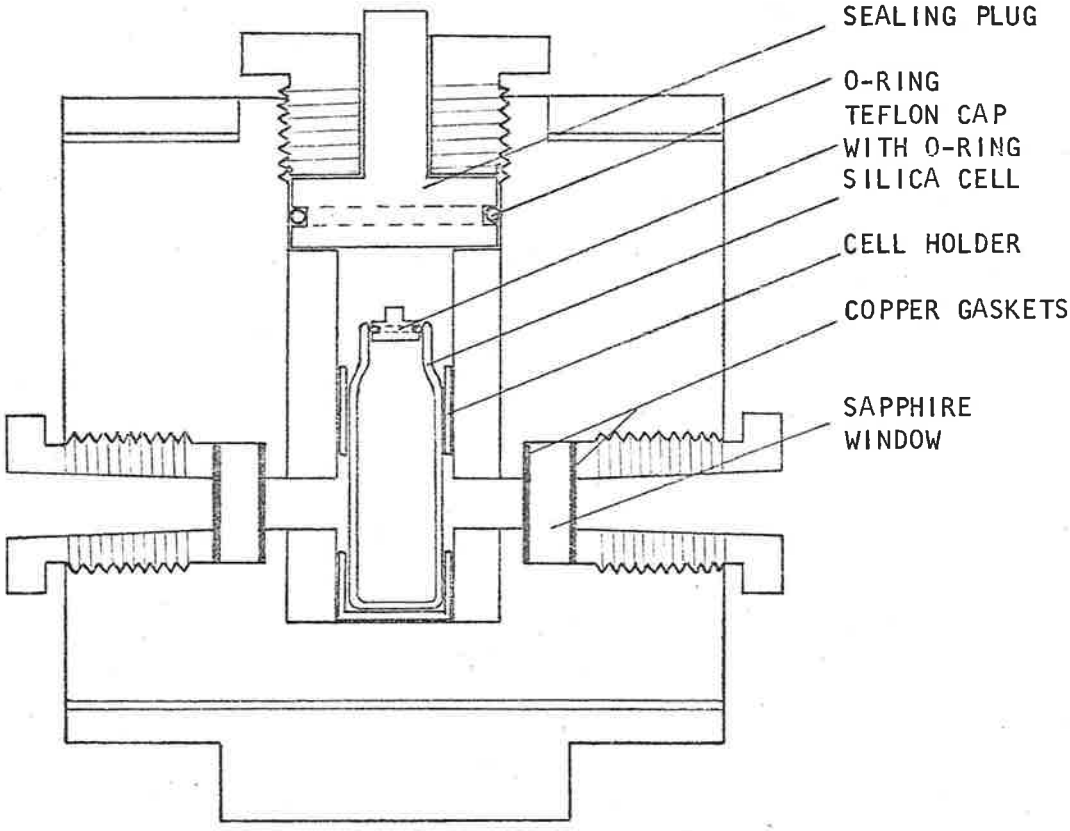

Figure 3.5(a) Optical Pressure Vessel (Vertical Section)

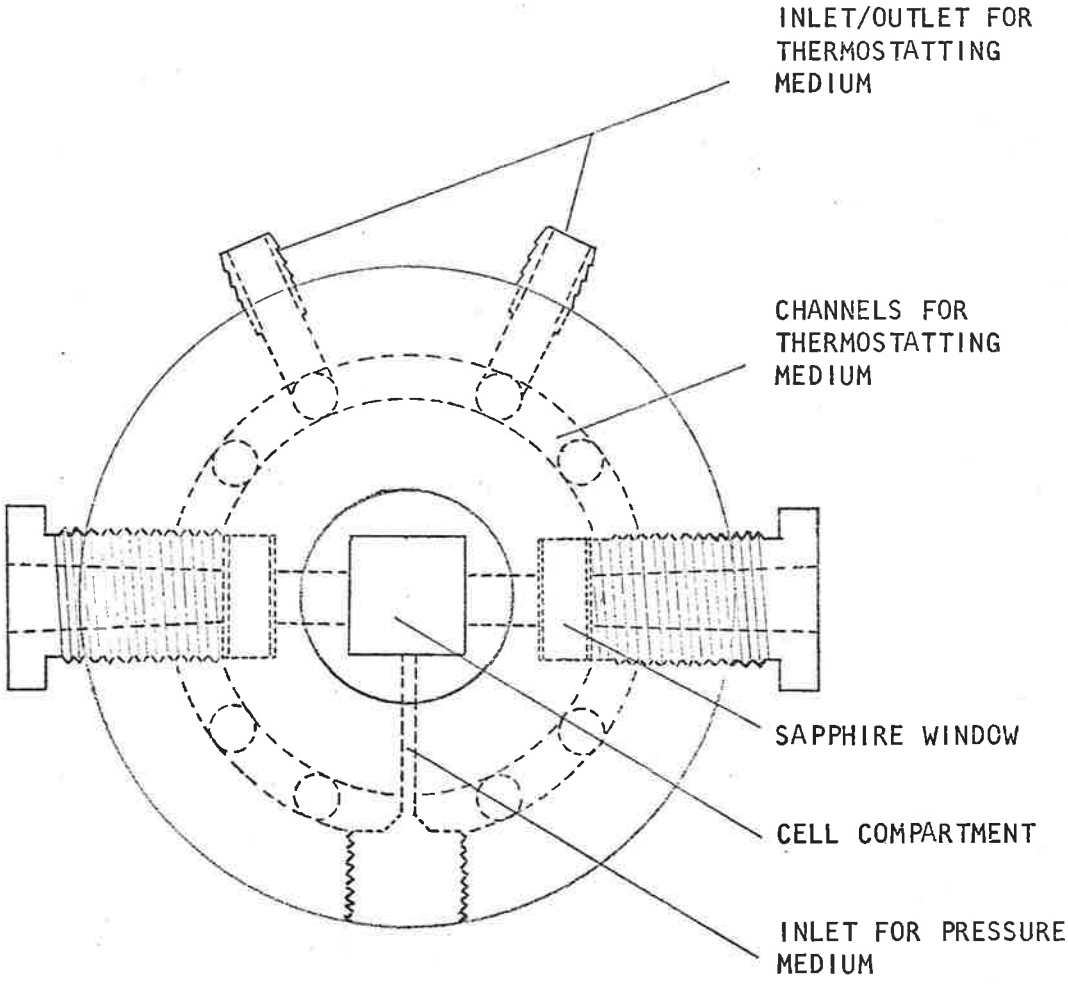

Figure 3.5(b) Optical Pressure Vessel (Transverse Section)

the results of experiments on the bursting pressure of various kinds of plate glass, Pugh, Hodgson and Gunn[60] found that a thickness to unsupported-diameter ratio (t/d) equal to 1 was satisfactory up to 12 kbar. A t/d ratio equal to 1 for this vessel should show no significant deformation of the windows, which would otherwise result in refractive losses.

3.3 General Pressure Equipment

Pressure Gauges

The pressures were measured with Budenburg Pressure Gauges, which are Bourdon-type gauges. The gauge was situated about mid-way along the pressure line between the pump and the pressure vessel. Two interchangeable gauges, with ranges of 0-25,000 p.s.i. (0-1.7 kbar) and 0-70,000 p.s.i. (0-4.8 kbar), were used, depending on the pressure required. These gauges were guaranteed by the manufacturers to have an error of not more than 1% of the maximum scale value, when operated within 10% and 90% of full scale. No calibration check was therefore considered necessary.

Hydraulic Pumps

The pressure was generated by a manual hydraulic pump, Blackhawk Enerpac Model P-228, rated at 40,000 p.s.i. (2.75 kbar). The pump was filled with Ondina 17 oil, supplied by the Shell Company, and this

was pumped directly through the pressure line into the pressure vessel.

High Pressure Tubing and Valves

The high pressure tubing used was of 316 stainless steel. The size used most frequently was 1/4" O.D. tubing, rated at 100,000 p.s.i. (6.9 kbar). Some 3/8" O.D. tubing, rated at 50,000 p.s.i. (3.4 kbar) was used as an oil reservoir. These tubings were supplied by the American Instrument Company. For the inlet to the spectrophotometer vessel, 1/8" O.D. was used, due to the greater ease in forming it to the shape required to exit it from the spectrophotometer. This tubing was rated at 90,000 p.s.i. (6.2 kbar) and was supplied by the Harwood Engineering Company, U.S.A. The T-piece connectors and valves were standard Aminco fittings, supplied by the American Instrument Company and all rated at 60,000 p.s.i. (4.1 kbar).

All connections with high pressure tubing were made using the standard line-seal method, created by a 59° cone-ending and a 60° cone-insert, as shown below (Figure 3.6).

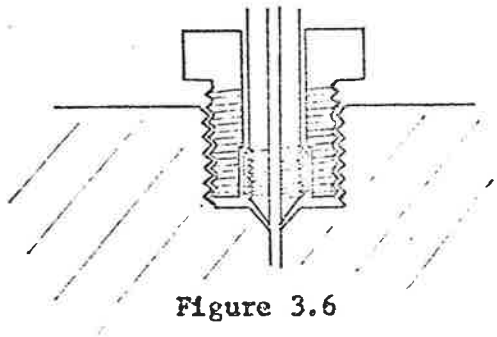

Figure 3.6

Pressure Medium Reservoirs

With the high pressure sampling vessel, after an aliquot of reaction solution had been withdrawn, the pressure was readjusted by pumping more oil into the pressure vessel. To maintain a constant temperature inside the vessel, then, it was necessary to have a reservoir of oil, situated immediately before the inlet to the pressure vessel and thermostatted to the same temperature as the pressure vessel.

Two types of reservoir were used. One consisted of a length of 3/8" O.D. high pressure tubing, containing 48 ml. of oil, coiled around the pressure vessel and leading directly into it. The other reservoir was, in effect, another pressure vessel, similar to the reaction pressure vessel, but without the outlet valve. This stood alongside the reactant pressure vessel and was connected directly to it.

The schematic diagrams below (Figure 3.7) show the arrangement of the apparatus, using the high pressure sampling vessel and each oil reservoir.

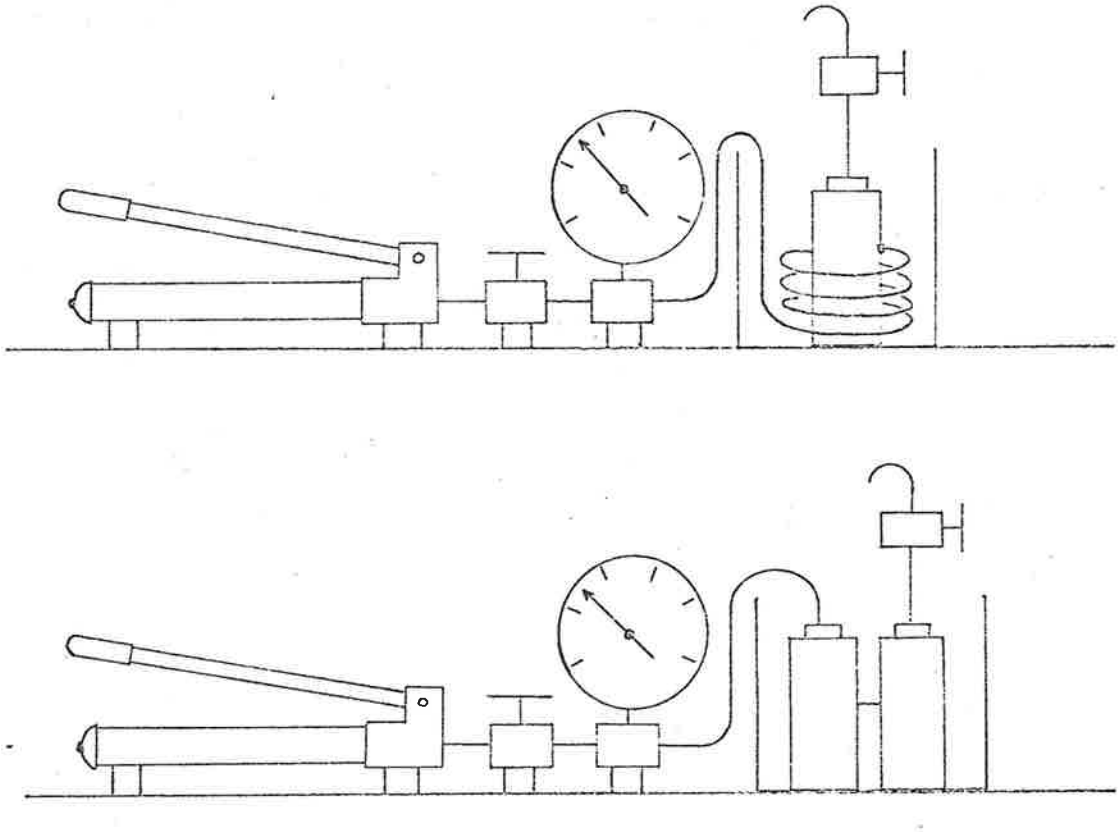

Figure 3.7

The temperature effects caused by pressurization were shown to be insignificant, except for the Fe^{2+}_{aq} - Fe^{3+}_{aq} system, and they are considered in detail in Chapter 6.

Chapter 4

The Effect of Pressure on the Co^{II}(EDTA) - Co^{III}(EDTA) System

The major part of the study described in this chapter concerned the electron exchange between Co^{II}(EDTA) and Co^{III}(EDTA). A subsidiary study of the pressure dependence of the equilibrium between the hexadentate and pentadentate forms of the Co(III) complex in acid solution was also undertaken.

A. The Effect of Pressure on the Co^{II}(EDTA) - Co^{III}(EDTA) Electron Exchange

4.1 Introduction

The electron exchange between Co^{II}(EDTA) and Co^{III}(EDTA) has been studied previously by Adamson and Vorres[61] and by Im and Busch.[62] Both groups studied the reaction as a function of temperature, and their measurements of the energy and entropy of activation, as well as the rate data, were in agreement. Independent methods of following the exchange were used in each study, the former workers using isotopic labelling and the latter employing optical activity.

This reaction was chosen for high pressure study because it appeared to be well characterised and it fulfilled the following conditions: (i) the reaction was slow enough to permit its study using high pressure techniques, and (ii) the exchange was believed to proceed by an outer-sphere mechanism, thus making it suitable for application of the Marcus-Hush theory. An outer-sphere mechanism

was considered operative in this system because of the substitution-inert character of Co(III) complexes and because of the evidence adduced in the second and more complete investigation of this system by Im and Busch, who proposed a mechanism involving an outer-sphere activated complex.

4.1.1 Nature of the Co-EDTA Species in Solution

There has been considerable discussion in the literature as to whether the ligand ethylenediaminetetraacetate ($EDTA^{4-}$) functions as a pentadentate or hexadentate ligand in aqueous solution.

From a spectrophotometric study of the EDTA complexes of Co(II), Cu(II) and Ni(II) in solutions of various pH values, Bhat and Krishnamurthy[63] concluded that the normal complex exists as hexacoordinated EDTA but on protonation at lower pH the ligand becomes pentadentate, presumably with the introduction of a water molecule into the first coordination sphere.

This view was supported by Sawyer and Tackett,[64] who compared the IR spectrum of the free ligand with that of the metal-ligand complex in aqueous solution. They concluded that under all conditions of acidity at which the Co(II)-EDTA complex forms (down to pH 0.9), the proton does not add to the nitrogen atom but to a carboxylate group. Hence the mono-protonated species has one free carboxylic acid group and the sixth coordination position would be occupied by a solvent water molecule.

More recently, Wilkins and Yelin[65] treated the Co(II)-EDTA complex at various acidities with a variety of rapidly reacting oxidants and examined the spectra of the resulting Co(III) complex soon after it was formed. Their calculations of the product distribution yielded a value of $\geq$ 80% hexadentate $Co(EDTA)^{2-}$ in the Co(II) solution at pH $\gtrsim$ 4.5. Higginson[66a] also, contrary to his earlier conclusions,[66b] believed that there was a predominance of the hexacoordinate EDTA in the Co(II) complex at these acidities (provisional results 77 $\pm$ 3%), but at lower pH the pentacoordinate EDTA predominated. His conclusions were based on measurements of the association constants of the protonated and unprotonated Co(II)-EDTA complexes with a variety of monodentate ligands.

The acidity constant for the protonated Co(II)-EDTA complex, $Co(HEDTA)H_2O^-$, has been measured under a variety of conditions,[62,67,68] and has the value of $pK_a \tilde{} 3$ at room temperature. Thus the exact proportions of protonated and unprotonated species present in solution can be calculated for a solution of any given pH.

Hence, in summary, it seems clear that for Co(II) the EDTA acts as a hexadentate ligand at pH $\gtrsim$ 4.5 and the predominant species will be $Co(EDTA)^{2-}$, while at pH $\lesssim$ 3 the protonated species will be dominant, with the EDTA now pentacoordinate and a water molecule in the sixth coordination position.

For the Co(III)-EDTA complex the situation is similar, except that the ligand appears to be unambiguously hexadentate at higher pH

and the conversion to the protonated, pentadentate form at lower pH is slow (as would be expected from the inert nature of the Co(III) ion) and is not so extensive.

A variety of early evidence[69-71] indicated that the Co(III) complex contained hexadentate EDTA in aqueous solution at normal pH. This has since been further supported. Weakliem and Hoard[72] showed conclusively that the Co(III)-EDTA complex was hexadentate in the solid state by a complete crystallographic structure determination. With this established, Gillard and Wilkinson[73] measured the IR spectrum of Co(III)-EDTA in heavy water and found there was a close correspondence of the IR spectrum in solution with that of the ion in the solid state. This implied that there was very little change in the structure of the ion in solution and so it must be hexadentate also in solution. Some recent evidence from viscosity measurements also confirms this conclusion.[74]

Higginson,[75] using spectrophotometric methods, has carried out a thorough investigation of the kinetics and equilibria existing between the various Co(III)-EDTA species in aqueous solution at different pH. He found that as the pH of the solution was changed, there was a rapid interconversion between the various pentadentate forms but that equilibria between the pentadentate and hexadentate forms were established slowly. The interconversion between the pentadentate forms could be represented as:

$$Co(HEDTA)H_2O \underset{\text{I}}{\overset{\text{fast}}{\rightleftharpoons}} Co(EDTA)H_2O^- + H^+ \underset{\text{II}}{\overset{\text{fast}}{\rightleftharpoons}} Co(EDTA)OH^{2-} + 2H^+$$

Equilibrium I had the value $pK_a \simeq 3$ and equilibrium II the value $pK_a \simeq 8$, indicating the predominant pentadentate species in solutions of different pH.

The equilibria between the pentadentate and hexadentate forms could be written as:

$$Co(HEDTA)H_2O \overset{\text{slow}}{\rightleftharpoons} Co(EDTA)^- + H^+ + H_2O$$

$$Co(EDTA)H_2O^- \overset{\text{slow}}{\rightleftharpoons} Co(EDTA)^- + H_2O$$

$$Co(EDTA)OH^{2-} \overset{\text{slow}}{\rightleftharpoons} Co(EDTA)^- + OH^-$$

Between pH 2.5-7.0 the conversion to $Co(EDTA)^-$ was found to be quantitative, but between pH 7-10, there was some loss ($\lesssim$ 5%) of $Co(EDTA)^-$, apparently with the formation of $Co^{II}(EDTA)^{2-}$. Between pH 0-2 an equilibrium was established between the hexadentate form, $Co(EDTA)^-$, and the protonated, pentadentate form, $Co(HEDTA)H_2O$:

$$Co(EDTA)^- + H^+ + H_2O \rightleftharpoons Co(HEDTA)H_2O$$

The equilibrium constant for this equilibrium was determined. Hence again, once equilibrium had been established, the proportion of each form present in a solution of given pH could be calculated.

4.1.2 pH Dependence of the Exchange Rate

The rate of electron exchange exhibits a pH dependence. This is shown in Figure 4.1, where the data of Im and Busch are reproduced, together with the results, corrected to 100°C, from a number of preliminary runs carried out in this present study. As might be expected, the plot of observed rate constant, k, against pH follows the pattern of a pH titration curve, with the inflection occurring around pH 3, corresponding to the acid dissociation constant, $pK_a = 3$, for the protonated Co(II)-EDTA complex:

$$Co(HEDTA)H_2O^- \rightleftarrows Co(EDTA)^{2-} + H_2O + H^+ \qquad pK_a = 3$$

Because, then, the protonated and unprotonated Co(II) complexes exchange at quite different rates with the Co(III) complex, it would be desirable to have all the Co(II) in the one form for rate studies. Accordingly, the plateau region of pH 4-6 appeared most suitable, since here both the Co(II) and Co(III) complexes were hexadentate, with charges of -2 and -1 respectively. A number of runs was carried out in this region, as indicated in Figure 4.1, but some difficulty was experienced. This was due, apparently, to the decomposition of some of the reactant to cobalt oxide at this higher pH and high temperature (95°C). Im and Busch also reported that reproducible data could be obtained only within the range pH 2-4.

Hence it was decided to study the exchange in the other plateau

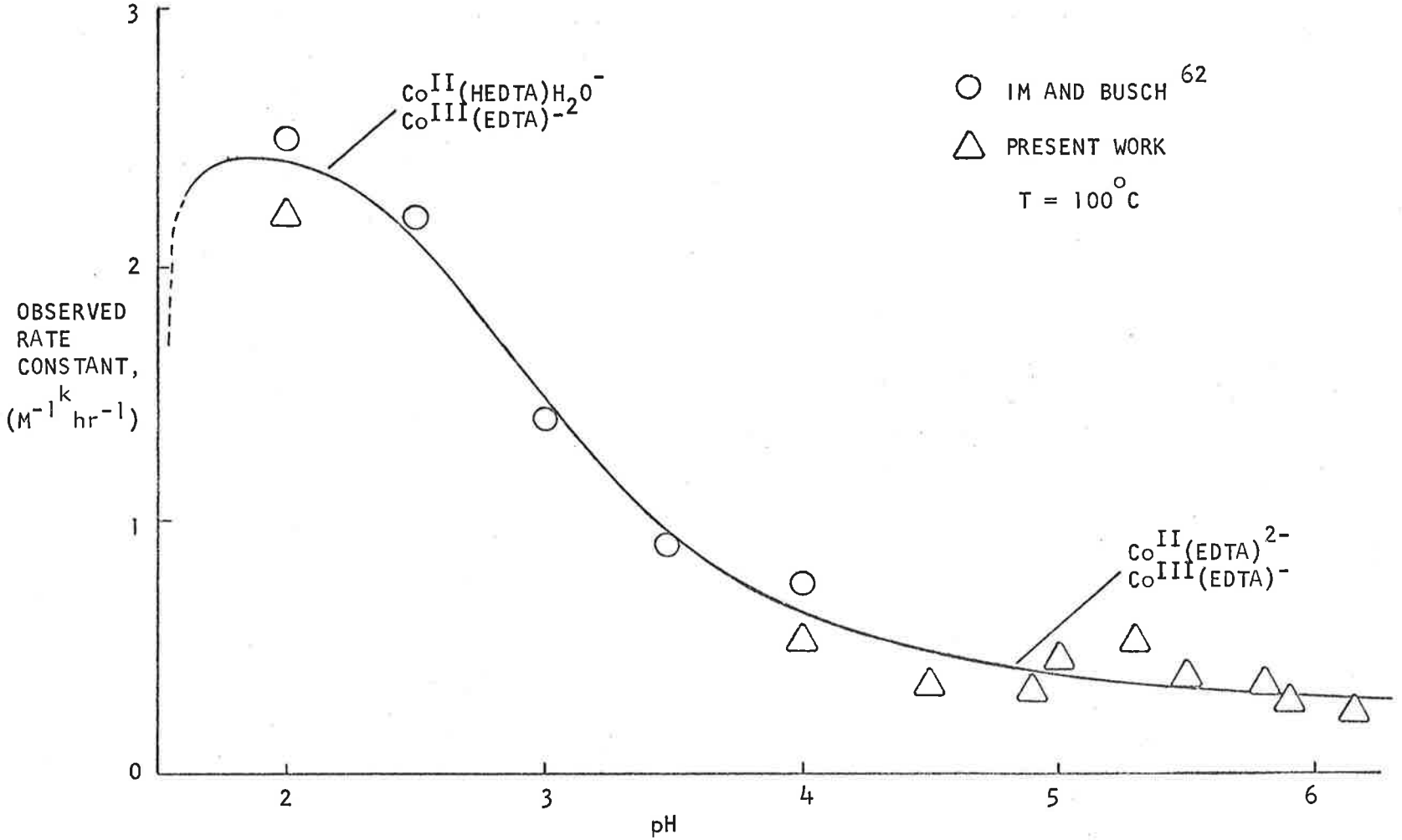

Figure 4.1 pH Dependence of Electron Exchange Rate

region at pH 2. Below about pH 1.8 the rate of exchange dropped away rapidly due to the destruction of the Co(II) complex. No exchange was observed to occur at all between Co^{2+}_{aq} and $Co^{III}(EDTA)^-$, as was reported also in both previous studies. This behaviour appears typical for Co^{2+}_{aq} - Co(III) systems, e.g. Co^{2+}_{aq} - $Co(en)_3^{3+}$, Co^{2+}_{aq} - $Co(NH_3)_6^{3+}$. Two further advantages of working at pH 2.0 were that the exchange proceeded at faster, more convenient rates than at higher pH, and that the pH of the solution was not so susceptible to change with pressure.

It will be shown in the Discussion below (section 4.4), that the only important pathway for exchange under these conditions was that involving the species $Co^{II}(HEDTA)H_2O^-$ and $Co^{III}(EDTA)^-$, i.e. the reaction can be represented by the equation

$$\overset{*}{Co}{}^{II}(HEDTA)H_2O^- + Co^{III}(EDTA)^- \rightleftarrows \overset{*}{Co}{}^{III}(EDTA)^- + Co(HEDTA)H_2O^-.$$

4.1.3 Ionic Strength Effect

Adamson and Vorres[61] found that increasing the ionic strength from 0.2 M to 0.7 M by the addition of $BaCl_2$ increased the rate of exchange by about 10%. Im and Busch[62] subsequently carried out a more detailed investigation on the effect of ionic strength on the exchange rate. They showed that this system was insensitive to changes in ionic strength, the rates being essentially the same in the absence of added salt (μ = 0.2 M) and at μ = 0.7 M in the presence of $NaNO_3$, KNO_3, $RbNO_3$ or CsCl. However, they also found that the rate of exchange was

accelerated by about 10% at μ = 0.7 M in the presence of $BaCl_2$, indicating that this was a specific ion effect. These present studies were carried out at constant ionic strength, μ = 0.5 M, using $NaClO_4$ as the supporting electrolyte.

A number of preliminary runs were carried out at 80°C, 85°C and 95°C. However, for the pressure dependence study it was found convenient to study the exchange rate at 85°C. Although a detailed study of the temperature effect was not made, from the limited data available from the preliminary runs, it was shown that the temperature dependence was consistent with an activation energy of 21-22 kcal. $mole^{-1}$, reported in both previous studies.[61,62]

Hence, the pressure dependence of the electron exchange rate between Co^{II}(EDTA) and Co^{III}(EDTA) was studied at 85°C in aqueous solution of pH 2.0 and total ionic strength 0.5 M.

4.2 Experimental

4.2.1 Apparatus

Pressure Vessels

The early part of this work was carried out using the set of individual pressure vessels, but these were replaced during the course of the work by the high pressure sampling vessel. These vessels have been described in Chapter 3.

Several modifications to the high pressure sampling vessel were found necessary. Initially, a length of stainless steel capillary tubing, inside the pressure tubing, was used as the outlet from the reaction vessel to the sampling valve block. The connection to the reaction vessel was made by means of a simple Luer lock, as shown below.

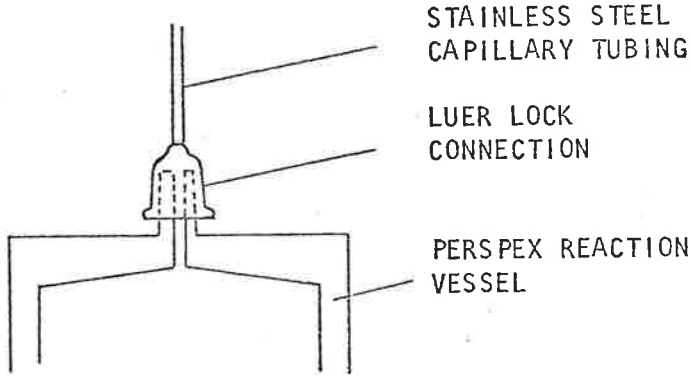

However, it was noticed that the optical absorbance of the reaction solution, measured at the lower absorption maximum of the Co(III) complex, steadily decreased during the course of a run by as much as 20-30%. That this was due to the loss of Co(III) complex was shown by the fact that the same fractional decrease in optical

absorbance occurred at both absorption maxima for the Co(III) complex, 382 nm and 538 nm, while there was no significant change at the absorption maximum of the Co(II) complex at 487 nm. It was further noticed that the metal connection was being etched. This effect occurred only at higher pressures and was not observed at atmospheric pressure. Any change in the pH of the solution was too small to measure accurately and tests to determine whether Co(II) was being formed were inconclusive. Whatever reaction was occurring was not investigated further.

To overcome this difficulty, the Luer lock was replaced by a connection with an O-ring seal and with the end of the outlet tubing that protruded into the reaction solution being gold-plated. This connection is shown in the diagram below.

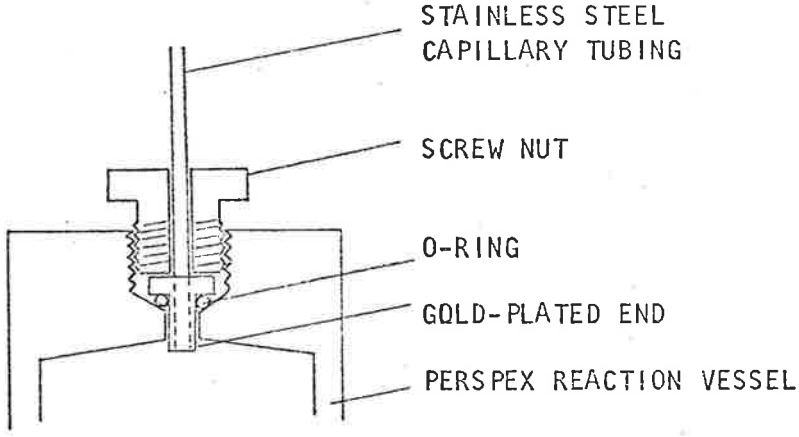

At first this was successful, but because the gold-plating was either too porous or too uneven, corrosion of the metal beneath the gold again

occurred after some hours in use, and this was accompanied by a similar loss of some of the Co(III) complex.

Finally, the entire stainless steel capillary was replaced by a Pt/Ir alloy tubing, with the connection as described in Chapter 3. The above effect was then eliminated.

Scintillation Counter

The activities of the sample solutions were determined using a Philips Scintillation Detector (PW4119), housed in a Philips Automatic Sample Changer (PW4003), with a Stabilised High Voltage Supply Unit (PW4025/10). This was coupled to an assembly consisting of a Scaler (PW4231), Stabilised Power Supply (PW4211), Amplifier (PW 4270), Timer (PW4261), Printer Control (PW4200) and Victor Digit-Matic printer. The scintillation crystal was a well-type thallium-activated sodium iodide crystal.

The tracer used in these experiments was ^{60}Co, which has a half-life of 5.27 years[76] and so any small time delays in counting separate samples were of no consequence. ^{60}Co emits two γ-rays of energies 1.33 Mev and 1.17 Mev.[76]

To obtain the optimum conditions for counting the ^{60}Co γ-rays, the control settings were systematically varied. The E.H.T. was set at 1300 V, which was about midway along the voltage plateau. The discriminator bias was set so that the lower threshold was just below

the energy of the ^{60}Co γ-rays, and the attenuation was set at X 10. These settings gave the maximum ratio of total count to background.

The scaler was used on a pre-set time setting. Each sample was counted for 200 seconds, and the total count was such that the standard deviation was not more than 1%. The counting time was probably longer than necessary to obtain this accuracy in the count rate, but as the instrument was automatic a minimum counting time was not important.

The Automatic Sample Changer had a capacity for 50 separate samples. The counting tubes were found to vary slightly in size, thus affecting the count rate. However, a number of tubes were selected which gave count rates which were reproducible to within 1% on samples of the same activity, and these were used throughout.

pH Meter

All pH measurements were made using a Doran Precision Universal pH Meter and D.C. Potentiometer, Model M4989. It consisted of an Electrometer Valve Potentiometer, reading to 0.001 pH units. The null detector used was a self-contained reflecting galvanometer. Automatic temperature compensation was provided, although manual control was also available. The electrodes used were a standard glass electrode and a calomel electrode.

Buffer solutions for standardising the instrument before use were

prepared from buffer tablets for the appropriate pH range, supplied by Marconi Instruments Ltd., England.

Spectrophotometers

For complete spectra in the U.V. and visible wavelength regions, Unicam S.P.700 and Unicam S.P.800 recording spectrophotometers were used.

All accurate absorbance measurements were made using a Shimadzu spectrophotometer, Model QR-50. This was a manual instrument and measurements on duplicate samples were reproducible to $\pm$ 0.001 optical absorbance units. Matched silica cells were used.

Temperature Control

For the first set of pressure vessels, temperature control was achieved by completely immersing the vessels in an oil bath maintained to within $\pm$ 0.1 degree of the required temperature by a solid-state proportional control heater, regulated by a thermistor probe.

The high pressure sampling vessel was similarly immersed in an oil bath, but only to the top of the main body. At the higher temperatures (above 40°C), heat loss from the exposed top of the pressure vessel caused a temperature difference up to 1°C between the reaction solution inside the pressure vessel and the oil surrounding the pressure vessel. Once thermal equilibrium had been attained, this

temperature difference remained constant, so by maintaining the oil bath at a slightly higher temperature than required, the desired temperature could be accurately obtained within the reaction vessel. At the lower temperatures such a temperature difference did not exist.

The heating effect on the reaction solution, caused by compression when generating the required pressure, amounted to some 2-3°C. However, tests with a thermocouple probe showed that this extra heat was largely dissipated within 15-20 minutes, after which time the temperature had come to within 0.2° of the required temperature. Because the reaction times for this system were of the order of hours, this heating effect was not significant.

The pressure medium reservoir ensured that the oil which replaced the volume of an aliquot after sampling was already at the required temperature.

4.2.2 Materials

Cobalt-60 Tracer

Cobalt-60 was obtained in the form of a small metal slug from the Australian Atomic Energy Commission, Lucas Heights. The slug was dissolved in 7 M HNO_3 and from this stock solution more dilute solutions were obtained with a specific activity of about 0.8 mC $ml.^{-1}$. 1-2 drops of this tracer solution were sufficient to label the reactant solution to a reasonable level of activity. The concentration of tracer in the

reactant solution was of the order of 10^{-7} M, which was insignificant compared to the concentrations of the other species in solution.

Sodium Ethylenediaminetetraacetatocobaltate(III), $NaCo(EDTA).4H_2O$

$NaCo(EDTA).4H_2O$, where EDTA represents the hexadentate ligand ethylenediaminetetraacetate, was prepared according to the method of Dwyer, Gyarfas and Mellor,[77] except that sodium acetate was used so as to prepare the sodium salt rather than the potassium salt.

Cobalt(II) chloride hexahydrate (56 g.), sodium acetate (117 g.) and ethylenediaminetetraacetic acid (70 g.) were heated in water to nearly boiling and then 210 ml. of 3% hydrogen peroxide solution gradually added to the deep red solution. The salt was precipitated by the addition of alcohol to the cooled deep violet-red solution, collected on a Buchner funnel and washed with alcohol. The product was then recrystallised twice, and after washing with alcohol, dried for several hours in an oven at 80°C. The purity was checked by analysis for carbon, nitrogen and hydrogen. The analysis figures are given below.

Analysis for $NaCo(EDTA).4H_2O$	C	N	H
Calculated for $NaCo(EDTA).4H_2O$	27.2%	6.34%	4.56%
Found	27.3	6.55	5.12

Stock solutions of this salt were prepared by direct weighing and dissolving in water.

All $Co^{III}(EDTA)^-$ solutions were determined spectrophotometrically at the absorption maximum at 382 nm, where absorption by the Co(II) complex was negligible. The molar extinction coefficient, ε, for the $Co^{III}(EDTA)^-$ complex at 382 nm was found to have the value $\varepsilon = 219 \pm 1\ M^{-1}cm^{-1}$, obtained from a Beer's law plot, which was linear within the concentration range used (.001-.002 M). The standard solutions used for the Beer's law plot were made up by direct weighing of the K Co(EDTA).$2H_2O$ salt, which is well characterised.[77-81] The salt was obtained from Dr. G.H. Searle and had been prepared by the method of Dwyer et al.,[77] recrystallised three times, washed with alcohol and acetone then dried in air. The purity of the compound was checked by analysis for carbon, nitrogen and hydrogen and for water content. Duplicate C, N, H analyses were carried out and the results are given below. The water content was determined by heating duplicate weighed samples at 80°C under reduced pressure over P_2O_5.

Analysis for K Co(EDTA).$2H_2O$	C	N	H
Calculated for K Co(EDTA).$2H_2O$	28.4%	6.63%	3.81%
Found	28.3	6.50	3.96
	28.1	6.52	3.75

Loss of water calculated for K Co(EDTA).$2H_2O$	8.5%	Found	8.5%

Cobalt(II) Perchlorate

Cobalt(II) perchlorate was prepared by fuming A.R. grade

cobalt(II) chloride hexahydrate with concentrated A.R. perchloric acid until no test for chloride was given with silver nitrate. The salt was recrystallised twice from water.

A 0.1 M stock solution of $Co(ClO_4)_2$ in 5×10^{-3} M $HClO_4$ was prepared by direct weighing and standardised by electrodeposition of cobalt using platinum electrodes. Triplicate analyses agreed within $\pm$ 0.4%.

Disodium Ethylenediaminetetraacetate Dihydrate, $Na_2H_2EDTA.2H_2O$

A.R. grade $Na_2H_2EDTA.2H_2O$ was dried overnight at 80°C to remove any trace of moisture and then a 0.1 M stock solution was prepared by direct weighing.

Ethylenediaminetetraacetatocobalt(II)

The Co(II)-EDTA complex was prepared at the beginning of a run by mixing solutions of $Co(ClO_4)_2$ and Na_2H_2EDTA, when the complex formed immediately. The EDTA ligand was in 35% excess, and using the values[67] of the appropriate formation constants, at 20°C, for the various species in solution, it can be shown that at pH 2.0 more than 99% of the Co(II) was coordinated.

No accurate data is available for the formation constants at 85°C, but within experimental error the heats of formation for the protonated ligand and for the Co(II) complex are the same,[67] and so the Co(II)

will be more than 99% coordinated at 85°C also.

Sodium Perchlorate

Sodium perchlorate, obtained from G.F. Smith Company, was recrystallised from water three times, then dried overnight at 130°C. A 2M stock solution was then prepared by direct weighing of the anhydrous salt.

Purified Water

All stock solutions and reaction solutions were prepared using demineralised water which had been redistilled from alkaline potassium permanganate and acidified sodium dichromate solutions to remove all traces of organic impurity.

All other materials used were A.R. grade or reagent grade, depending on their use.

4.2.3 Procedure for Exchange Runs

The reactant solutions for the exchange runs were prepared by adding 10.0 ml. of 0.1 M $Co(ClO_4)_2$ solution to 10.0 ml. of 0.13 M Na_2H_2EDTA solution, thus forming the Co(II)-EDTA complex *in situ*. The EDTA concentration was in 35% excess over the Co(II) concentration to ensure virtually complete coordination of all the Co(II). To this

solution was added 20.0 ml. of $NaCo^{III}$(EDTA) solution and 10.0 ml. of 2 M $NaClO_4$ solution to adjust the ionic strength to 0.5 M. The solution was then labelled by adding 1-2 drops of ^{60}Co tracer in the form of cobalt(II) nitrate solution. Each reaction solution had a total activity of approximately 20 μC. The pH of the solution was then adjusted to pH 2.00 by the addition of a few drops of $HClO_4$ or NaOH solution. The volume increase that this represented was insignificant compared to the total volume of the solution and so concentrations were not affected. For the pressure runs, this reactant solution was then transferred to the reaction vessel and loaded in the pressure vessel. For the thermal runs, the reactant solution was placed in a stoppered glass conical flask which was then placed in the thermostatted bath. Tests showed (see section 4.3.3) that there was no significant surface catalysis, and that the rates in each type of reaction vessel were identical under similar conditions.

Unlike the cobalt-amine systems, this reaction is not oxygen-sensitive, and so the solutions could be freely handled in air. They did, however, have to be brought up to the higher temperature soon after adjusting the pH, otherwise some of the EDTA would precipitate due to its low solubility at pH 2 at room temperature.

Because the solutions had to be labelled before they were raised to 85°C, it was not possible to obtain a true zero-time sample. However, careful estimations indicated that if any zero-time exchange occurred

it did not exceed 2%.

At the completion of most of the runs, the pH of the reactant solution was checked and the optical absorbance was measured at 382 nm (the absorption maximum for the Co(III)-EDTA complex). It was found that, within the accuracy of reading ($\pm$ 0.01), the pH of the reactant solutions remained the same, and that the concentration of the Co(III) complex did not change by more than 1% in any run. This was contrary to the results of Adamson and Vorres,[61] who found that during the course of a run, the pH of the reactant solution rose as much as several tenths of a pH unit. They concluded that some decomposition had occurred and assumed that Co(II) was being formed although they had no direct evidence for its formation.

4.2.4 Sampling and Separation Procedures

Separation of the Co(II) and Co(III) was achieved by quenching a sample in acid, then passing the acidified solution through a cation exchange column to remove the cationic Co^{2+}_{aq}. The resin used was Zeo-carb 225 in the H-form. This is a cross-linked polystyrene sulphonic acid resin, and being a strongly acidic type resin, its exchange capacity is virtually independent of the pH of the solution.

Accurate 2.0 ml. aliquots were taken. For the runs where the set of individual pressure vessels were used, the vessel to be sampled was taken from the thermostatted bath and quickly placed on the pressure line.

The pressure was checked as described earlier, then the polypropylene reaction vessel removed and a 2.0 ml. aliquot withdrawn with a pipette. This whole operation took about four minutes. Because the reaction was slow and the time taken for sampling was virtually constant, no significant error was introduced here. When using the continuous sampling vessel, the first 1-1.5 ml. of solution (which contained the solution in the capillary outlet tubing) was discarded. A further 2.5 ml. of solution was discharged into a glass test-tube and the 2.0 ml. aliquot withdrawn by pipette. For the thermal runs carried out in the glass vessel, the aliquots were withdrawn directly from the reaction vessel.

The aliquot was then quenched by discharging into 3 ml. of 4 M perchloric acid, which had already been placed on top of the ion exchange column, together with some Co^{2+} carrier. The acid destroyed the labile Co(II) complex, while leaving the inert Co(III) complex intact. The liberated Co^{2+} was adsorbed on the column and the anionic Co(III) complex was washed through the column with 50 ml. of water. Its progress down the column could be followed visually because of its intense red-purple colour. When the Co(III) effluent had been collected, the Co(II) was eluted with conc. HCl. This formed the bright green cobalt tetrachloride, $CoCl_4^{2-}$, which being anionic could now be eluted from the column. The elution process was relatively slow, requiring about 2 hours and 100 ml. of conc. HCl before all the Co(II) had been

removed. Both the Co(II) and Co(III) fractions were collected in volumetric flasks so that their specific activities could be calculated. Tests with solutions containing Co^{2+}_{aq}, of known specific activity, and $Co^{III}(EDTA)^-$ indicated that better than 99% separation of the Co(II) and Co(III) was achieved by this ion-exchange method.

Although not necessary for calculating the fraction of exchange, accurate aliquots of the same volume were taken each time so that a check could be made on the efficiency of the separation and assay procedure, by comparing the total count obtained for each aliquot.

For activity determinations, 10.0 ml. aliquots of the separated Co(II) and Co(III) fractions were used each time.

Because the half-time for the exchange process was so long, it was impractical to determine experimentally the infinite time value for the specific activity of the Co(III), which was necessary for calculating F, the fraction of exchange. Instead this was calculated using the mass-balance equation, (4.1), which assumes a distribution of the ^{60}Co tracer between the two Co species proportional to their molar concentrations at infinite time. The mass-balance is given by

$$(a + b)x_\infty = ax_T \qquad (4.1)$$

where a and b represent the concentrations of Co(II) and Co(III) respectively, x_∞ the specific activity of the Co(III) at infinite time, and x_T the total specific activity of the solution.

Each kinetic run was followed for approximately $1\ ^{1}/_{2}$ half-times.

4.3 Results

4.3.1 Evaluation of Kinetic Data

The electron exchange reaction can be represented by the equation:

$$^{*}Co^{II}(EDTA) + Co^{III}(EDTA) \rightleftharpoons {}^{*}Co^{III}(EDTA) + Co^{II}(EDTA)$$

where $Co^{II}(EDTA)$ and $Co^{III}(EDTA)$ represent all forms of the EDTA complexes of Co(II) and Co(III). The rate of electron exchange, R, is given by the McKay equation, (1.1),

$$\text{i.e. } R = -\frac{2.303}{t}\,\frac{[Co^{II}][Co^{III}]}{[Co^{II}] + [Co^{III}]}\,\log(1 - F) \qquad (4.2)$$

$[Co^{II}]$ and $[Co^{III}]$ represent the total molar concentrations of Co(II) and Co(III) complex respectively.

For each kinetic run, the rate of exchange was obtained by plotting log (1 - F) against time. A typical exchange plot is shown in Figure 4.2. The second order rate constant, k, was calculated from the expression

$$k = \frac{0.693}{t_{1/2}}\,\frac{1}{[Co^{II}] + [Co^{III}]} \qquad (4.3)$$

where $t_{1/2}$ is the half-time for the exchange.

4.3.2 Order of Reaction

The electron exchange was shown to be described by the second order

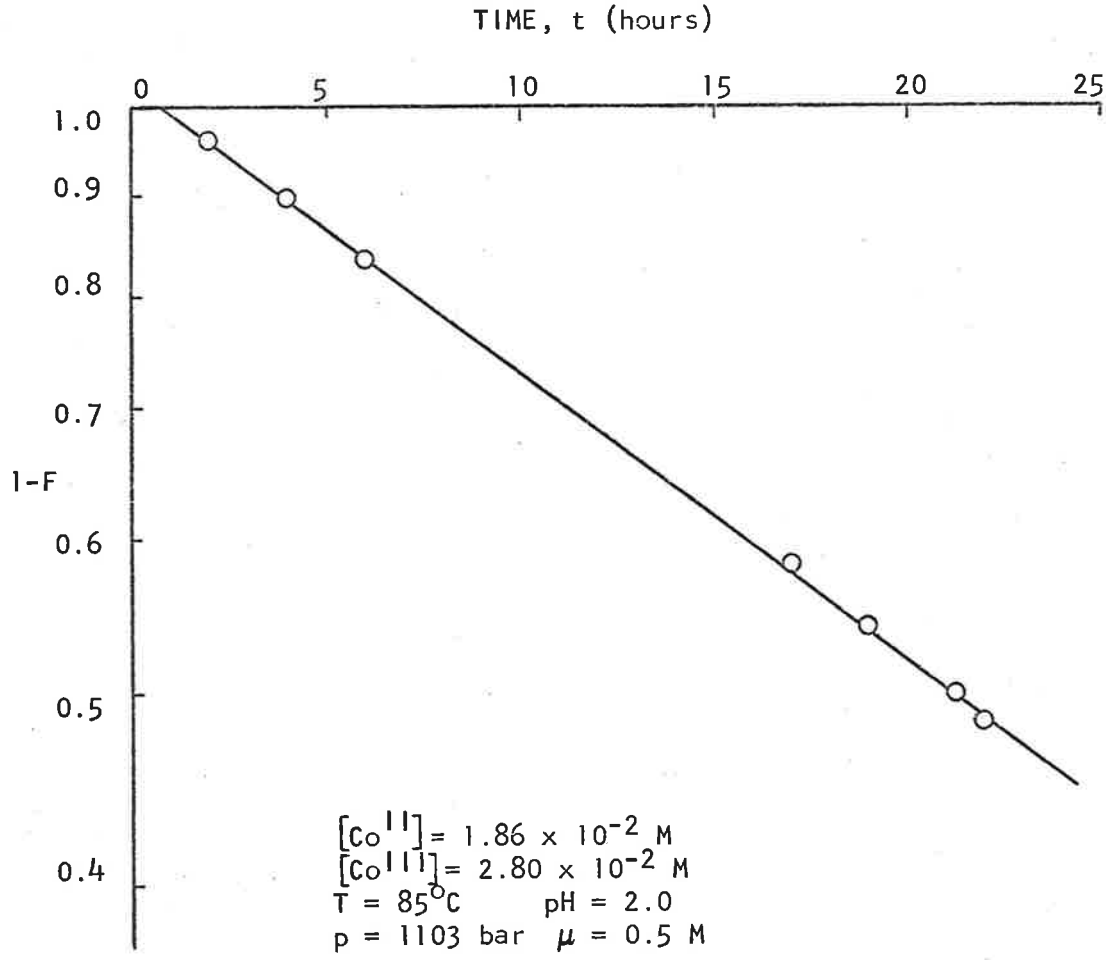

Figure 4.2 Typical Exchange Plot

rate law,

$$R = k[Co^{II}][Co^{III}], \qquad (4.4)$$

by the constancy of the second order rate constant, k, with varying concentrations of both reactants. This can be seen from the results given in Table 4.1.

Table 4.1

Constancy of Second Order Rate Constant, k, with Varying Reactant Concentrations

T = 80°C pH = 2.00

$[Co^{III}] \times 10^2$ M	$[Co^{II}] \times 10^2$ M	k (M^{-1} $hr.^{-1}$)	No. of Runs
2.88	2.23	.41	4
2.88	2.79	.39	1
3.00	1.86	.41	9
4.00	3.72	.39	1
		(S.D. = 0.03)	

In this Table the rate constants have been assigned an uncertainty of $\pm$.03 M^{-1} $hr.^{-1}$, which was the standard deviation of k calculated from the results of the set of nine identical runs.

The observation of second order kinetics is in agreement with the results reported in the previous studies[61,62] of this system.

4.3.3 Surface Catalysis

The results given below in Table 4.2 show that the rate of electron exchange was the same in both the Perspex vessels (used in pressure runs) and in glass vessels (used in thermal runs).

It is also seen from Table 4.2 that there was evidence for very slight surface catalysis of the exchange rate for a 50-fold increase in surface area. This result is consistent with the observation of Adamson and Vorres,[61] who reported a 6-fold increase in rate with a 2000-fold increase in surface area. However, this effect is small, as would be expected with an anionic system since silica adsorbs cations. The contribution from any surface exchange can be neglected for the purpose of this present study.

Table 4.2

Effect of Surface on Exchange Rate

$T = 80°C$ $pH = 2.00$

$[Co^{III}] = (2.88 - 4.00) \times 10^{-2} M$ $[Co^{II}] = (1.86 - 3.72) \times 10^{-2} M$

Nature of Surface	k (M^{-1} $hr.^{-1}$)	No. of Runs
Perspex	.41 ± .03	9
glass	.41 ± .02	6
glass (50 x surface area)	.53 ± .03	1

4.3.4 Effect of Pressure on the Electron Exchange Rate

A number of runs was carried out at atmospheric pressure to establish

the value of the rate constant at this pressure with a minimum of error. This value, together with those obtained for each of the other pressures studied, are given in Table 4.3.

All of the high pressure measurements were made in the range 1-2 kbar. Having made these measurements first, it was evident that there was no point in doing any runs in the range 0-1 kbar. This was because the effect of pressure on the exchange rate was small, and any acceleration of the rate by pressures less than 1 kbar would be of the same order of magnitude as the uncertainty in the rate measurements themselves. It was for this reason that a greater number of runs than usual was carried out at atmospheric pressure to determine this value accurately.

The uneven distribution of pressures was due largely to the fact that, when using the set of individual pressure vessels, the pressure developed at 85°C, after pressurizing the vessel at room temperature, could not be determined accurately beforehand, as explained in Chapter 3.

The value obtained for k at 1 bar, $0.64 \pm .03$ M^{-1} $hr.^{-1}$, agrees fairly well with the values of 0.75 M^{-1} $hr.^{-1}$ and 0.55 M^{-1} $hr.^{-1}$, reported by the previous workers[61,62] for the same conditions of temperature and pH.

Table 4.3

Effect of Pressure on Electron Exchange Rate

T = 85°C pH = 2.00 μ = 0.5 M

$[Co^{III}] = 2.88 \times 10^{-2} M$ $[Co^{II}] = 1.86 \times 10^{-2} M$

p (bar)	k (M^{-1} $hr.^{-1}$)	No. of Runs
1	.64	9
1103	.72	2
1585	.73	1
1722	.78	2
1861	.78	1
2070	.80	2
2280	.82	4

(S.D. = 0.03)

The values of k in Table 4.3 have been assigned an uncertainty of $\pm$ 0.03 M^{-1} $hr.^{-1}$, which is the standard deviation calculated from the sets of 9 runs and 4 runs under identical conditions.

The pressure dependence of the electron exchange rate is shown in Figure 4.3, where the values from Table 4.3 are plotted as log k against pressure.

Because the effect of pressure on the rate of exchange was small, no curvature is evident in this plot, and the straight line of best fit, calculated by the "least squares" procedure, was taken to best represent the experimental data. This line of best fit is shown in

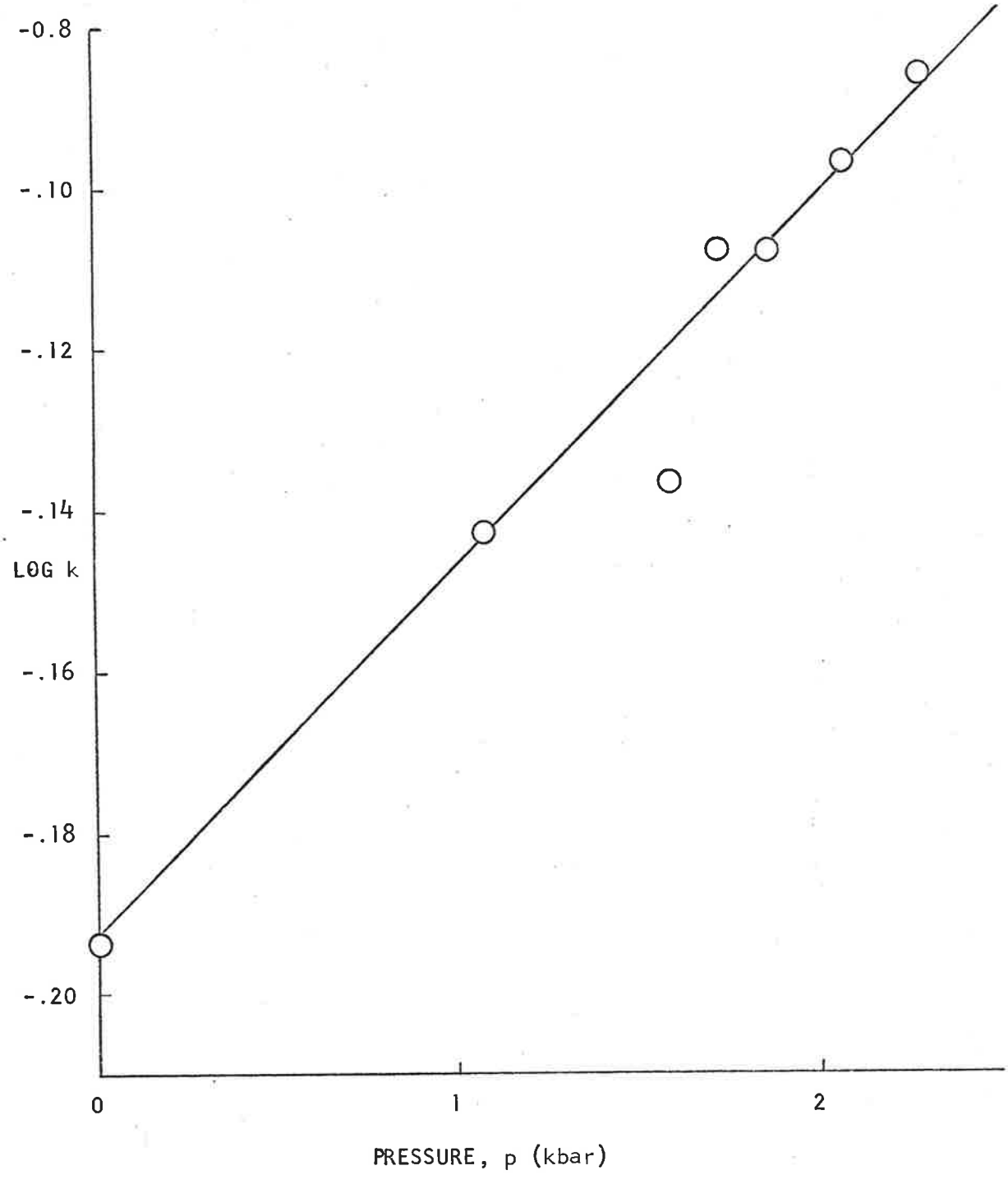

Figure 4.3 Pressure Dependence of Electron Exchange Rate

Figure 4.3. The volume of activation was calculated from the slope of this line, using equation (2.20). Using the value[76] $\beta = 4.65 \times 10^{-5}$ bar^{-1} for the isothermal compressibility of water at 85°C, the term $RT\beta$ amounts to 1.38 c.c. $mole^{-1}$. The standard error of the slope of the line of best fit, calculated by the method of least squares, leads to an uncertainty of $\pm$ 0.22 c.c. $mole^{-1}$ in the measured value of $\Delta V^{\ddagger}$. A more realistic estimate of the uncertainty would be $\pm$ 0.5 c.c. $mole^{-1}$, largely because of the assumption of linear dependence of log k on the pressure. Hence, for the electron exchange between Co(II)-EDTA and Co(III)-EDTA at 85°C in aqueous solution of pH 2.0 and ionic strength 0.5 M, the volume of activation, $\Delta V^{\ddagger}$, corrected for the term $RT\beta$, was found to be -4.5 ± 0.5 c.c. $mole^{-1}$.

4.4 Discussion

4.4.1 Nature of the Exchanging Species

Because at pH 2.0 the Co(II) and Co(III) complexes exist as equilibrium mixtures of the pentadentate and hexadentate forms, electron exchange could proceed by any of the following pathways:

$$\overset{*}{Co}^{II}(EDTA)^{2-} + Co^{III}(EDTA)^{-} \rightleftarrows \overset{*}{Co}^{III}(EDTA)^{-} + Co^{II}(EDTA)^{2-} \quad (A)$$

$$\overset{*}{Co}^{II}(HEDTA)H_2O^{-} + Co^{III}(EDTA)^{-} \rightleftarrows \overset{*}{Co}^{III}(EDTA)^{-} + Co^{II}(HEDTA)H_2O^{-} \quad (B)$$

$$\overset{*}{Co}^{II}(EDTA)^{2-} + Co^{III}(HEDTA)H_2O \rightleftarrows \overset{*}{Co}^{III}(HEDTA)H_2O + Co^{II}(EDTA)^{2-} \quad (C)$$

$$\overset{*}{Co}^{II}(HEDTA)H_2O^{-} + Co^{III}(HEDTA)H_2O \rightleftarrows \overset{*}{Co}^{III}(HEDTA)H_2O + Co^{II}(HEDTA)H_2O^{-} \quad (D)$$

Equations (B) and (C) imply that the rate of electron exchange is slow compared with the rate of equilibration between pentadentate and hexadentate Co(III). From Higginson's data,[75b] using the values of 23.4 kcal. mole^{-1} and 25.6 kcal. mole^{-1} for the activation energies of the forward and backward reactions for this equilibration, it can be shown that at 85°C the half-time for pentadentate-hexadentate equilibration is of the order of 10^{-2} min.; this is very fast compared with the electron exchange rate.

The extent of the contribution of any one of these pathways to the overall rate of exchange will be determined by the relative proportions of each species and their relative rates of exchange.

For the Co(III) complex, the equilibrium constant at 85°C for the hexadentate-pentadentate equilibrium can be estimated from Higginson's data,[75b] assuming ΔH = 2.22 kcal. mole^{-1}, to be 0.64 $\pm$ 0.2 M^{-1}. This equilibrium constant has a pressure dependence, which has been measured at 25°C (see section 4.7.3 below). If we assume only a negligible temperature dependence of $\Delta V^{\neq}$, the equilibrium constant at 85°C and 2 kbar is estimated to be 0.83 $\pm$ .08 M^{-1}. Hence, in solutions of pH 2.0, it can be shown that > 99% of the Co(III) complex will exist as the hexadentate, unprotonated form, $Co^{III}(EDTA)^-$.

The pK_a for the protonated Co(II) complex at 85°C can be estimated from the data of Im and Busch[62] to be 2.9 $\pm$ 0.1. The pressure dependence of this equilibrium is not known, but if it is assumed to be the same as for the Co(III) complex, then the pK_a for $Co^{II}(HEDTA)^-$ can be estimated as 3.0 $\pm$ 0.1 at 2 kbar and 85°C. Hence, at pH 2.0 the Co(II) complex will exist as a mixture of 89-91% in the protonated form and 9-11% in the unprotonated form at pressures between 0 and 2 kbar.

From a study of the pH dependence of the exchange rate, Im and Busch[62] have calculated the rate constants for the paths involving the protonated Co(II) (equation B) and the unprotonated Co(II) (equation A). From their data it can be estimated that at 85°C the rate of exchange via the protonated form of Co(II) is about 4 times faster than for the unprotonated form. This can be seen qualitatively from Figure 4.1.

The relative contributions, then, to the overall rate of exchange from each pathway can be calculated to be as follows:

Pathway A: 2.7%

Pathway B: 97.3%

Pathway C: negligible

Pathway D: negligible

Thus, it is evident that the measured volume of activation refers to the process described by pathway B, given above, i.e.

$$\overset{*}{Co}^{II}(HEDTA)H_2O^- + Co^{III}(EDTA)^- \rightleftarrows \overset{*}{Co}^{III}(EDTA)^- + Co^{II}(HEDTA)H_2O^-$$

4.4.2 Comparison of Measured and Predicted $\Delta V^{\ddagger}$ Values

The measured value of $\Delta V^{\ddagger}$ can be compared to that calculated from the Marcus-Hush theory, in the manner described in Chapter 2. The contributions to $\Delta V^{\ddagger}$, calculated from equation (2.26), are made up in the following way:

$$\Delta V^{\ddagger}_{calc} = \Delta V^{\ddagger}_{coulombic} + \Delta V^{\ddagger}_{solvent\ rearr.}$$

where

$$\Delta V^{\ddagger}_{coulombic} = \frac{NZ_1Z_2e^2}{\sigma} \frac{\partial}{\partial p}\left(\frac{1}{\varepsilon}\right)_T \qquad (4.5)$$

$$\Delta V^{\ddagger}_{solvent\ rearr.} = \frac{Ne^2}{4}\left\{\frac{1}{2r_1} + \frac{1}{2r_2} - \frac{1}{\sigma}\right\}\left\{\frac{\partial}{\partial p}\left(\frac{1}{\varepsilon_o}\right)_T - \frac{\partial}{\partial p}\left(\frac{1}{\varepsilon}\right)_T\right\} \qquad (4.6)$$

N is Avogadro's number, introduced to bring these quantities to the molar scale, since equation (2.26) refers to the volume change per molecule. Assuming the close-contact outer-sphere model, the values of r_1, r_2 and σ may be estimated from the crystal radii of Co(II) and Co(III) and from the Van der Waal's radii of the ligand atoms. For the Co(II) complex this gives an effective radius, r_1, of 4.13 Å and for the Co(III) complex a value for r_2 of 3.98 Å. Hence, σ, the internuclear distance in the transition state, can be put equal to 8.1 Å. For solvent water, the term $(\partial(1/\varepsilon)/\partial p)_T$ may be calculated as -1.049×10^{-6} bar^{-1} at 85°C, assuming that $\partial\varepsilon/\partial p$ is independent of temperature and using the values $\partial \ln \varepsilon/\partial p = (1/\varepsilon)(\partial\varepsilon/\partial p) = 4.71 \times 10^{-5}$ bar^{-1} at 25°C,[6] and $\varepsilon = 59.37$ at 85°C.[76] The term $\partial(1/\varepsilon_o)/\partial p$ is taken to have the value -1.20×10^{-5} bar^{-1}, calculated from the data of Owen and Brinkley[82] at 25°C. Hence, from equations (4.5) and (4.6), we obtain the following values:

$$\Delta V^{\ddagger}_{\text{coulombic}} = -1.80 \text{ c.c. mole}^{-1}$$

$$\Delta V^{\ddagger}_{\text{solvent rearr.}} = -4.88 \text{ c.c. mole}^{-1}$$

To these terms must be added a further term, $\Delta V^{\ddagger}_{\text{D.H.}}$, to correct for finite ionic strength effects. These are probably most satisfactorily described by the modified Debye-Hückel equation for a second order reaction:

$$\ln k_\mu = \ln k_o + \frac{2Z_1 Z_2 A\sqrt{\mu}}{1 + Ba\sqrt{\mu}} + 2C\mu \qquad (4.7)$$

where k_o and k_μ are respectively the rate constants at ionic strengths zero and μ. A and B are parameters given by expressions involving fundamental constants and the dielectric constant of the medium and the absolute temperature. The linear term $C\mu$ is added to improve this theoretical expression in describing sets of experimental data. The parameter C is often expressed as $C = 0.1|Z_1Z_2|\mu$. The parameter a is the estimated encounter distance for the two ions.

On differentiating equation (4.7) with respect to pressure, we obtain

$$\left(\frac{\partial RT \ln k_\mu}{\partial p}\right)_T = \left(\frac{\partial RT \ln k_o}{\partial p}\right)_T + \left(\frac{\partial RT \ln \Phi}{\partial p}\right)_T \qquad (4.8)$$

$$\text{i.e.} \quad -\Delta V^{\neq} = -\Delta V_o^{\neq} + RT(\partial \ln \Phi/\partial p)_T \qquad (4.9)$$

where Φ is the function describing the ionic interaction. The term $RT(\partial \ln \Phi/\partial p)_T$ is thus the correction, $\Delta V^{\neq}_{D.H.}$, arising from finite ionic strengths, to be made to the calculated value of $\Delta V^{\neq}$.

The calculated value of $\Delta V^{\neq}$ to be compared to the measured $\Delta V^{\neq}$, is then given by

$$\Delta V^{\neq}_{calc} = \Delta V^{\neq}_{coulombic} + \Delta V^{\neq}_{solvent\ rearr.} - \Delta V^{\neq}_{D.H.} \qquad (4.10)$$

The explicit expression for the term $\Delta V^{\neq}_{D.H.} = RT(\partial \ln \Phi/\partial p)_T$ is obtained as:

$$\Delta V^{\ddagger}_{D.H.} = RT\, Z_1 Z_2 \{\frac{A\sqrt{\mu}}{1 + Ba\sqrt{\mu}} (\frac{3}{\varepsilon}\frac{\partial \varepsilon}{\partial p} - \beta)$$

$$- \frac{ABa\mu}{(1 + Ba\sqrt{\mu})^2} (\frac{1}{\varepsilon}\frac{\partial \varepsilon}{\partial p} - \beta - \frac{2\partial \ln a}{\partial p}) + 0.2\mu\beta\} \qquad (4.11)$$

For $Z_1 = Z_2 = -1$, $\mu = 0.5$ and putting $\underline{a} = 4$ Å and using the values[53] $A = 0.5842\ M^{-1/2} deg.^{3/2}$, $B = 0.3440 \times 10^8\ cm.^{-1} M^{-1/2} deg.^{1/2}$ and $\beta = 4.65 \times 10^{-5}\ bar^{-1}$ (the isothermal compressibility of water at 85°C),[76] we obtain from equation (4.11),

$$\Delta V^{\ddagger}_{D.H.} = 0.96 \text{ c.c. mole}^{-1}.$$

Thus, the volume of activation calculated for comparison with the measured value is, from equation (4.10),

$$\Delta V^{\ddagger}_{calc} = -1.80 - 4.88 - 0.96 = -7.64 \text{ c.c. mole}^{-1}.$$

The measured volume of activation, $\Delta V^{\ddagger}_{meas} = -4.5 \pm 0.5$ c.c. mole^{-1}. There is thus a difference of approximately 3 c.c. mole^{-1} between the measured and the predicted values.

In estimating the calculated value of $\Delta V^{\ddagger}$, there are several sources of uncertainty. Built into the Marcus-Hush theory are several simplifying assumptions. The main assumptions are that the ions are spherical and that the solvent is a continuous dielectric and the dielectric properties do not change down to the closest distance of approach, σ. These assumptions could lead to errors in the values

calculated by the theory to represent the real situation. However, inasmuch as these assumptions are part of the theory, the comparison of calculated and experimental values will measure their validity.

More specific sources of error arise from the values of the quantities used in the calculations. For lack of data, the properties of the solution are taken to be those of pure water. From a comparison of the value of the compression of water, calculated from the data of Bridgman,[83] with that of 0.5 M $NaClO_4$ solution, determined by Swaddle,[84] it can be shown that the difference in compressibility may be only 2% greater for 0.5 M $NaClO_4$ solution than for water. Hence, using the value of the compressibility, β, of pure water would not lead to a significant error.

The estimation of the quantity $(1/\varepsilon)(\partial\varepsilon/\partial p)$ is less certain. Again the value for pure water is used, and although values of $1/\varepsilon$ at different temperatures are known, the term $\partial\varepsilon/\partial p$ at different temperatures is not. However, recent experiments by Franck[85] indicate that, at least up to about 200°C, $\partial\varepsilon/\partial p$ is virtually independent of temperature, so the value of $\partial\varepsilon/\partial p$ at 25°C can be used for the higher temperatures, without introducing significant error. Whether the value of the term $(1/\varepsilon)(\partial\varepsilon/\partial p)$ is the same for a mixed electrolyte solution of ionic strength 0.5 M as for pure water is not known, and not even the sign of $\partial\varepsilon/\partial p$ for an electrolyte solution is known. It has been assumed here that there is not a significant difference between the two. A more

serious uncertainty arises in the term $(\partial(1/\varepsilon_o)/\partial p)_T$. It is not possible to estimate this term at 85°C, since no data is available. Its value at 25°C can be calculated from the data of Owen and Brinkley[82] and this value was used, together with the value for $(\partial(1/\varepsilon)/\partial p)_T$ at 25°C, to calculate the term $\{(\partial(1/\varepsilon_o)/\partial p)_T - (\partial(1/\varepsilon)/\partial p)_T\}$ in equation (4.6) for $\Delta V^{\ddagger}_{\text{solvent rearr.}}$. This was done in the hope that the temperature dependence of $\partial(1/\varepsilon_o)/\partial p$ is similar to that of $\partial(1/\varepsilon)/\partial p$, so that the difference in these two terms would be the same at 85°C as at 25°C.

The uncertainty in the value of σ arises from the possible uncertainties in the Van der Waal's radii of the ligand atoms. If the uncertainties in the radii of the two ions are 0.1 Å, and hence 0.2 Å for σ, this will lead to an uncertainty of $\pm$ 0.16 c.c. mole^{-1} in $\Delta V^{\ddagger}$.

If the compressibility of the ions is taken into account, the term representing the internal rearrangement of the ions in the equation for $\Delta G^{\ddagger}$, (1.15), leads to an additional term in the expression for $\Delta V^{\ddagger}$. It has been estimated[86] that for +2, +3 transition metal ions, this additional term will contribute about 0.4 c.c. mole^{-1} to $\Delta V^{\ddagger}$.

For the sources of error in the calculations, just described, the corrections, wherever an estimate could be made, would tend to reduce the difference between the calculated and measured values of $\Delta V^{\ddagger}$.

Also, in estimating the measured value of $\Delta V^{\ddagger}$, a linear dependence of ln k on pressure was assumed. If $\Delta V^{\ddagger}$ were itself pressure

dependent, as is generally to be expected, then the line of best fit used to represent the data in Figure 4.2 would be concave downwards. This would result in a greater value of the initial slope and hence a larger value of $|\Delta V^{\ddagger}|$, which would adjust the measured $\Delta V^{\ddagger}$ in the direction of the calculated $\Delta V^{\ddagger}$.

If there were a small contribution to the observed rate of exchange from a pathway involving an inner-sphere activated complex, this would further reduce the small difference between the calculated value and measured value of $\Delta V^{\ddagger}$ for an outer-sphere mechanism. This is because the inner-sphere mechanism would be expected to contribute a positive term to the measured value of $\Delta V^{\ddagger}$, and hence the measured value of $\Delta V^{\ddagger}$ which is to be compared with the calculated value would be more negative than that reported. It is possible that such a pathway, albeit minor, does exist, owing to the labile nature of the Co(II) complex.

4.4.3 Possibility of an Inner-Sphere Mechanism

Because of the equilibria between the pentadentate and hexadentate forms of the two reactant ions, the group in the sixth coordination position is apparently moderately labile. Hence we can consider the possibility of a bridged, inner-sphere activated complex being involved in the predominant pathway for exchange. Presumably this would involve the expulsion of the water molecule from the first coordination shell

of one of the ions and bridging by a carboxylate group from the other ion.

Im and Busch,[62] as a result of their extensive studies of this reaction (especially the isotope-effect experiments in D_2O) discounted any mechanism involving either direct bridging between the metal ions, bridging by hydrogen atoms, or hydrogen atom transfer. They proposed an outer-sphere activated complex, with a hydrogen ion symmetrically disposed between the two complex ions, serving merely to reduce electrostatic interactions between the reactants. This model is consistent with the results obtained in these studies.

Furthermore, we might expect that the individual contributions to the value of $\Delta V^{\ddagger}$ from the coulombic, solvent rearrangement and Debye-Hückel terms would not differ greatly in the inner-sphere case from those calculated above for the outer-sphere case. However, there would be an additional contribution resulting from the expulsion of the water ligand from the first coordination shell of the ion into the solvent. In the limit, this would amount to +18 c.c. $mole^{-1}$, the partial molar volume of water, and the actual value would be expected to be close to this figure. The overall value of $\Delta V^{\ddagger}$, then, for an inner-sphere mechanism would be expected to be distinctly positive (in the limit, approximately -8 + 18 = +10 c.c. $mole^{-1}$). This is not observed. The measured value of $\Delta V^{\ddagger}$ is, however, close to that predicted for an outer-sphere mechanism. Hence, from this and the more

extensive chemical evidence, this reaction would appear to involve an outer-sphere activated complex.

4.4.4 Conclusion

The $Co^{II}(EDTA)$ - $Co^{III}(EDTA)$ electron exchange has been chosen as a reaction believed to proceed by an outer-sphere mechanism. The pressure dependence of this reaction has been measured, yielding the value $\Delta V^{\ddagger} = -4.5 \pm 0.5$ c.c. $mole^{-1}$. The Marcus-Hush theory, which assumes an outer-sphere mechanism, has been used to calculate a predicted value of $\Delta V^{\ddagger}$. Bearing in mind the uncertainties in the values used for the various quantities in these calculations, the calculated value of -7.6 c.c. $mole^{-1}$ agrees fairly well with the measured value. This apparent agreement is an indication of the degree of adequacy of the Marcus-Hush theory in providing a description of the outer-sphere mechanism for electron transfer in solution.

B. Effect of Pressure on the $Co^{III}(EDTA)^-$ - $Co^{III}(HEDTA)H_2O$ Equilibrium

4.5 Introduction

As mentioned in the introduction to this Chapter, the kinetics and equilibria existing between the various Co(III)-EDTA species in aqueous solution have been studied by Higginson.[75] He found that in solutions of pH < 2.5, the equilibrium between the hexadentate and pentadentate forms,

$$Co(EDTA)^- + H^+ + H_2O \rightleftarrows Co(HEDTA)H_2O \qquad K \approx 1$$

was established slowly.

Since this reaction is relatively slow and the extinction curves[75] for the pentadentate and hexadentate forms are different enough to provide a convenient means of following the reaction, an investigation of the pressure dependence of the equilibrium was undertaken.

To evaluate the pressure dependence of the forward and back reactions, it was necessary also to determine the effect of pressure on the position of equilibrium.

The rate of approach to equilibrium, and the shift in equilibrium position, were studied at 25°C in 1.00 M perchloric acid at pressures between 0 and 2 kbar.

4.6 Experimental

4.6.1 Apparatus

Pressure Vessel

These studies were conducted in the optical pressure vessel, described in Chapter 3.

Spectrophotometer

The pressure vessel was mounted inside the cell compartment of a Unicam S.P.800 Spectrophotometer. This is a double beam instrument, in which the beam is switched alternately through the sample and reference cells 25 times per second. The pressure vessel was aligned in the sample beam while the reference beam was left clear.

Absolute values of optical absorbance could not be measured; however, for the present work this was not important since only changes in optical absorbance needed to be measured. The optical path length of the reactant solution was approximately 1 cm. but it was not accurately known, and the pressure vessel, with only water in the reaction cell, had a "background" optical absorbance of about 0.7. This was mainly due to loss of light from the sample beam resulting from the small aperture (1/4" diameter) of the pressure vessel windows compared to the cross-section area of the reference beam, all of which was transmitted. These factors remained constant, though, throughout a run, and so changes in optical absorbance of the reaction solution with time could be measured accurately.

The normal full-scale range for the instrument was 0-2 optical absorbance units, but it was equipped with an S.P.850 Scale Expansion Accessory, which provided an electrical signal suitable for driving a potentiometric slave recorder. Since the total change in absorbance for a run was never more than 0.07, the scale was expanded by factors of 10 or 20, depending on the total change in absorbance.

For the accurate measurement of the absolute values of absorbances of equilibrium solutions, the Shimadzu manual spectrophotometer was used.

Temperature Control

The reaction vessel was thermostatted by the rapid circulation of constant temperature water through the casing of the pressure vessel. By the use of a calibrated thermistor it was shown that the temperature of the reactant solution was held within $\pm$ 0.1°C of the required temperature. The reservoir of water was contained in a thermostatted tank, maintained at the desired temperature by a solid-state proportional control heater.

Tests showed that the heat generated when raising the pressure on the reactant solution (causing temperature rises up to 2°C) was effectively dissipated within 3-4 minutes. The first readings were not taken until several minutes after pressurizing the solution, so this heating effect was not important.

4.6.2 Materials

Sodium ethylenediaminetetraacetatocobaltate(III), $NaCo(EDTA).4H_2O$

The $NaCo(EDTA).4H_2O$ salt used for these studies was the same as was used for the electron exchange studies, and has been described in section 4.2.2.

Perchloric Acid

1 M $HClO_4$ was prepared from conc. Analar $HClO_4$ by dilution with doubly-distilled water, and standardised against A.R. mercuric oxide and potassium iodide.

4.6.3 Procedure for Equilibrium Measurements

To determine the effect of pressure on the position of equilibrium between the pentadentate and hexadentate forms of the Co(III) complex, a weighed amount of the $NaCo(EDTA).4H_2O$ salt was dissolved in 1.0 M $HClO_4$. This solution was then divided, half being allowed to stand overnight at 25°C at atmospheric pressure, and half being kept at a pressure of 1.8 kbar at 25°C. The high pressure sampling vessel was used for this purpose. When these solutions had equilibrated after several hours, their optical absorbances were measured at 500 nm, where the greatest difference occurs in the extinction coefficients of the two species, $Co^{III}(EDTA)^-$ and $Co^{III}(HEDTA)H_2O$. Since the rate of attainment of equilibrium was slow at 25°C ($t_{1/2}$ = 22 min.), the solution which was under pressure could be withdrawn and quickly

measured, without any appreciable change in composition.

4.6.4 Procedure for Kinetic Runs

To initiate a run, a weighed amount of the salt, $NaCo(EDTA).4H_2O$, which contained Co(III) in the hexadentate form, was dissolved in 1 M $HClO_4$ inside the reaction cell. The acid had previously been equilibrated to 25°C. The cap was put on the cell, and then the cell quickly placed in the pressure vessel and the pressure raised to the required value. As the pressure was increased some distortion of the sapphire windows apparently occurred. It was found that it took about 5 minutes before steady optical readings could be obtained. The first readings for a run were always taken 7-10 minutes after the reaction solution had been placed in the pressure vessel and subjected to pressure.

The runs were followed by recording on a slave recorder the change with time in optical absorbance of the solution at 500 nm, using the Scale Expansion Accessory with the spectrophotometer.

4.7 Results

4.7.1 Evaluation of Kinetic Data

Plots of log $(D_t - D_\infty)$ against time, where D_t and D_∞ are the observed optical absorbances of the solution at times t and infinity respectively, were linear. Hence, the reaction was first order, or pseudo first order, since the Co(III) concentration was about 1.5×10^{-3} M in each run and the acid concentration was 1 M. This observation was in agreement with the results of Higginson,[75] who reported first order kinetics.

Since neither a zero-time nor infinite-time reading could be readily obtained, a run was followed for 4 to 5 half-times and the rate constant was found using the Guggenheim method.[26] Values of log $(D_t - D'_t$ were plotted against time, where D_t and D'_t were optical absorbances of the solution at times t and $t + \Delta$ respectively, Δ being a constant time increment equal to about 2 or 3 half-times of the reaction. The slope of this plot was then equal to $-k_{obs}/2.303$, the observed rate constant. A typical recorder trace of a kinetic run and the corresponding Guggenheim plot are shown in Figures 4.4(a) and 4.4(b).

4.7.2 Accuracy of Results

The accuracy of the results was severely limited by the small changes in optical absorbance of the solution. The total change for a run was never more than 0.07, and sometimes only half that value.

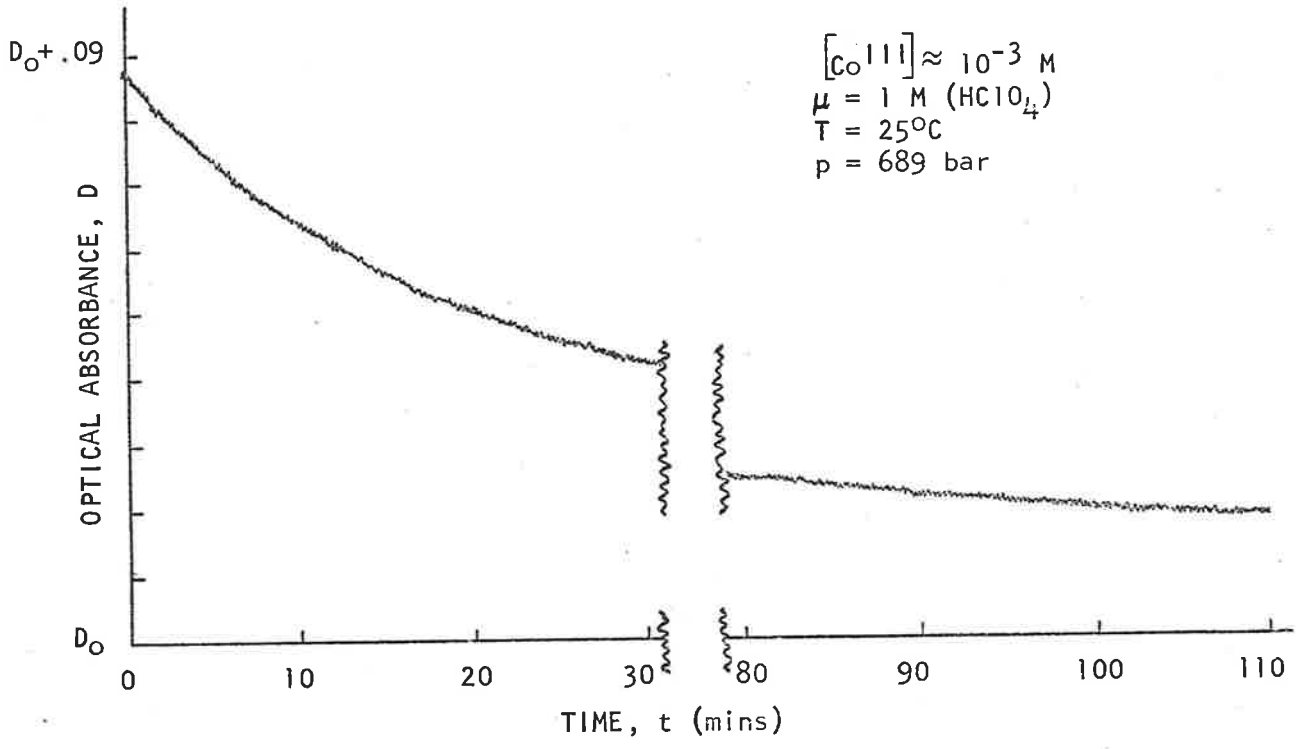

Figure 4.4(a) Typical Recorder Trace of a Kinetic Run

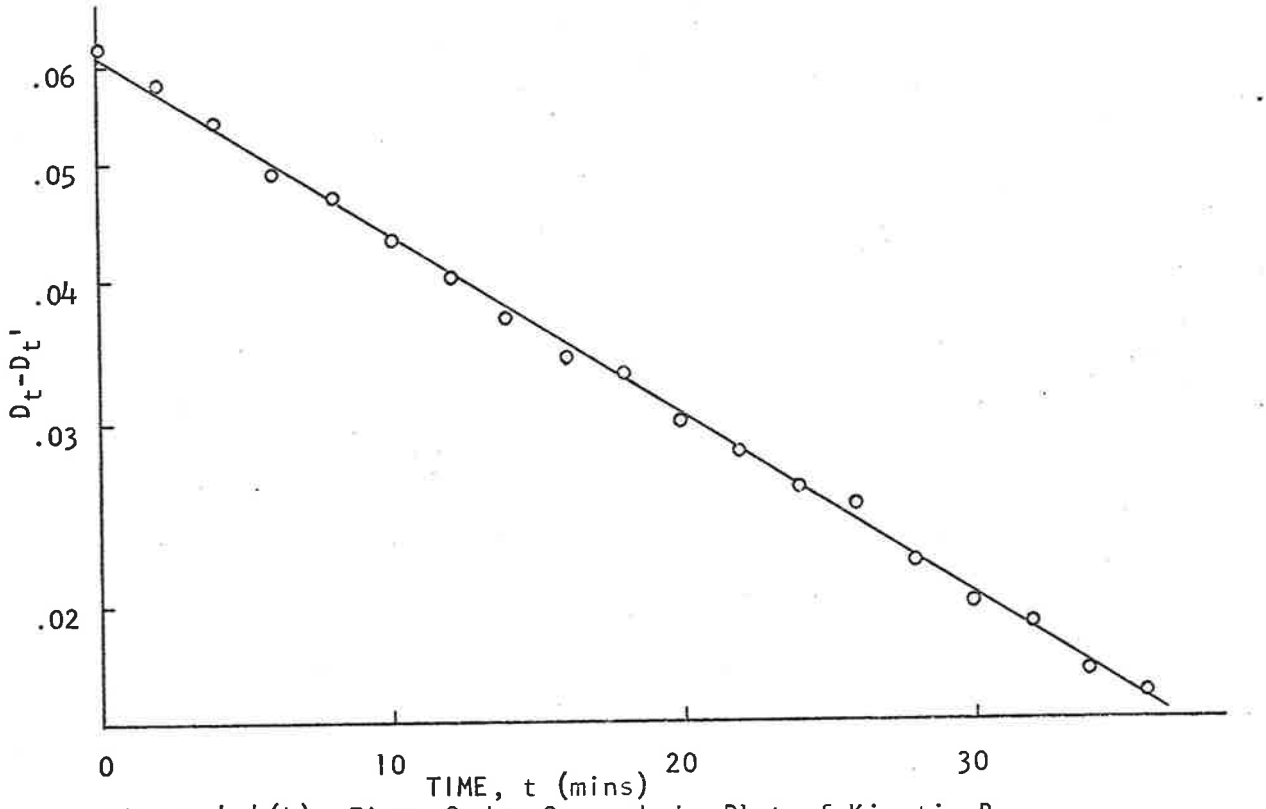

Figure 4.4(b) First Order Guggenheim Plot of Kinetic Run

The readings were recorded using a scale expansion factor of either 10 or 20, and the increased sensitivity required was accompanied by more "noise" in the instrument, which introduced greater uncertainty in the readings. Moreover, the runs were followed for a period of 100 to 120 minutes. Slight drifts in the recording instruments were bound to occur over this length of time, again adding to the uncertainty of the readings. Nevertheless, despite these difficulties, the accuracy of the readings was sufficient to obtain reproducible results, to the degree of accuracy reported in Table 4.4.

4.7.3 Pressure Dependence of the Rate of Attainment of Equilibrium

The rate constant, k_{obs}, for attainment of equilibrium for the reaction,

$$Co^{III}(EDTA)^{-} + H^{+} + H_2O \underset{k_b}{\overset{k_f}{\rightleftarrows}} Co(HEDTA)H_2O,$$

where k_f and k_b are the rate constants for the forward and back reactions, was determined at four different pressures. Because of the inherent inaccuracies involved in the measurements, 8 to 9 individual runs were conducted at each pressure. The results obtained are given in Table 4.4. The uncertainties quoted for the values of k_{obs} are the standard deviations for the set of runs at each pressure.

Table 4.4

Variation of Observed Rate Constant, k_{obs}, with Pressure

$[Co(EDTA)^-]_{t=0} \simeq 1.5 \times 10^{-3}$ M pH = 0 (1 M $HClO_4$)

T = 25°C μ = 1 M

p (bar)	$k_{obs} \times 10^2$ (min.$^{-1}$)	No. of Runs
1	3.17 ± .18	9
689	2.99 ± .31	9
1379	2.43 ± .19	8
2068	2.17 ± .34	9

The value for k_{obs} at 1 bar is in precise agreement with the value obtained by Higginson[75b] under the same reaction conditions, $(3.17 \pm .07) \times 10^{-2}$ min.$^{-1}$.

The measured rate constant, k_{obs}, can be written in terms of the rate constants for the forward and back reactions, i.e.,

$$k_{obs} = k_f + k_b. \qquad (4.12)$$

Also, the equilibrium constant, K, which is given by

$$K = \frac{[Co(HEDTA)H_2O]}{[Co(EDTA)^-][H^+]}, \qquad (4.13)$$

can be written in terms of k_f and k_b:

$$K = k_f/k_b \qquad (4.14)$$

To obtain the values of k_f and k_b at each pressure, it was therefore necessary to know the variation of K with pressure.

At 1.8 kbar, the optical absorbance of the equilibrated solution was found to decrease by (3.14 $\pm$ 0.5)%. Taking the literature values[75b] of the molar extinction coefficients, ε, of each species at 500 nm, i.e. ε($Co(EDTA)^-$) = 235 M^{-1} $cm.^{-1}$ and ε($Co(HEDTA)H_2O$) = 134 M^{-1} $cm.^{-1}$ and the value of K = 1.28 at 25°C, the equilibrium constant at 1.8 kbar and 25°C was found to have the value, K = 1.62 $\pm$ 0.17 M^{-1}.

Since there was only a very small shift in equilibrium with pressure, resulting in changes in absorbances of the solutions of only about .007, measurements were made at only the one high pressure (1.8 kbar) and a linear dependence of log K on pressure was assumed. The values of K, calculated assuming this linear relationship, for the pressures at which the rate measurements were made are given in Table 4.5, together with the corresponding values of k_f and k_b, calculated using equations (4.12) and (4.14).

Table 4.5

Variation of K, k_f and k_b with Pressure

T = 25°C μ = 1 M ($HClO_4$)

p (bar)	K (M^{-1})	$k_f \times 10^2$ ($min.^{-1}$)	$k_b \times 10^2$ ($min.^{-1}$)
1	1.28	1.78 ± .18	1.39 ± .12
689	1.40	1.74 ± .24	1.25 ± .16
1379	1.54	1.47 ± .18	0.96 ± .11
2068	1.68	1.36 ± .26	0.81 ± .15
	(± 11%)		

The variations of k_f and k_b are shown in Figures 4.5 and 4.6, where log k_f and log k_b have been plotted against pressure. Because of the small dependences on pressure, resulting in the uncertainties in the measurements being of the same order of magnitude as the changes being measured, the straight line of best fit has been drawn through the experimental data. Values of $\Delta V^{\neq}$ have been calculated from the slopes of these lines, using equation (2.20). The volumes of activation, corrected for the term in $RT\beta$, for the forward and back reaction of the equilibrium between hexadentate and protonated pentadentate Co(III)-EDTA at 25°C were found to be

$$\Delta V^{\neq} (k_f) = 1.5 \pm 2 \text{ c.c. mole}^{-1}$$

$$\Delta V^{\neq} (k_b) = 6.6 \pm 1.5 \text{ c.c. mole}^{-1}.$$

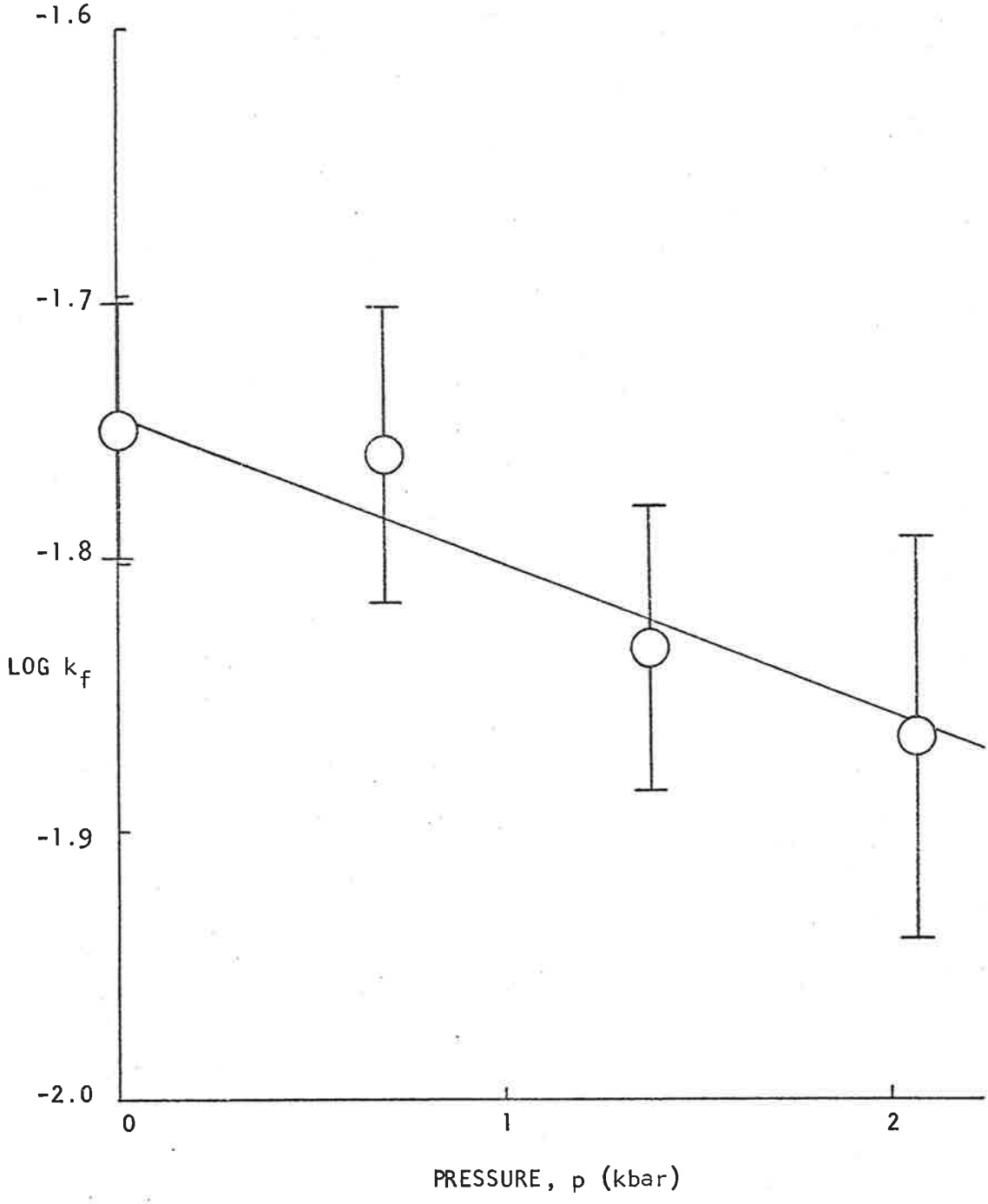

Figure 4.5 Pressure Dependence of Rate Constant, k_f

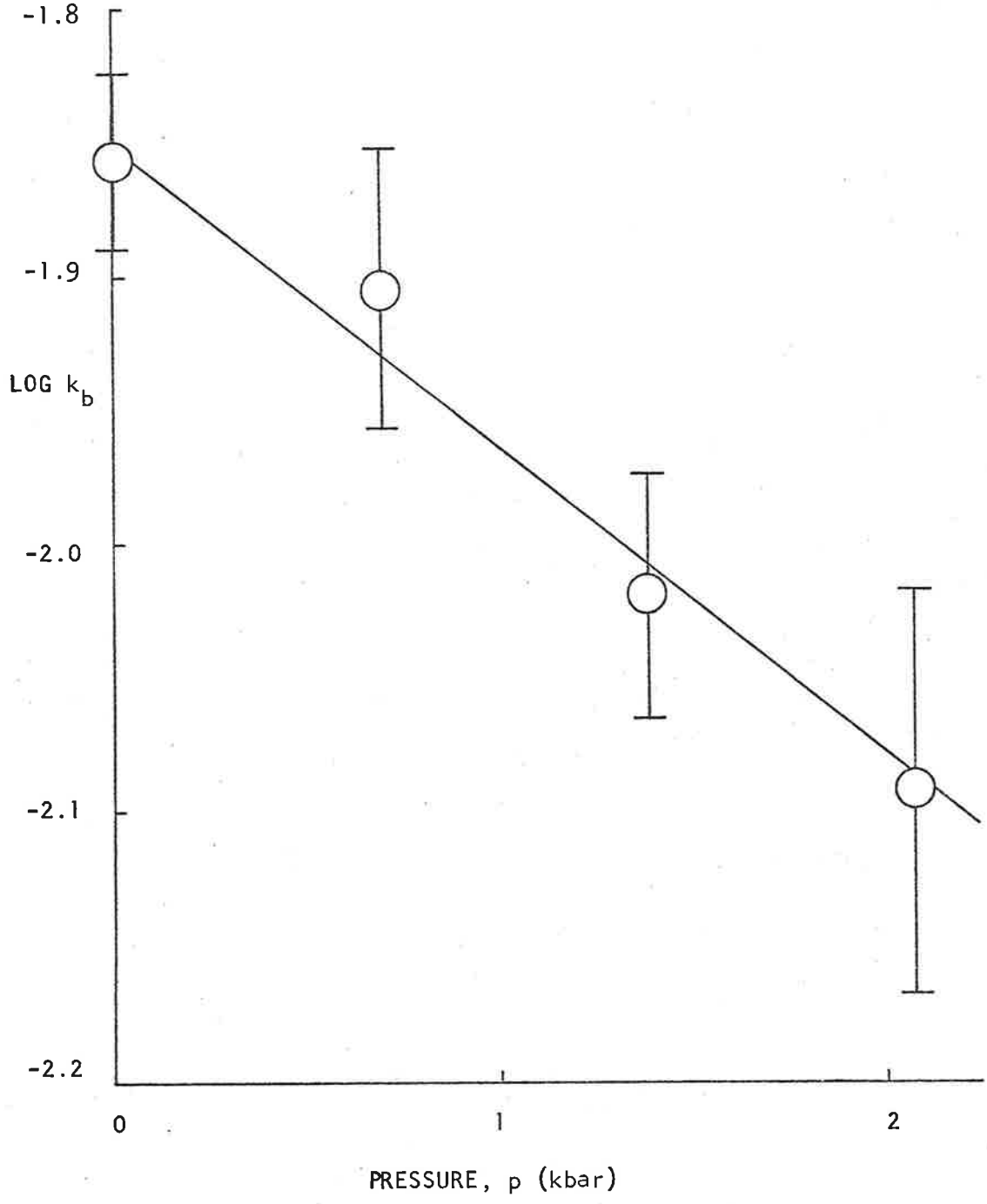

Figure 4.6 Pressure Dependence of Rate Constant, k_b

4.8 Discussion

4.8.1 Effect of Pressure on the Pentadentate-Hexadentate Equilibrium

The influence of pressure on a chemical equilibrium can be expressed in terms of $\Delta\bar{V}$, defined by equation (2.18). $\Delta\bar{V}$ represents the excess of the partial molar volumes of the products over those of the reactants in the prevailing medium.

For the equilibrium between the pentadentate and hexadentate forms of the Co(III)-EDTA complex,

$$Co^{III}(EDTA)^{-} + H_2O + H^{+} \rightleftarrows Co^{III}(HEDTA)H_2O,$$

the value of $\Delta\bar{V}$ can be evaluated from the measurements reported in Table 4.5, using equation (2.18). Taking the value $\beta = 4.57 \times 10^{-5}$ bar^{-1} for the compressibility of water at 25°C,[76] the term in $RT\beta$ amounts to 2.2 c.c. $mole^{-1}$. Hence, for the pentadentate-hexadentate equilibrium at 25°C and ionic strength 1 M, $\Delta\bar{V}$ was found to have the value -5.5 ± 1.4 c.c. $mole^{-1}$.

Since $\Delta\bar{V}$ is equal to the difference in partial molar volumes between the products and reactants, an estimate of the difference in the volumes of the pentadentate and hexadentate forms of the complex can be obtained. The partial molar volume of water is 18 c.c. $mole^{-1}$ and that of H^{+}, at infinite dilution, is believed to be close to zero.[45] Hence, the difference between the partial molar volume of $Co(HEDTA)H_2O$ and that of $Co(EDTA)^{-}$ is $-5.5 + 18 = 12.5$ c.c. $mole^{-1}$. This difference

in volume would be due to a difference in the effective radii of the two ions and to a difference in the interaction between the solvent and each complex, $Co(EDTA)^-$ having a formal charge of -1 and $Co(HEDTA)-H_2O$ having zero formal charge. Ignoring the specific interaction of the different parts of each complex with the solvent, we can estimate the difference for the interaction of each complex with the solvent by using the electrostriction equation, (2.30), which assumes a spherical particle and an even distribution of charge. Taking the radius of the $Co(EDTA)^-$ ion as 4 Å, this gives a difference for the ions of 1.5 c.c. $mole^{-1}$ due to electrostriction of the solvent. Thus there would be a difference of approximately 11 c.c. $mole^{-1}$ in the size of the ions. Again taking the radius of the $Co(EDTA)^-$ ion as 4 Å, this value of 11 c.c. $mole^{-1}$ represents an increase of about 7% in the volume of the $Co(HEDTA)H_2O$ complex, and an increase of in the radius of less than 0.1 Å.

4.8.2 Effect of Pressure on the Rate of Attainment of Equilibrium

For the back reaction of the equilibrium,

$$Co(HEDTA)H_2O \rightarrow Co(EDTA)^- + H^+ + H_2O,$$

Higginson has proposed three alternative mechanisms. These can each be considered in terms of the measured volume of activation determined in the present studies.

The first mechanism[75a] is of the S_N1 type, envisaged as consisting of three steps: first, the loss of the coordinated water molecule to form a 5-coordinate intermediate, followed by the rapid ionisation of the free carboxylic acid group and then coordination of the carboxylate group in the sixth coordination position. The first step is slow and rate determining. This mechanism can be represented as:

$$Co(HEDTA)H_2O \xrightarrow{slow} \text{Co}\overline{}\text{COOH} + H_2O \xrightarrow{fast} Co(EDTA)^- + H^+ + H_2O$$

(5-coordinate intermediate)

If this mechanism were operative, the volume of activation would be expected to be close to +18 c.c. $mole^{-1}$, since the formation of the transition state involves, in the limit, only the release of a water molecule to the bulk solvent. This does not accord with the measured $\Delta V^{\ddagger}$ of +6 c.c. $mole^{-1}$, and so this limiting S_N1 mechanism does not seem likely.

The other two mechanisms proposed[75b] are of the S_N2 type. They differ from each other only in that one uses the coordinated water to help ionise the carboxylic acid group while the other uses a solvent water molecule. These mechanisms involve the same three steps described above for the S_N1 mechanism, but here they occur in a concerted action. The reaction described in these terms may be represented as:

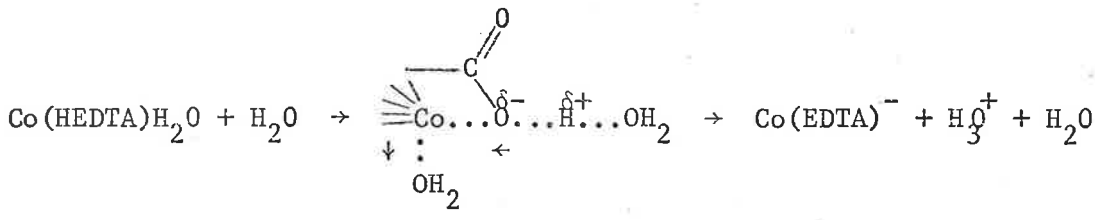

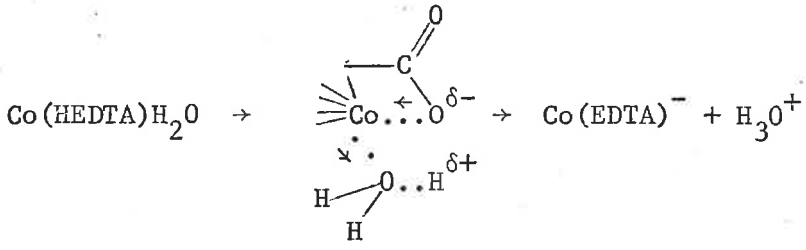

If the reaction proceeded via either of these pathways and the transition state configuration resembled the products, the volume of activation would be expected, in the limit, to be equal to the molar volume change for the ionisation of a carboxylic acid plus the molar volume of a water molecule. It has been found[45] that almost all carboxylic acids ionise with a contraction of about 12 c.c. mole^{-1}. Hence the volume of activation would be close to the value +18 - 12 = +6 c.c. mole^{-1}. If, in the transition state, the two processes of acid ionisation and water expulsion were nearly complete (i.e. transition state resembles products) then the contributions would be numerically slightly less than 18 and 12, and the difference between the two values would still be about +6 c.c. mole^{-1}. These mechanisms are thus quite consistent with the measured value of $\Delta V^{\ddagger}$ = +6 c.c. mole^{-1}.

It appears, then, from the results of these pressure studies that an S_N2 type mechanism is more probable than a limiting S_N1 type for the back reaction of the Co(III) equilibrium.

The forward reaction of the equilibrium,

$$Co(EDTA)^- + H^+ + H_2O \rightarrow Co(HEDTA)H_2O,$$

can also be considered in terms of either an S_N1 or S_N2 type mechanism. The S_N1 type mechanism would consist of a slow "ring-opening" process, as one of the carboxylate groups dissociates from the central Co ion and becomes protonated, followed by the rapid introduction of a water molecule into the vacant sixth coordination site. This could be represented thus:

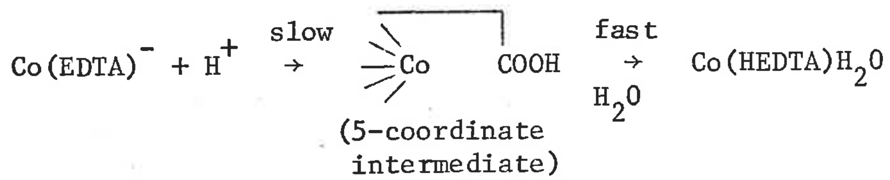

The formation of the transition state on this scheme is just the reverse of the ionisation of a carboxylic acid, and so the volume of activation would be expected to be close to +12 c.c. mole^{-1}. This does not agree well with the measured value of +1 c.c. mole^{-1}.

A possible S_N2 type mechanism for the forward reaction would be just the reverse of that proposed for the back reaction. In that scheme it was proposed that the transition state resembled the products, which

for the forward reaction would be the reactants. Hence if a similar mechanism were operative for the forward reaction, the transition state would resemble the reactants and the expected volume of activation would be close to zero. Within experimental error this is observed to be so.

Thus it is seen that the measured volumes of activation for the forward and back reaction of the Co(III) hexadentate-pentadentate equilibrium are consistent with an S_N2 mechanism, which is the same for both forward and back reactions.

Chapter 5

The Effect of Pressure on the $Co(en)_3^{2+}$ - $Co(en)_3^{3+}$ Electron Exchange Reaction

5.1 Introduction

The electron exchange reaction between $Co(en)_3^{2+}$ and $Co(en)_3^{3+}$ is generally believed to be an example of the outer-sphere mechanism.[20] This is because of the substitution inert character of the $Co(en)_3^{3+}$ ion, and, in perchlorate medium, because of the lack of a suitable bridging ligand. For example, even the base hydrolysis of the $Co(en)_3^{3+}$ ion proceeds with half-times of the order of hundreds of hours at temperatures similar to those employed in the present study,[87] yet the half-time observed for electron exchange was less than ten hours. Hence it does not seem possible that the electron exchange could proceed by an inner-sphere mechanism, which would require substitution into the first coordination sphere of the $Co(en)_3^{3+}$ ion.

The thermal, homogeneous electron exchange has previously been studied by Lewis, Coryell and Irvine,[88] who used the radio-isotope method to follow the reaction, and by Dwyer and Sargeson,[89] who used the racemisation method. Their results were substantially in agreement.

In the early part of these present studies, a considerable number of runs (not reported here) was carried out, but despite the greatest care to ensure purity of reagents and exclusion of oxygen, reproducible rates could not be obtained. Similar difficulties appear to have

plagued the first workers[88] on this system. Early evidence indicated that this was due to oxygen catalysis.

If oxygen, even a very small amount, was present at the commencement of a run, severe catalysis occurred. This showed as a distinct curvature in the log (1 - F) vs. time plots. However, this effect was transitory and disappeared after a couple of hours when the exchange plots became linear. It led, then, to an apparent ordinate intercept on these plots. Lewis, Coryell and Irvine[88] reported as much as 20% zero-time exchange. In these present studies, less than 2% zero-time exchanges were obtained. However, even this refinement did not lead to satisfactorily reproducible results. It seemed that a second type of catalysis was occurring which was permanent throughout a run.

All of these early runs, in which this trouble was encountered, were carried out at 25°C. It was then found that, when the temperature was raised to 65°C, reproducible rates could be obtained. It appears significant that the later workers, Dwyer and Sargeson[89] and Stranks,[90] who did not report any difficulties of this nature with this system, carried out their studies at 98°C (although some runs were done at 25°C) and 50°C respectively. This suggests that the suspect "oxy species" is decomposed at higher temperatures. Accordingly, all of the work reported in this present study was carried out at 65°C, where the rates were reproducible.

Lewis, Coryell and Irvine[88] found that there was a dependence of the exchange rate on the total ionic strength, μ, of the solution. Dwyer and Sargeson subsequently made a more detailed investigation of the effect of ionic strength on the rate, and showed that log k increased linearly with $\sqrt{\mu}$. They also showed that there was no dependence on specific anions.

These present studies of the effect of pressure on the rate of electron exchange between $Co(en)_3^{2+}$ and $Co(en)_3^{3+}$ were carried out at 65°C in solutions of total ionic strength 0.5 M.

5.2 Experimental

5.2.1 Materials

Ethylenediamine

Analar B.D.H. ethylenediamine was twice distilled at atmospheric pressure and the fraction boiling at 118-118.5°C collected and stored under nitrogen in a dark bottle. From this supply of pure ethylenediamine, aqueous stock solutions of 0.5 M ethylenediamine were prepared and then standardised against 0.1 M perchloric acid.

Nitrogen

The nitrogen used was "high purity oxygen-free" grade, supplied by Commonwealth Industrial Gas Company. To ensure that the last traces of oxygen were removed, the gas was scrubbed immediately before entering the reaction vessel, as described below.

Trisethylenediaminecobalt(III) perchlorate, $Co(en)_3(ClO_4)_3$

The perchlorate salt of trisethylenediaminecobalt(III) was prepared directly by using all perchlorates as starting materials. 61 g. of 30% ethylenediamine was poured into a solution of 36.5 g. of $Co(ClO_4)_2.6H_2O$ in 75 ml. of water, and then about 8 ml. of concentrated perchloric acid was slowly added to partly neutralise the ethylenediamine. The Co(II) was oxidised by bubbling a vigorous stream of air through the solution for 3 hours. The volume of the

solution was then reduced on a steam bath until some product began to crystallise. Some lithium perchlorate was added to precipitate more product and the solution cooled and allowed to stand in a refrigerator to crystallise. The product was filtered off and twice recrystallised from water. The final product was washed with alcohol, then ether, and dried for several minutes in an oven at 80°C.

The purity of the salt was checked by analysis for carbon, hydrogen and nitrogen. The analysis figures are given in Table 5.1.

Table 5.1

Analysis for $Co(en)_3(ClO_4)_3$	C	N	H
Calculated for $Co(en)_3(ClO_4)_3$	13.41%	15.63%	4.50%
Found	13.65	15.35	4.67

Trisethylenediaminecobalt(II), $Co(en)_3^{2+}$

The trisethylenediaminecobalt(II) ion was prepared *in situ* at the beginning of each run by mixing solutions of $Co(ClO_4)_2$ and ethylenediamine. The ethylenediamine concentration was at least 16 times in excess of the Co^{2+} concentration in each run, thus ensuring that full coordination was virtually 100% complete. The value of the formation constant, β_3, for the reaction,

$$Co^{2+} + 3\ en \rightleftarrows Co(en)_3^{2+}$$

calculated at 65°C, using the literature values[67] for the formation

constant at 25°C and the heat of formation, was log β_3 = 12.04. Using this value, it can be shown that the ratio $[Co(en)_3^{2+}]/[Co^{2+}] > 10^{10}$ for the concentrations of reactants employed in these studies.

The addition of the ethylenediamine to the aqueous Co(II) solution had to be carried out in an oxygen-free atmosphere, since the Co^{2+}/ethylenediamine mixture was very susceptible to formation of peroxo dicobalt species and oxidation to Co(III). The peroxo species act as a homogeneous catalyst for the electron exchange.

All other materials used have been described earlier.

5.2.2 Apparatus

Glass Reaction Vessel

Because the $Co(en)_3^{2+}$ - $Co(en)_3^{3+}$ exchange is profoundly catalysed by even traces of oxygen, an air-tight all-glass vessel, of about 50 ml. effective capacity, was constructed so that the reactant solutions could be de-oxygenated and mixed entirely under an atmosphere of nitrogen. This vessel is shown in Figure 5.1.

A number of thermal runs was carried out completely in this vessel, and for the pressure runs it was used for the preparation of the reaction solution, prior to loading in the pressure vessel. For this purpose the vessel had an outlet, D, sealed with an air-tight rubber serum cap.

Initially the separate reactant solutions were placed in the vessel,

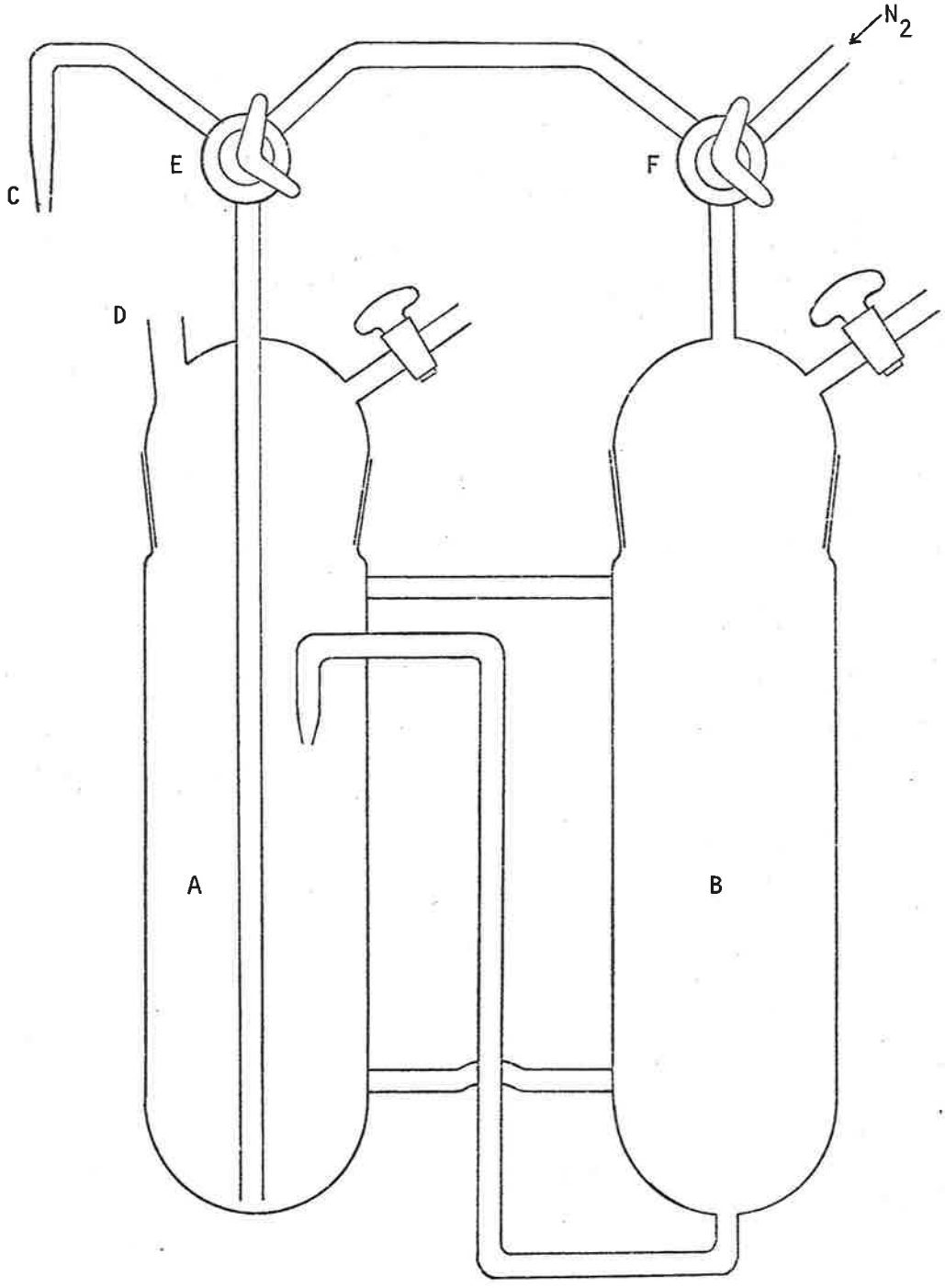

Figure 5.1 Glass Reaction Vessel

with the ethylenediamine solution in A and $Co(ClO_4)_2$ solution in B, or *vice versa* - it made no difference which. Likewise the placement of the other components, sodium perchlorate solution and trisethylenediaminecobalt(III) perchlorate, proved to be immaterial. Normally the Co(III) complex and ethylenediamine solution were placed in A and the labelled $Co(ClO_4)_2$ and sodium perchlorate solutions in B.

These solutions were then de-oxygenated for 1-1 $^1/_2$ hours by bubbling purified nitrogen from left to right through the vessel. The nitrogen flow was then reversed, forcing the solution from B into A and thus mixing the reactant solutions. The $Co(en)_3^{2+}$ formed immediately, thus initiating the exchange. No observable exchange occurs between Co^{2+}_{aq} and $Co(en)_3^{3+}$.

Measurements showed that not less than 99.5% of the solution in B was forced into A by the nitrogen pressure, so that transfer was essentially quantitative. To remove a sample for analysis during a run carried out in this vessel, nitrogen was passed from right to left through the vessel, forcing reaction solution through the opened sample outlet, C. The first 1-2 ml., containing the solution remaining in the outlet tube since the previous sample, were rejected, then a 1 $^1/_2$ - 2 ml sample was run directly into quenching solution. All taps were then closed and the nitrogen supply turned off. Before removing a sample, purified nitrogen was first passed through the nitrogen inlet tubing with the two 2-way taps, E and F, in the by-pass position. This removed

any oxygen that had diffused into the plastic tubing between samples. This source of contamination was found to be significant in runs with half times of several hours.

A schematic representation of the arrangement of the apparatus using the glass reaction vessel is given in Figure 5.2.

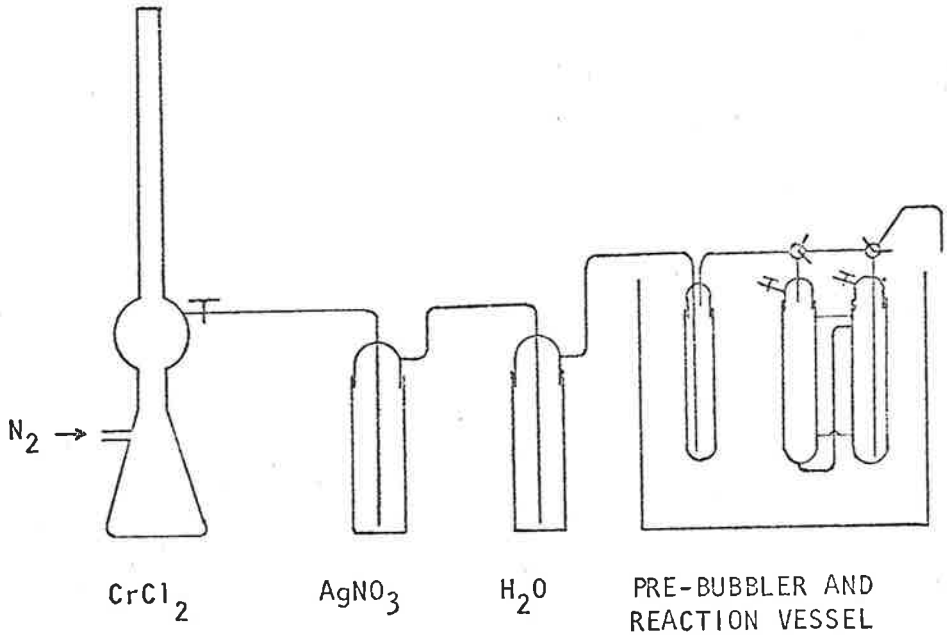

Figure 5.2

The scrubbing of the nitrogen to remove any residual oxygen impurity was achieved by passing the nitrogen through a 1 m. column packed with glass helices, through which 0.2 M chromous chloride was percolated. The chromous chloride was continuously regenerated with

zinc amalgam at the bottom of the column. The nitrogen was then washed by bubbling through 10% silver nitrate solution and finally water.

Another pre-bubbler, containing water, was included in the flow-line immediately before the reaction vessel, and was kept at the same temperature as the reaction solutions. This pre-bubbler was important during the preliminary de-oxygenating periods, especially at hig er temperatures, to prevent loss of volume from the reactant solutions.

For the runs conducted in the pressure vessel, the reactant solutions were first de-oxygenated and mixed in the glass vessel, as described above. Then, with nitrogen flowing through the vessel, the self-sealing rubber serum cap was pierced by the outlet needle of the partly-assembled pressure vessel. After flushing the perspex reaction vessel and outlet tubing with nitrogen, the outlet needle was lowered into the mixed reaction solution, which was then drawn back into the reaction vessel by withdrawing the plunger. In this way the reaction vessel was filled without having the reaction solution come into contact with air. The reaction vessel was then placed in the pressure vessel and the pressure adjusted to the required value.

Pressure Vessel

The pressure vessel used for this system was the high pressure sampling vessel, described in Chapter 3. It was impractical to use

the Pt/Ir outlet tubing for this reaction, since the extremely small bore of this tubing made it virtually impossible to fill the Perspex reaction vessel in the manner described in the previous paragraph. The stainless steel capillary outlet tubing was used, and this was found satisfactory, although it had to be renewed during the course of the studies.

It was found after a number of runs that the measured rates of the exchange reaction began to increase. This was apparently due to some interaction between the reaction solution and the stainless steel capillary tubing, probably while the reaction solution was being drawn into the reaction vessel through the tubing. When both the outlet needle and the tubing connecting the reaction vessel to the valve block were replaced with new tubing, the inconsistency in the reaction rates ceased. The tubing was renewed twice during these studies.

5.2.3 Method of Analysis for Co(II)

In the early part of these studies each kinetic run was analysed spectrophotometrically for Co(II) at the beginning and end of the run to determine whether any oxidation had occurred. It was found that not more than 1% oxidation ever occurred, and this was close to the limit of accuracy for the analytical method.

The method of analysis was as follows: A 5.0 ml. sample of reaction

solution was quickly withdrawn with a pipette and discharged directly into 10.0 ml. of 6 M HCl. 5.0 ml. of this quenched solution was made up to 25.0 ml. in a volumetric flask and then 2.0 ml. of this solution was made up to 25.0 ml. with 1 ml. of 7 M NH_4CNS, 1.0 ml. of water and 21 ml. of acetone. The optical absorbance of this solution was measured at 621 nm, corresponding to the absorption maximum of the blue tetrathiocyanatocobalt(II) species, $Co(SCN)_4^{2-}$. The Co(II) concentration was then determined using the molar extinction coefficient at this wavelength.

The value of the molar extinction coefficient at 621 nm was found to be 1935 $M^{-1}cm.^{-1}$. This was determined by preparing several standard solutions of composition similar to the prepared sample solutions, but with different Co(II) concentrations, covering the range to be employed in the reaction solutions. The optical absorbances of these solutions were measured and were found to be described by Beer's law over the concentration range used.

5.2.4 Sampling and Separation Procedures

An approximately 2 ml. aliquot of reaction solution was discharged directly from the outlet needle into 3 ml. of 6 M HCl. The inert Co(III) complex was unaffected, while the labile Co(II) complex was immediately decomposed. The electron exchange was instantly quenched, since no observable exchange occurs between Co^{2+} and $Co(en)_3^{3+}$. The quenched

solution was then added to about 17 ml. of 2 M NH_4CNS solution and 23 ml. of a 15% v/v solution of pyridine in chloroform. This mixture was shaken thoroughly in a separating funnel and then the two immiscible phases allowed to separate. The lower phase, containing the Co(II) in the form of the $Co(py)_4(SCN)_2$ complex, was run off and made up to 25.0 ml. in a volumetric flask. Similarly the upper layer, containing the $Co(en)_3^{3+}$, was made up to 25.0 ml. Then 10.0 ml. of each of these solutions were taken for radiometric assay.

It was found unnecessary to wash each phase with more reagent solution, as tests indicated that a single separation was more than 99% efficient.

Further tests also showed that the counting efficiency was the same for both the aqueous and chloroform solutions. This was to be expected using a scintillation counter, which detects γ-rays; but it was not the case for a G.M. tube, which detects β-rays.

5.3 Results

5.3.1 Order of Reaction

Previous studies[88,89] have reported that this exchange is a second order reaction, first order in both the concentrations of $Co(en)_3^{2+}$ and $Co(en)_3^{3+}$. Accordingly, plots of reaction rate, R, against $[Co^{II}][Co^{III}]$ should be linear. A number of runs was carried out with varying Co(II) and Co(III) concentrations, and the results obtained are given in Table 5.2.

Table 5.2

Variation of Exchange Rate, R, with $[Co(en)_3^{2+}]$ and $[Co(en)_3^{3+}]$

T = 65°C μ = 0.5 M

$[Co(en)_3^{2+}]$ (M)	$[Co(en)_3^{3+}]$ (M)	R x 10^4 (M $hr.^{-1}$)
.0186	.0200	13.8
.0186	.0169	12.1
.0186	.0200	14.2
.0093	.0100	5.81
.0093	.0100	6.83
.0372	.0400	33.4
.0558	.0600	63.5
.0279	.0300	24.4
.0279	.0700	33.2
.0093	.0200	8.76
.0186	.0250	17.8

The results (except for the two runs at the highest values of $[Co^{II}][Co^{III}]$) are shown in Figure 5.3, where R has been plotted against $[Co(en)_3^{2+}][Co(en)_3^{3+}]$. It was found, as can be seen from this graph, that as the Co(III) concentration was increased the plot became curved, and was linear only at the low concentrations.

This effect was also noted by Lewis, Coryell and Irvine,[88] who quoted reaction orders as low as 0.58 for Co(III) dependence. They, however, used higher Co(III) concentrations (0.017 to 0.089 M).

This deviation from linearity at the higher Co(III) concentrations can be attributed to a second order salt effect, which results from the high contribution to the total ionic strength of the solution from the highly charged $Co(en)_3^{3+}$ ion. A common assumption is that the activity coefficients of the solute species, regardless of their charge type, will remain constant in the presence of a swamping electrolyte. In the present case, although the calculated ionic strength, μ $(= \frac{1}{2} \Sigma c_i Z_i^2)$, was held constant, the added electrolyte ($NaClO_4$) contributed less than half of the total ionic strength at Co(III) concentrations greater than 2×10^{-2} M. The prediction that the reaction order should approach unity as the ionic strength is increased was verified by Lewis, Coryell and Irvine.[88] In the present studies it was not considered more satisfactory to work in a medium of higher ionic strength, since this would lead to an inordinately large correction to the calculated volume of activation through the term

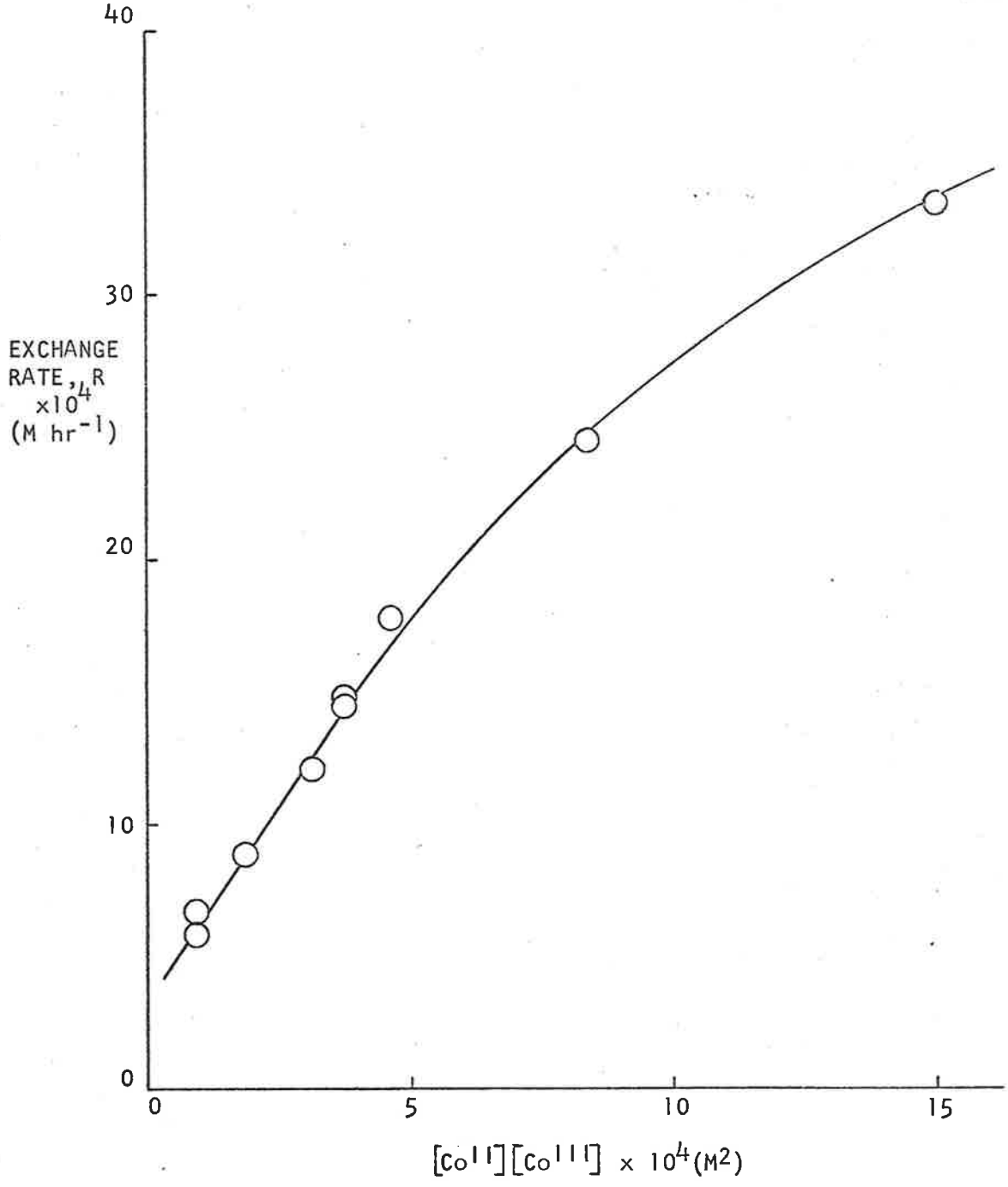

Figure 5.3 Non-Linear Variation in Rate, R, with Increasing Cobalt(III) Concentration

$\Delta V^{\ddagger}_{D.H.}$. This would introduce a considerably larger uncertainty in the value of $\Delta V^{\ddagger}$. Instead, the reaction was studied in a medium of ionic strength 0.5 M, using concentrations of the reactants within the range where the reaction was found to be satisfactorily of first order in each reactant, i.e. for $Co(en)_3^{3+}$, (1.00 to 2.00) x 10^{-2}M and for $Co(en)_3^{2+}$, (0.93 to 1.86) x 10^{-2}M.

5.3.2 Dependence on Free Ethylenediamine Concentration and Hydroxide Ion

Since there was excess ethylenediamine present in the reaction solutions, the pH of these solutions was approximately 10. A possible dependence of the exchange rate on the concentration of free (unbound) ethylenediamine and on hydroxide ion was therefore examined. This question had previously been studied by both Lewis, Coryell and Irvine[88] and Dwyer and Sargeson,[89] and so was only checked in these present studies.

The previous workers found that the exchange rate was independent of free ethylenediamine concentration, at least up to 1.05 M, and independent of hydroxyl ion concentration in solutions of pH 9.5 - 11.6. These results were confirmed in the present studies, as can be seen from the results in Table 5.3.

Table 5.3

Absence of Rate Dependence on Free Ethylenediamine Concentration and pH

$T = 65°C$ $\mu = 0.5$ M $[Co^{II}] = 0.0186$ M $[Co^{III}] = 0.0200$ M

[en] (M)	k (M^{-1} $hr.^{-1}$)	$[en]_{free}$ (M)	pH
.08	2.6	.024	10.9
.3	2.7	.244	11.4

Although the exchange rate has been found independent of hydroxide ion concentration in the narrow range pH 9.5 - 11.6, Stranks[90] has reported that in solutions up to 0.01 M in hydroxide, the exchange rate was first order in $[OH^-]$. In the present studies the total ethylenediamine concentration was 0.3 M in each run. This gave the reaction solution a pH of about 10. At this hydroxide ion concentration, the contribution to the rate due to hydroxide ion catalysis would be negligible, as was found.

5.3.3 Heterogeneous Catalysis

If the electron exchange proceeded entirely by a homogeneous, second order mechanism, then the measured exchange rate, R, would be given by $R = k[Co(en)_3^{2+}][Co(en)_3^{3+}]$. A graphical plot of R vs. $[Co(en)_3^{2+}][Co(en)_3^{3+}]$ should be linear with zero intercept. However, as seen from Figure 5.3, a plot of R vs. $[Co^{II}][Co^{III}]$, although linear at low values of $[Co^{II}][Co^{III}]$, has a non-zero intercept. This suggests

some heterogeneous catalysis of the exchange rate. The rate data can be described by the rate law

$$R = k[Co^{II}][Co^{III}] + S \qquad (5.1)$$

where k is the second order homogeneous exchange rate constant and S is the heterogeneous contribution to the observed rate, R. The heterogeneou contribution is evidently independent of $[Co^{II}]$ and $[Co^{III}]$. This would be due to complete coverage of the surface at the bulk concentrations of reactants employed. This concentration independence of the heterogeneous rate has been verified by detailed studies of the heterogeneous reaction in these laboratories.[91]

From Figure 5.5 it can also be seen that the heterogeneous contribution to the observed rate shows a pressure dependence, since the intercept increases with increasing pressure. However, no detailed study of this pressure dependence was undertaken, as we are only concerned here with the effect of pressure on the homogeneous exchange rate, which is obtained from the slope of each plot.

Lewis, Coryell and Irvine[88] also found evidence of some heterogeneou catalysis, which varied slightly depending on the type of surface employed. In the present study an insufficient number of runs under the same conditions was carried out to enable an accurate comparison of the rates in the glass and Perspex vessels respectively. The difference, if any, appeared small. Moreover, this was of no real

consequence for the present purpose as all the runs in the pressure dependence study were conducted in the Perspex reaction vessel inside the pressure vessel, and only the homogeneous rate was of interest.

5.3.4 Evaluation of Second Order Rate Constants

The observed rates of electron exchange for the reaction

$$\overset{*}{Co}(en)_3^{2+} + Co(en)_3^{3+} \rightleftharpoons \overset{*}{Co}(en)_3^{3+} + Co(en)_3^{2+}$$

were again obtained using the equation:

$$R = -\frac{1}{2.303\ t}\frac{[Co^{II}][Co^{III}]}{[Co^{II}] + [Co^{III}]}\log\ (1 - F) \qquad (5.2)$$

where $[Co^{II}]$ and $[Co^{III}]$ represent the total concentrations of $Co(en)_3^{2+}$ and $Co(en)_3^{3+}$ respectively. Due to the long half-times of exchange, the specific activity of the Co(III) at infinite time was calculated for each run, again using the condition for material balance, given by equation (4.1). A typical exchange plot is shown in Figure 5.4. The half-times of exchange were obtained from these plots and then the observed rates of exchange, R, were calculated using equation (1.3). From the variation of R with $[Co^{II}]$ and $[Co^{III}]$, the second order homogeneous exchange rate constant, k, at each pressure was obtained from a plot of R vs. $[Co^{II}][Co^{III}]$, using equation (5.1).

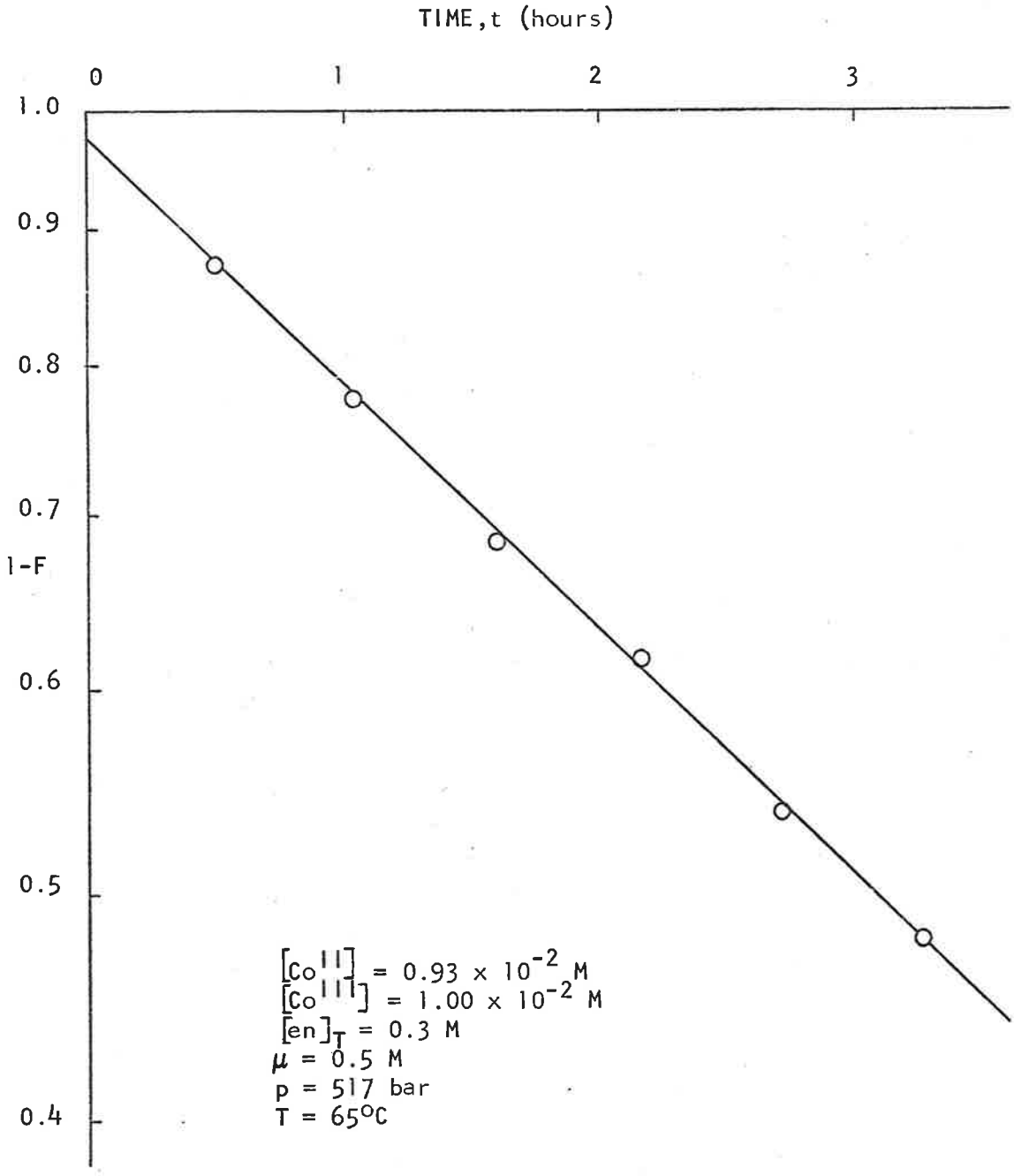

Figure 5.4 Typical Exchange Plot

5.3.5 The Effect of Pressure on the Exchange Rate

The rate of electron exchange between $Co(en)_3^{2+}$ and $Co(en)_3^{3+}$ was studied at pressures between 0 and 2 kbar using reactant concentrations of $(0.93 - 1.86) \times 10^{-2}$ M for Co(II) and $(1.00 - 2.00) \times 10^{-2}$ M for Co(III). The results are given in Table 5.4, where the values of R have been assigned an estimated uncertainty of $\pm$ 5%, based mainly upon the errors involved in the measured quantities used in evaluating R.

Table 5.4

Variation of Observed Exchange Rate, R, with Pressure

T = 65°C μ = 0.5 M

[Co(II)] (M)	[Co(III)] (M)	R x 10^4 (M $hr.^{-1}$)
	p = 1 bar	
.0093	.0100	5.81
.0093	.0200	8.80
.0186	.0169	12.0
.0186	.0200	13.6
.0186	.0200	14.2
	p = 517 bar	
.0093	.0100	11.3
.0093	.0200	14.2
.0186	.0150	20.2
.0186	.0200	21.9
	p = 1034 bar	
.0093	.0100	13.9
.0093	.0200	21.0
.0186	.0150	24.0
.0186	.0200	29.5

(contd.)

Table 5.4 (contd.)

[Co(II)] (M)	[Co(III)] (M)	R x 10^4 (M $hr.^{-1}$)
	p = 1552 bar	
.0093	.0100	18.8
.0093	.0200	27.0
.0186	.0150	32.5
.0186	.0200	39.3
	p = 2068 bar	
.0093	.0100	22.3
.0093	.0200	30.4
.0186	.0150	39.7
.0186	.0200	47.0
.0186	.0200	47.0

The values of R in the Table are subject to an uncertainty of ± 5%.

In Figure 5.5, these observed rates, R, have been plotted against $[Co^{II}][Co^{III}]$ for each pressure. The straight lines drawn through these data are the lines of best fit, calculated using the "least squares" method. The values of the rate constants, k, and their standard deviations, obtained from the slopes of these lines, are listed in Table 5.5.

Table 5.5

Variation of Second Order Rate Constant, k, with Pressure

T = 65°C μ = 0.5 M

p (bar)	k (M^{-1} $hr.^{-1}$)
1	2.84 ± .15
517	4.07 ± .59
1304	5.36 ± .56
1552	7.22 ± .24
2068	8.90 ± .24

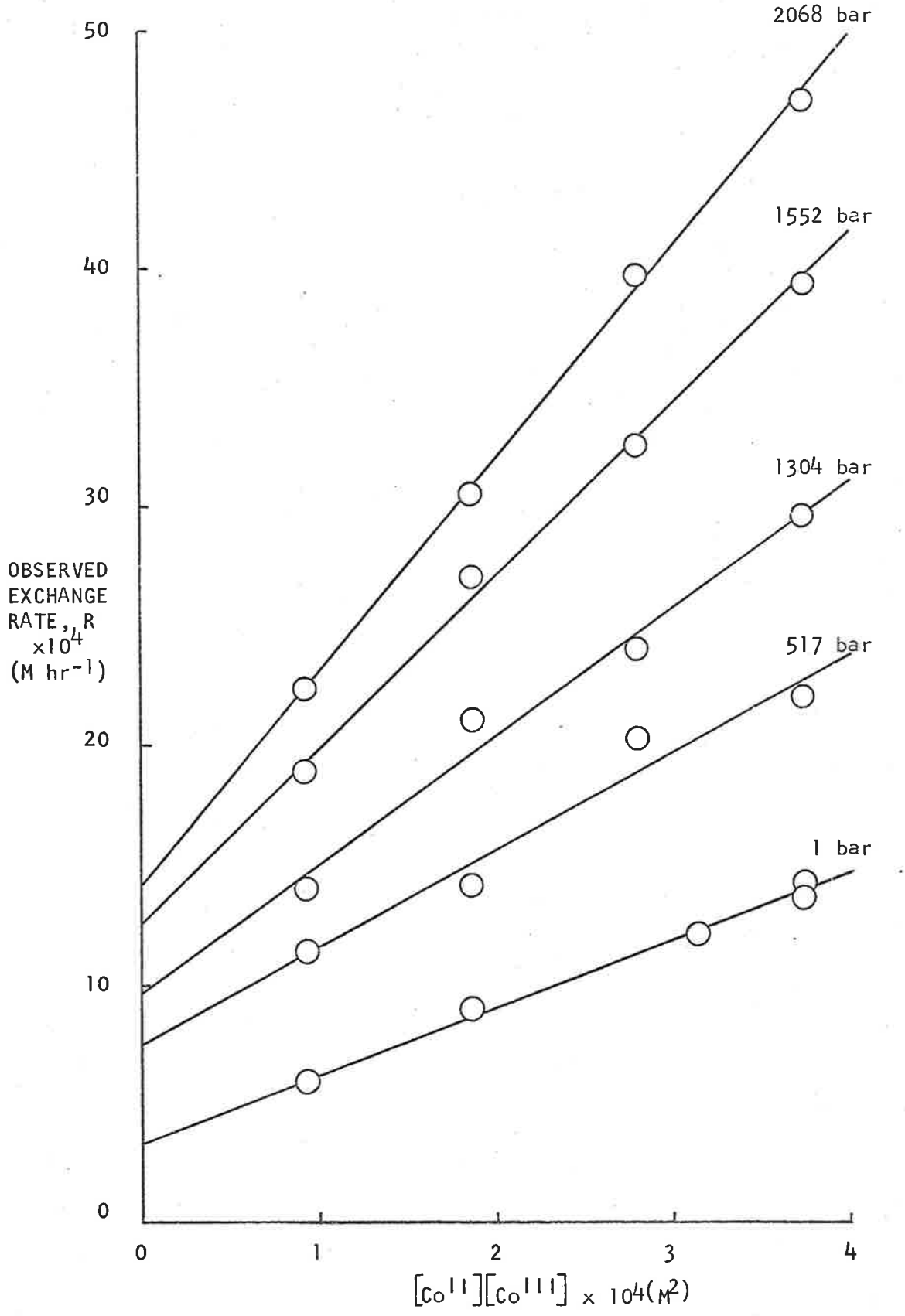

Figure 5.5 Pressure Dependence of Observed Exchange Rate, R

The rate constant for the homogeneous exchange at 1 bar pressure, 65°C and ionic strength 0.5 M, was found to be 2.84 ± 0.15 M^{-1} $hr.^{-1}$. This is consistent with the value of 3.2 M^{-1} $hr.^{-1}$ calculated from the data of Dwyer and Sargeson[89] and corrected to the same conditions of temperature and ionic strength. No useful comparison can be made with the results of the other previous studies, due to insufficient data on ionic strength effects in the one case[90] and too unreliable data in the other.[88]

The variation of rate constant, k, with pressure is shown in Figure 5.6, where log k is plotted against pressure. The pressure dependence is seen to be non-linear. The volume of activation at any pressure must be calculated, then, using the differential equation for $\Delta V^{\ddagger}$, equation (2.20).

To obtain the value of the derivative, $(\partial \log k/\partial p)_T$, a curve was fitted to the experimental data of p and log k using a least-squares polynomial computer program.[92] This program calculates, for a set of data, the curve of best fit in the form of a polynomial up to degree six. The values of log k were weighted according to their standard errors, given in Table 5.5. It was found that the data could be equally well represented, over the range of pressures employed, by either a polynomial of degree 2 or 3. Taking the simpler equation, then the curve of best fit was a second order polynomial of the form

$$\log k = a + bp + cp^2. \qquad (5.3)$$

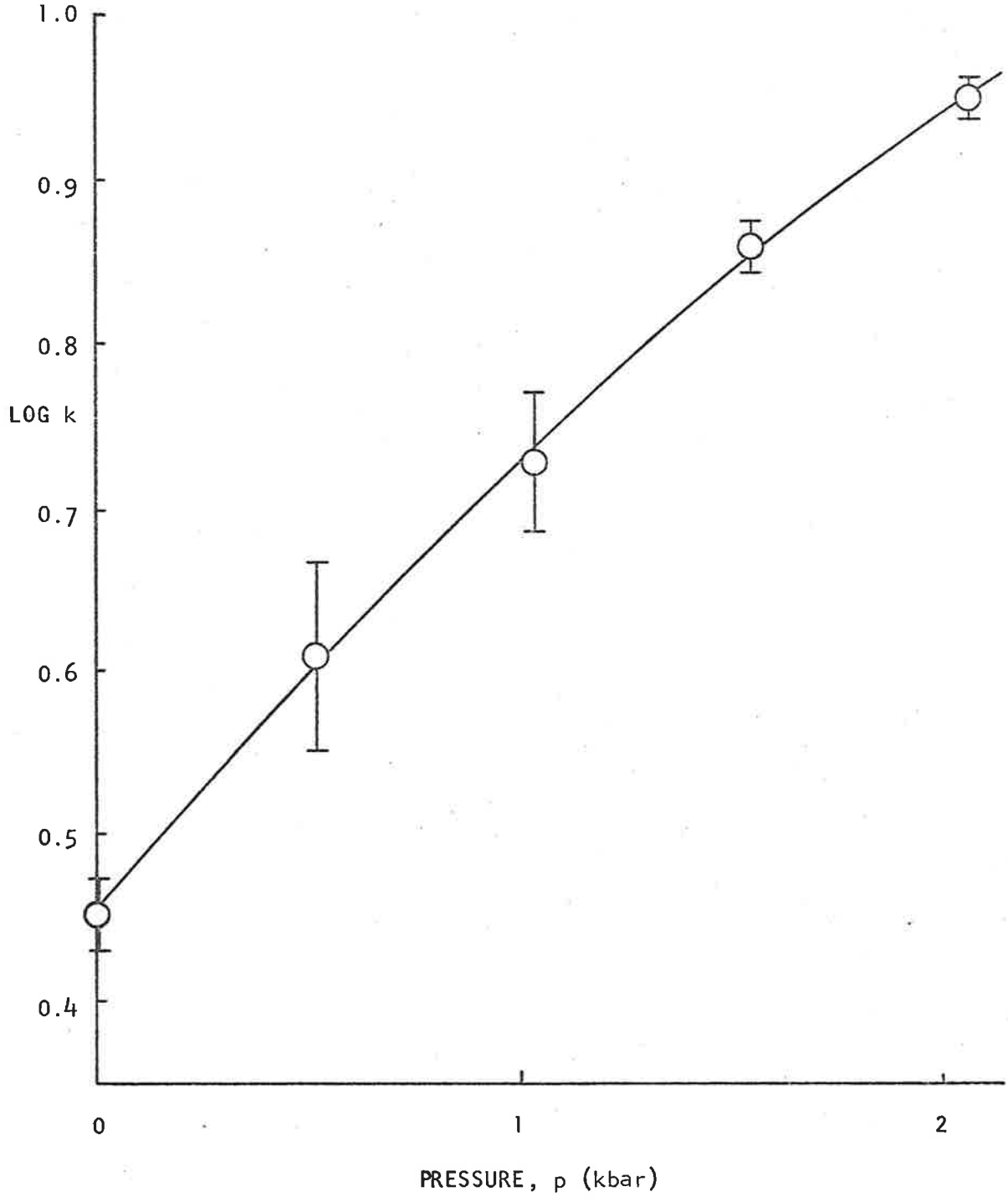

Figure 5.6 Pressure Dependence of Rate Constant, k

With p expressed in bar, the values of the coefficients were:

$a = .4545$

$b = 3.069 \times 10^{-4}$

$c = -3.236 \times 10^{-8}$

Equation (5.3) is represented in Figure 5.6 as a continuous line through the points representing the experimental data.

The volume of activation was calculated at several different pressures, using equation (2.20), with the values of $(\partial \log k/\partial p)_T$ obtained from the first derivative of equation (5.3). These values of $\Delta V^{\ddagger}$, which have been corrected for the term $RT\beta$, are given in Table 5.6. The value of β was taken to be 4.48×10^{-11} cm.^{2} dyne^{-1}, which is the value for water at 65°C.[76] The value of the term $RT\beta$ was thus 1.3 c.c. mole^{-1}.

The values of $\Delta V^{\ddagger}$ listed in Table 5.6 have been assigned an uncertainty of $\pm$ 1.5 c.c. mole^{-1}, based on the uncertainties in the quantities used in estimating $\Delta V^{\ddagger}$.

Table 5.6

Variation of $\Delta V^{\ddagger}$ with Pressure

T = 65°C $\qquad$ μ = 0.5 M

p (bar)	$\Delta V^{\ddagger}$ (c.c. mole^{-1})
1	-21.1
517	-19.0
1034	-16.9
1552	-14.7
2068	-12.6
	($\pm$ 1.5)

The volume of activation, $\Delta V^{\ddagger}$, for the homogeneous electron exchange between $Co(en)_3^{2+}$ and $Co(en)_3^{3+}$ at 1 bar in aqueous solution at 65°C and ionic strength 0.5 M, was found to be -21.1 ± 1.5 c.c. $mole^{-1}$.

5.4 Discussion

5.4.1 Comparison of Measured and Predicted $\Delta V^{\ddagger}$ Values

A comparison of the measured and predicted $\Delta V^{\ddagger}$ values can be made in the same manner as in the previous chapter.

The values of r_1, r_2 and σ, in the Marcus-Hush equation, can again be estimated from the crystal radii of Co(II) and Co(III) and from the Van der Waal's radii of the ligand atoms. The value of r_1, the effective radius of $Co(en)_3^{2+}$, is estimated as 4.13 Å and the value of r_2, for $Co(en)_3^{3+}$, as 3.98 Å. The value of σ is thus 8.11 Å. Taking the value for the dielectric constant of water as $\varepsilon = 65.21$ at 65°C,[76] the value of $(\partial(1/\varepsilon)/\partial p)_T$ may be calculated as before to be -8.699×10^{-7} bar^{-1}. The term $\{(\partial(1/\varepsilon_o)/\partial p)_T - (\partial(1/\varepsilon)/\partial p)_T\}$ is again calculated from the values at 25°C. Hence, from equations (4.5) and (4.6), the contributions to $\Delta V^{\ddagger}$ predicted by the Marcus-Hush theory are calculated to be:

$$\Delta V^{\ddagger}_{\text{coulombic}} = -8.94 \text{ c.c. mole}^{-1}$$

$$\Delta V^{\ddagger}_{\text{solvent rearr.}} = -4.89 \text{ c.c. mole}^{-1}$$

The correction for finite ionic strength effects is made in the same way as before. Taking the values[53,76] $A = 0.5558\ M^{-1/2}\ \text{deg.}^{3/2}$, $B = 0.3384 \times 10^{8}$ cm.$^{-1}\ M^{-1/2}\ \text{deg.}^{1/2}$ and $\beta = 4.48 \times 10^{-5}$ bar^{-1}, all at 65°C, and putting $Z_1 = 2$, $Z_2 = 3$, $\mu = 0.5$ and $\underline{a} = 4$ Å, we obtain from equation (4.11),

$$\Delta V^{\ddagger}_{D.H.} = 4.80 \text{ c.c. mole}^{-1}$$

The predicted volume of activation to be compared with the measured value is thus,

$$\Delta V^{\ddagger}_{calc} = -8.94 - 4.89 - 4.80 = -18.63 \text{ c.c. mole}^{-1}.$$

The measured volume of activation was found to be $\Delta V^{\ddagger}_{meas} = -21.1 \pm 1.5$ c.c. mole^{-1}. There is thus a reasonably close agreement between the two values.

The uncertainties in the calculated value of $\Delta V^{\ddagger}$ arise from the same sources as mentioned in the previous chapter for the Co-EDTA reaction. These are the use of the values of pure water for the compressibility and dielectric properties of the mixed electrolyte solution, the uncertainties in the values themselves used for the dielectric terms, the uncertainties in the values of r_1, r_2 and σ, and the assumption that the ions are incompressible.

If the compressibility of the ions is taken into account, it has been estimated[86] that this would lead to a correction of about 0.4 c.c. mole^{-1} in the value for $\Delta V^{\ddagger}$. If the uncertainties in r_1, r_2 and σ are taken to be 0.1 Å and 0.2 Å respectively, this gives a correction of 0.36 c.c. mole^{-1}. It is difficult to estimate the errors arising from the various dielectric terms, due to lack of data, but it is considered that they are not too serious.

Considering the uncertainties in the values obtained for both the

measured and predicted volumes of activation, it has been found, then, that they are equal within experimental error.

5.4.2 Compressibility of the Activated Complex

It was mentioned in Chapter 2 that frequently plots of log k vs. p are found to be curved. This can be explained in terms of the compressibility of the activated complex. If the compressibilities of the activated complex and the reactant ions were the same, this would require that $\Delta V^{\ddagger}$ be independent of pressure. Since $\Delta V^{\ddagger}$ is often found to be dependent on pressure, this suggests that the compressibility of the activated complex is different from those of the reactants. It has been pointed out by Hamann,[6] that where the volume changes are caused mainly by electrostriction, the curvature in the log k vs. pressure plots is most evident. This is understandable because of the changing interaction between the transition state and the solvent with change of pressure. Hence we might expect that reactions involving highly charged ions would show this curvature. The electron exchange between $Co(en)_3^{2+}$ and $Co(en)_3^{3+}$ shows a distinct curvature in the log k vs. pressure plot, shown in Figure 5.6.

If we define a quantity, $\kappa^{\ddagger} = (\partial \Delta V^{\ddagger}/\partial p)_T$, and call this the "compressibility of the transition state", we can attempt an order-of-magnitude comparison between the predicted and observed values. The observed value of $\kappa^{\ddagger}$ can be found from the values of $\Delta V^{\ddagger}$ at different

pressures listed in Table 5.6. The measured value of $\kappa^{\ddagger}$ thus obtained is $\kappa^{\ddagger} = -4 \times 10^{-3}$ c.c. mole^{-1} bar^{-1}.

The predicted value for $\kappa^{\ddagger}$ can be obtained by differentiating equation (2.26) with respect to pressure. Introducing Avogadro's number, N, to give molar quantities, we then have,

$$\kappa^{\ddagger} = \frac{NZ_1Z_2e^2}{\sigma} \frac{\partial^2}{\partial p^2}\left(\frac{1}{\varepsilon}\right) + \frac{Ne^2}{4}\left\{\left(\frac{1}{2r_1} + \frac{1}{2r_2} - \frac{1}{\sigma}\right) \frac{\partial^2}{\partial p^2}\left(\frac{1}{\varepsilon_o} - \frac{1}{\varepsilon}\right)\right\} \tag{5.4}$$

The value of $(\partial^2(1/\varepsilon_o)/\partial p^2)_T$ can be estimated from the data of Owen and Brinkley[82] to be -1.36×10^{-9} bar^{-2} at 25°C. Similarly, the value of $(\partial^2(1/\varepsilon)/\partial p^2)_T$ can be estimated as -0.914×10^{-20} bar^{-2} at 25°C. Using this value, together with the values of 78.54 for the dielectric constant of water at 25°C[76] and 3.699×10^{-3} bar^{-1} for the term $(\partial\varepsilon/\partial p)_T$ at 25°C, the value of $(\partial^2\varepsilon/\partial p^2)$ can be calculated as 9.122×10^{-7} bar^{-2} at 25°C. If it is assumed that $(\partial^2\varepsilon/\partial p^2)_T$ has the same value at 65°C, the term $(\partial^2(1/\varepsilon)/\partial p^2)_T$ can be evaluated as -1.158×10^{-20} bar^{-2} at 65°C, using the value of $\varepsilon = 65.21$ at 65°C.[76] This gives the first term of equation (5.4) the value of -1.19×10^{-3} c.c. mole^{-1} bar^{-1}. For the second term, the quantity $\{\partial^2(1/\varepsilon_o)/\partial p^2 - \partial^2(1/\varepsilon)/\partial p\}$ is evaluated using the values at 25°C, again in the hope that the difference between these values is the same at 65°C. The second term of equation (5.4) can then be calculated to have the value -0.544×10^{-3} c.c. mole^{-1} bar^{-1}. The predicted value of $\kappa^{\ddagger}$ at 65°C, is thus $\kappa^{\ddagger} = -1.7 \times 10^{-3}$ c.c. mole^{-1} bar^{-1}.

The uncertainties in the values of both the observed and calculated $\kappa^{\ddagger}$ are such that both could have an error of $\pm$(50-100)%. The values of -4×10^{-3} c.c. mole^{-1} bar^{-1} for the observed value of $\kappa^{\ddagger}$ and -2×10^{-3} c.c. mole^{-1} bar^{-1} for the predicted value of $\kappa^{\ddagger}$ can thus be taken to be in substantial agreement.

Hence, we can see that an explanation of the observed curvature in log k vs. pressure plots can be given in terms of the interaction between the reactant ions and the solvent. In an idealised model a reactant ion is often considered as the central metal ion plus its first coordination shell, distinct from the bulk solvent. The reality is that the influence of the central metal ion extends beyond the first coordination shell and we must regard the transition state as involving the second and perhaps the third solvent shells around the ion. When we regard it as such, the "compressibility of the transition state" is understandable in terms of the dependence on pressure of the first and second order differentials of the dielectric constant of the medium.

5.4.3 Conclusion

The pressure dependence of the homogeneous electron exchange rate between $Co(en)_3^{2+}$ and $Co(en)_3^{3+}$ has been studied, and the measured volume of activation thus obtained has been compared to the value predicted from the Marcus-Hush theory. The values have been seen to be in quite good agreement. An explanation of the curvature of log k

vs. pressure plots has also been given in terms of the pressure dependence of the dielectric constant of the medium.

This apparent success of the Marcus-Hush theory in predicting values of $\Delta V^{\ddagger}$ for outer-sphere electron exchange reactions, gives added confidence in the use of the theory for distinguishing outer-sphere reactions by a comparison of their calculated and observed volumes of activation. This criterion will now be applied to the $Fe^{2+}_{aq} - Fe^{3+}_{aq}$ electron exchange, where there exists some ambiguity in the mechanism involved.

Chapter 6

The Effect of Pressure on the Fe^{II}_{aq} - Fe^{III}_{aq} Electron Exchange Reaction

6.1 Introduction

The Fe^{II}_{aq} - Fe^{III}_{aq} electron exchange reaction was one of the earliest exchange systems to be investigated, and since the first successful attempt by Silverman and Dodson[93] to measure the rate of exchange, it has been the subject of a number of subsequent studies. A comprehensive review of all Fe(II) - Fe(III) electron exchange reactions that have been studied has been published by Reynolds and Lumry.[23]

Fe(III) forms complexes with a large number of anions, and these anions catalyse the electron exchange. The present studies have been carried out in perchlorate media, where association, if any, is minimal.

The Fe(II) - Fe(III) exchange has been well characterised, and from variations in [Fe(II)][Fe(III)] and $[H^+]$, the reaction has been shown to be described by second order kinetics, first order in both [Fe(II)] and [Fe(III)], and to exhibit an inverse hydrogen ion dependence. In the present studies, the first order dependence on each reactant has been assumed, but the inverse hydrogen ion dependence has been verified. From these results, it has been postulate that in the absence of added complexing anions, the electron exchange proceeds via two main pathways:

$$Fe(H_2O)_6^{2+} + {}^{*}Fe(H_2O)_6^{3+} \rightleftarrows Fe(H_2O)_6^{3+} + {}^{*}Fe(H_2O)_6^{2+} \qquad (A)$$

$$Fe(H_2O)_6^{2+} + {}^{*}Fe(H_2O)_5OH^{2+} \rightleftarrows Fe(H_2O)_5OH^{2+} + {}^{*}Fe(H_2O)_6^{2+} \qquad (B)$$

Because of the lability of both the Fe(II) and the Fe(III) ions, the mechanisms for these pathways is not known.[94] Several possible activated complexes can be proposed, and these will be considered in the light of the present studies in the Discussion at the end of this Chapter.

To obtain the rate constants for the hexaquo and the hydroxo pathways, given by equations (A) and (B) respectively, the $Fe^{II}_{aq} - Fe^{III}_{aq}$ electron exchange was studied as a function of $[H^+]$. The relatively fast rate of exchange permitted runs to be carried out only in the range $[H^+]$ = 0.5 to 0.08 M, using iron concentrations of the order of 10^{-5} M. At each hydrogen ion concentration employed, the rate of exchange was studied as a function of pressure in the range 0 to 1.4 kbar. The rates of exchange were measured at T = 2°C, although, as will be explained in Section 6.3.1, the temperature was not precisely constant throughout a run and corrections had to be made to allow for this.

6.2 Experimental

6.2.1 Materials

Ferric Perchlorate, $Fe(ClO_4)_3.9H_2O$

A ferric perchlorate stock solution was prepared from Purum grade Fluka $Fe(ClO_4)_3.9H_2O$. The solution was acidified with perchloric acid to prevent hydrolysis.

Ferrous Perchlorate, $Fe(ClO_4)_2.6H_2O$

Ferrous perchlorate is extremely difficult to obtain pure and always contains some ferric ions. This is due to the relative ease of aerial oxidation and to the presence of perchlorate ion, which is an oxidising agent. Non-ferrous impurities can be removed by the usual means of recrystallisation.

A ferrous perchlorate stock solution was prepared using $Fe(ClO_4)_2.6H_2O$, supplied by G.F. Smith Co. and recrystallised from 1 M perchloric acid. The recrystallised salt contained approximately 10% ferric ion. This was not important in the present studies, since only the total iron concentration, [Fe(II)] + [Fe(III)], had to be known. This stock solution was stabilised by the addition of perchloric acid.

Iron Solutions for Exchange Runs

From the stock solutions of ferric and ferrous perchlorate, just described, a set of four solutions was prepared by mixing the

appropriate volumes of each stock solution to give a molar ratio of ferrous to ferric ion equal to approximately 4:1, with a total iron concentration of 3.48×10^{-5} M. For each solution, sufficient perchloric acid was added to give the desired $[H^+]$, and the total ionic strength of each solution was made up to 0.5 M by the addition of sodium perchlorate. There was thus a set of four solutions, identical in [Fe(II)], [Fe(III)] and total ionic strength, but different in $[H^+]$. These were the solutions used for the kinetic runs.

Iron-59 Tracer

The radioisotope Fe-59 emits two main γ-rays of energies 1.3 Mev and 1.1 Mev, and has a half-life of 45 days.[76] Since the energies of the emitted γ-rays are very similar to those of Co-60, they could be counted using the scintillation counter with the same settings as for the Co-60 isotope. These same settings were checked and indeed fou to be the optimum settings for counting the Fe-59 isotope.

Since the half-times for the electron exchange, under the experimental conditions employed, and the assay times, were very short compared to the half-life of the isotope, no correction to the observed count rates was necessary to allow for the decay of the isotope.

The Fe-59 was obtained from the Radiochemical Centre, Amersham, in the form of ferric chloride in 0.1 M hydrochloric acid, with an initial specific activity of 16 mC per milligram $FeCl_3$. This was

fumed to dryness several times in a platinum crucible with A.R. conc. $HClO_4$ and a few drops of A.R. "100 volume" H_2O_2. The final residue was redissolved in 1 M perchloric acid and made up to such a volume as to give a specific activity suitable for labelling the exchange runs.

Sodium Acetate and Aluminium Perchlorate Solution

Stock solutions, 2 M in sodium acetate and 0.2 M in aluminium perchlorate, for use in separating the Fe(II) and Fe(III), were prepared by direct weighing of the salts. Univar A.R. sodium acetate and aluminium perchlorate, obtained from B. Newton Maine Ltd., were used.

α,α'-Bipyridyl

Stock solutions of 0.04 M α,α'-bipyridyl were prepared by direct weighing of B.D.H. Analar α,α'-bipyridyl and dissolving in absolute ethanol.

Standard Sodium Hydroxide Solution

1 litre of standard 0.1 M sodium hydroxide solution was prepared from a phial of "Volucon" pre-standardised sodium hydroxide concentrate, supplied by May and Baker Ltd.

All other materials used have been described previously.

6.2.2 Apparatus

Pressure Vessel

The high pressure sampling vessel was used for the study of this reaction. It was necessary to use the inert Pt/Ir capillary outlet tubing, since the reaction solutions were quite strongly acid. The vessel was sealed using Neoprene O-rings, and with these, sealing was instantaneous upon application of pressure. Since the reaction times were of the order of minutes, the O-rings provided an advantage over the copper gaskets, which took 1 or 2 minutes to seal.

Temperature Control

The rate of electron exchange was studied at 2.0°C. The pressure vessel was thermostatted to this temperature by immersion in a well-stirred glycerol/water mixture contained in an insulated tank.

Temperature control of the bath to $\pm$ 0.1°C was achieved with a refrigerating unit operating continuously in opposition to a solid-state proportional heater, regulated by a thermistor probe.

The refrigerating unit was a Rheinische Thermostatic Refrigerator Type TK1. Cooling was achieved by immersing the evaporator bulb of the unit in the medium to be cooled.

Atomic Absorption Spectrometer

Analyses for the total iron content of the reaction solutions were carried out using a Unicam S.P.90A Atomic Absorption Spectrometer. Calibration curves were prepared using standard iron solutions, prepared by dissolving pure iron wire in hydrochloric acid.

Temperature Measurement of Solutions Under Pressure

The rise in temperature of the reactant solutions caused by pressurisation was important in the study of this reaction, since the time taken for complete dissipation of this heat was comparable to the half-times of reaction. It was necessary, then, to know the temperature of the solution as the reaction progressed.

Temperatures of the solution inside the Perspex reaction vessel were measured using an S.T.C. Type F thermistor, which had a 2 kΩ resistance and nominal temperature coefficient at 20°C of -3.1 %/°C. The thermistor is shown diagramatically in Figure 6.1(a). As supplied, it was a vacuum-filled, glass-sealed type, but for our purposes a small hole was made in the glass wall near the upper end, as shown. The inside was then filled with pure conductivity water, which did not significantly affect the resistance properties of the thermistor. This enabled the thermistor to be put under pressure without shattering it.

The leads were connected to a length of double-cored Pyrotenax cab.

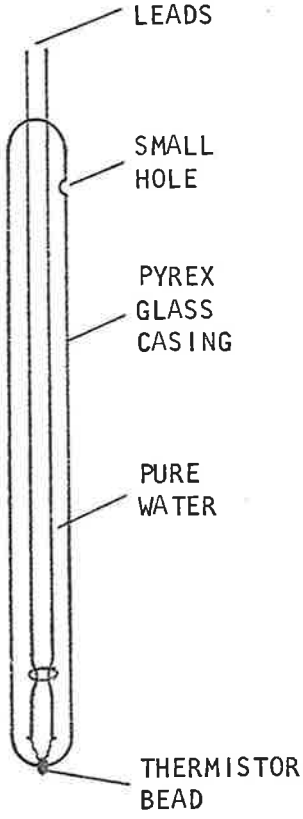

Figure 6.1(a)

Modified Thermistor

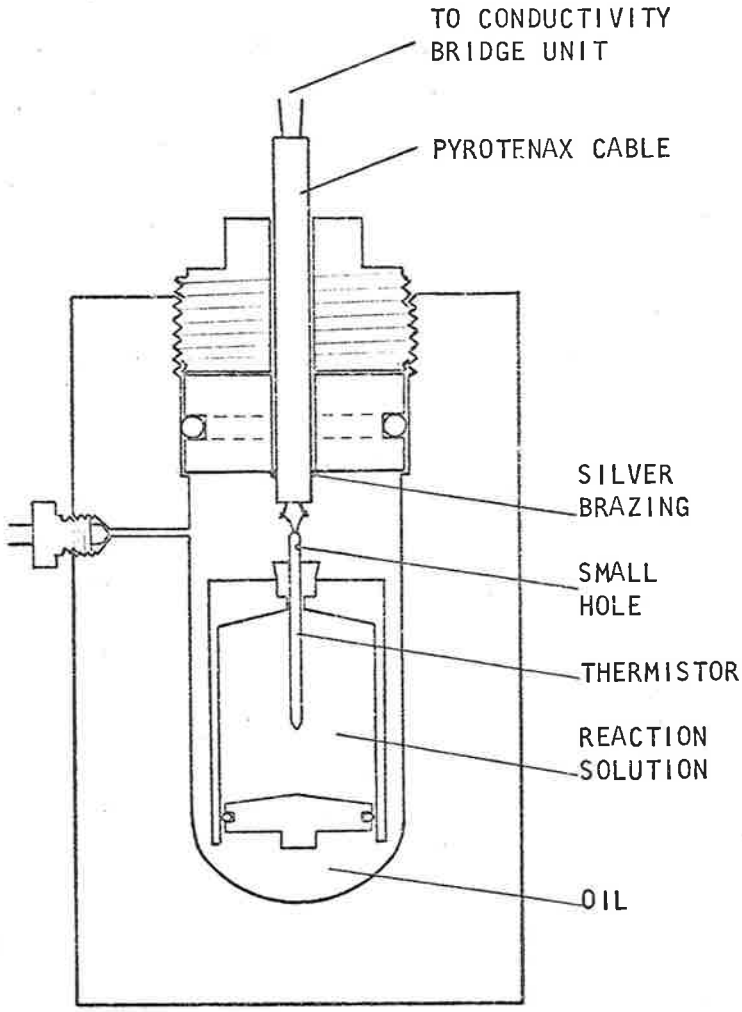

Figure 6.1(b)

Apparatus for Measuring Temperature Changes due to Pressurization

which was sealed into a sealing plug of the pressure vessel. The arrangement is shown in Figure 6.1(b).

The resistance of the thermistor was measured using a conductivity bridge unit, incorporating a 10 kΩ decade resistance box, connected to a C.R.O. for quick, visual detection of the null point.

The sensitivity of this arrangement was such as to be able to measure changes in temperature of 0.014°C.

The variation with time of the temperature of the solution inside the reaction vessel was measured at each of the pressures employed in the kinetic runs, and hence corrections could be made to the values for each run, depending on the pressure used.

6.2.3 Procedure for Kinetic Runs

About 30 ml. of the stock reaction solution, containing the required concentrations of Fe^{2+}, Fe^{3+}, $HClO_4$ and added $NaClO_4$, was placed in the Perspex reaction vessel. The Teflon plunger was placed in position and the entire vessel was almost fully immersed in the thermostatted bath and left to equilibrate for 1 $^{1}/_{2}$ hours. Tests showed that it took about 75 minutes for the reaction solution to cool from room temperature to 2.0°C.

The vessel was then quickly withdrawn, and after labelling the solution with one drop of Fe-59 tracer through the outlet opening,

the vessel was attached to the outlet tubing, shaken to mix the tracer uniformly and then lowered into the pressure vessel. All this took about $^{1}/_{2}$ - $^{3}/_{4}$ minute. Tests showed that during this time the temperature of the solution rose by not more than 0.3°C and usually by less than this.

The pressure was then raised to the required value and at predetermined time intervals, aliquots were taken for sampling. The reaction was normally followed for 1 - 1 $^{1}/_{2}$ half-times. The half-times of exchange varied from 42 to 155 minutes.

Aliquots were taken by discharging into graduated glass tubes about 1 ml. of reaction solution which was discarded, followed by another 1.5 ml. of reactant solution. 1 ml. of this was withdrawn with a pipette and run into the quenching mixture and then the Fe(II) and Fe(III) separated for radiometric assay. The 1 ml. pipette used was coated with "Repelcote", a water-repellant silicone compound. This enabled the 1 ml. aliquot to be quickly and accurately discharged into the quenching mixture. The sampling operation took about 30 seconds.

Two "infinite time" samples were taken after times greater than ten half-times for the exchange.

6.2.4 Procedure for Separation of Fe(II) and Fe(III)

The separation scheme employed here was essentially the method of Silverman and Dodson.[93] This method has been used almost

exclusively in the many subsequent studies, with minor modifications. Few of these modifications have been reported in much detail, and in most part they seem to have been appropriate only to the conditions under which the reaction was studied.

The basis of the method was to add the aliquot of reaction mixture to a solution of α,α'-bipyridyl in an acetate buffer of pH 5 and precipitate hydrated ferric oxide with ammonia. The Fe(II) remained in solution as the $Fe(dipy)_3^{2+}$ complex.

A number of preliminary tests were carried out to determine the best conditions for effecting this separation. The effectiveness and reproducibility of the separation was subject to the usual conditions of concentrations of reagents, order of mixing and time intervals between steps.

It was found that

(i) a pH of about 5 in the quenching mixture was best, but a value within about 2 pH units above or below this value was suitable;

(ii) the ammonia solution should be added as soon as possible after the aliquot was added to the bipyridyl solution;

(iii) there was no difference in the separation whether the mixture wa allowed to stand, after adding the ammonia solution, for 5 minut or 125 minutes before centrifuging; but it was preferable to leave it standing for at least 10-15 minutes to ensure complete precipitation of the Al^{3+} co-precipitant, otherwise some

continued to precipitate on the walls of the counting tubes;

(iv) it made no difference to the separation whether the mixture, after adding the ammonia solution, was kept in ice or at room temperature, but it was preferable to let stand at room temperature to give a heavier, more flocculent precipitate;

(v) the concentration of the bipyridyl in the quenching mixture was immaterial, provided it was present in excess;

(vi) the concentration of the Al^{3+} was immaterial, provided it was sufficient to give a reasonable volume of precipitate.

The following was the actual method used in these studies:

2 ml. of a solution of 2 M sodium acetate and 0.2 M aluminium perchlorate, together with 1 ml. of an alcoholic solution of 0.04 M bipyridyl, were placed in a 10 ml. volumetric flask and cooled in ice. Immediately before sampling the reaction mixture, a standard-size $^{1}/_{4}$" magnetic follower, coated with Teflon, was put in the flask and the flask placed on a magnetic stirrer. On sampling, the accurate 1 ml. aliquot was discharged into the stirred quenching mixture, followed immediately by 1 ml. of .880 S.G. ammonia solution. The quenched solution was stirred for 5 minutes, then the volume made up to the mark with water and left to stand, unstirred, for a further 10 minutes. After this time the mixture was centrifuged for about 2 minutes and then 5.0 ml. of the supernatant solution was withdrawn with a pipette, transferred to a counting tube and assayed in the

scintillation counter for 200 seconds.

Since the volume of each aliquot of the reaction solution, the final volume of the quenching mixture and the volume of supernatant solution counted were the same for each sample taken, the actual count recorded could be used in calculating the fraction of exchange, F, instead of the specific activity.

6.3 Results

6.3.1 Heating Effect of the Adiabatic Pressure Change

Stainless steel is not an efficient thermal conductor and because the walls of the pressure vessel were 1 in. thick, the contents of the vessel were substantially insulated from the surrounding thermostatting medium. Hence, because the time taken to raise the pressure inside the vessel was less than 3 minutes, this process was essentially an adiabatic one. The work done, then, in applying pressure to the vessel's contents, disregarding friction losses, appeared largely in the form of heat, the thermodynamic relation for an adiabatic compression being

$$\left(\frac{\partial T}{\partial p}\right)_s = \frac{T}{c_p}\left(\frac{\partial V}{\partial T}\right)_p \qquad (6.1)$$

where s is the entropy, V the volume and c_p the constant-pressure heat capacity of the liquid.

At the commencement of the pressure studies reported in this work, an estimate of the temperature rise, caused by pressurizing a reaction solution at the start of a pressure run, was determined using a copper-constantan thermocouple (see Chapter 4). It was found that raising the pressure to a value between 1.4 and 2 kbar caused a rise in temperature of 2° to 3°C. The sensitivity of the instrumentation, though, was only such as to give an uncertainty of approximately $\pm$ 0.5°C. For the previous two reactions, reported in Chapters 4 and 5, an initial temperature rise of this order of

magnitude was not important, because the half-times of reaction were of the order of hours. Compared to this, the time taken to arrive at thermal equilibrium with the surrounding thermostatting medium was short.

However, in the case of the Fe(II) - Fe(III) reaction, temperature rises of this magnitude were significant, due to the relatively short half-times of reaction (of the order of tens of minutes at 2°C).

There appeared to be two methods of overcoming this problem. The first was to have a thermostatting coil around the Perspex reaction vessel inside the pressure vessel, and to circulate through it the water/glycerol mixture from the surrounding bath. If this were thermally efficient, then the temperature of the reaction solution could quickly be brought to 2.0°C and the reaction carried out at constant temperature. Coils of various size tubing, made from both copper and nickel, were tried, but none was satisfactory, due either to collapsing under pressure or to thermal inefficiency.

The second solution was to measure the temperature accurately as the reaction progressed and to correct the observed rates, knowing the activation energy of the reaction. This was the method adopted. Accordingly, an accurate study of the effect of change of pressure on the temperature of the reaction solution was undertaken, using the thermistor as described in Section 6.2.2.

The thermistor was first calibrated accurately by measuring its resistance, Q, at several known temperatures, T, between 2° and 4°C. Over this narrow range, Q varied linearly with T. A plot of Q against T gave a slope, $\partial Q/\partial T$, of 68 $\pm$ 1 ohm. deg.$^{-1}$. This calibration was performed at pressures of 1 bar and 350 bar, and although the absolute values of Q were slightly different at each pressure, the slopes, $\partial Q/\partial T$, were the same within experimental error. Hence, the temperature coefficient of the thermistor was substantially unaffected by pressures.

The reaction vessel was filled with water and the apparatus assembled as described in Section 6.2.2 (see Figure 6.1). The vessel was then left in the thermostatted bath for 1 $^{1}/_{2}$ hours to come to thermal equilibrium at 2.0°C. (Earlier tests showed that it required about 75 minutes for a solution inside the Perspex reaction vessel, initially at room temperature, to cool to 2.0°C within the pressure vessel.)

The pressure was then raised to the desired value and readings of the thermistor resistance were taken at various time intervals until there was no further change in the reading. This final reading corresponded to 2.0°C. The pressure was then released and again readings of the resistance were taken until there was no further change. The final reading again corresponded to 2.0°C. This procedure was repeated at pressures of 345, 689, 1034 and 1379 bar.

The plot of Q against time, t, for p = 345 bar is shown in

Figure 6.2. This plot is typical for each of the pressures. The initial rapid fall in Q corresponded to the heating of the solution as the pressure was raised. This was followed by a gradual rise in Q as the heat generated was conducted away, and the value of Q levelled out as the temperature of the solution approached 2.0°C, the temperature of the outside bath. The subsequent rapid rise in Q corresponded to the release of pressure, and this was again followed by a gradual fall in Q as the temperature of the solution rose to 2.0°C again.

The reason for the slight difference in the value of Q at the three points A, C and E is obscure. However, it is clear that these values each corresponded to a temperature of 2.0°C under the conditions of pressure at those points.

It can be seen from Figure 6.2 that $\Delta Q_{heating}$ was slightly greater than $\Delta Q_{cooling}$. This was due to a gradual fall in pressure from 345 bar at B to 303 bar at C, brought about by the cooling of the solution in going from B to C. $\Delta Q_{heating}$, then, corresponded to the rise in temperature in going from p = 1 bar to p = 345 bar, while $\Delta Q_{cooling}$ corresponded to the temperature fall in going from p = 303 bar to p = 1 bar. If the system were completely adiabatic, we should expect $\Delta Q_{heating}$ to equal $\Delta Q_{cooling}$ for the same pressure change. It was found that this was very nearly the case. This observation is important because it indicates that, in the kinetic runs, the net

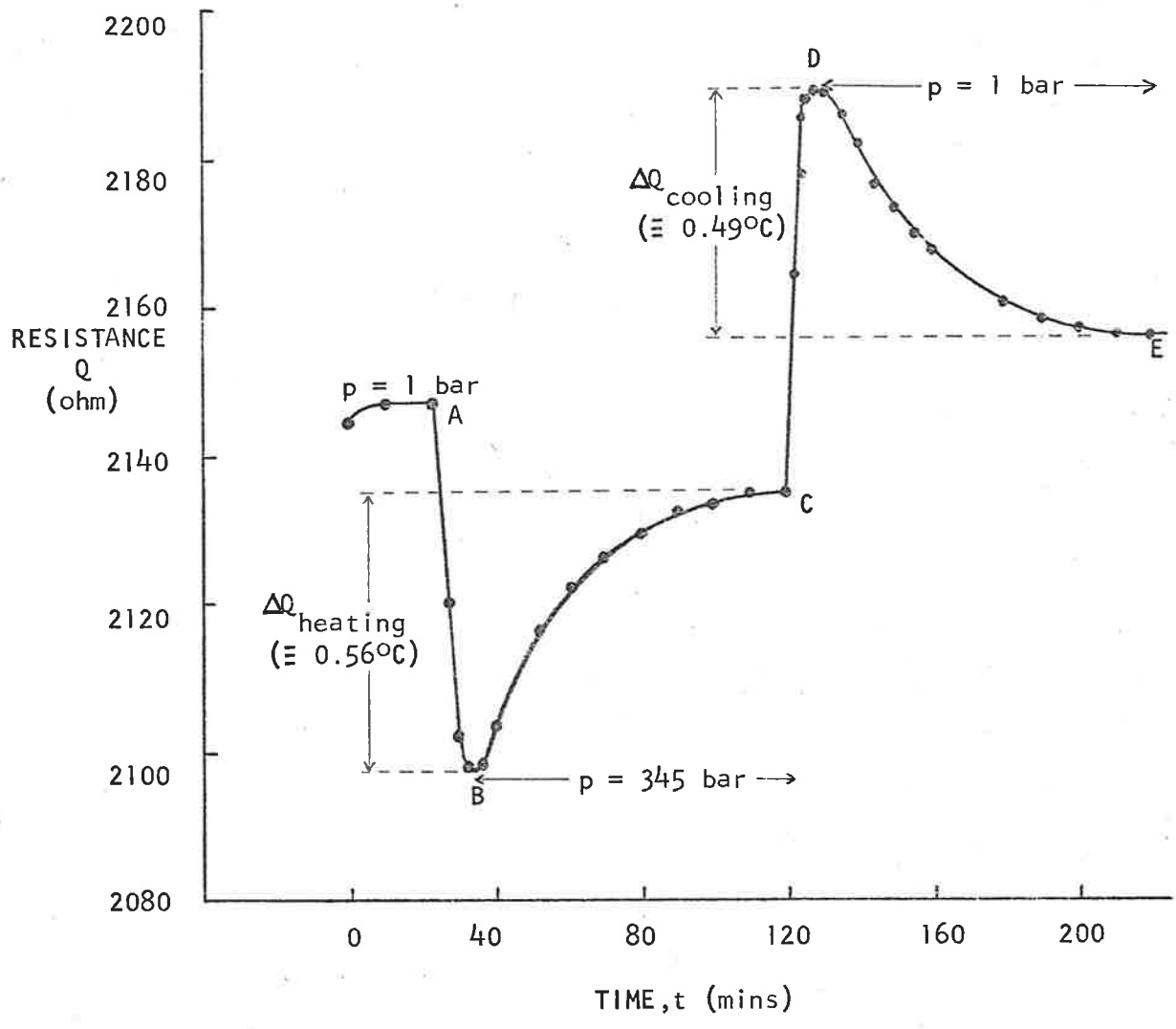

Figure 6.2 Heating and Cooling Effect on Reaction Solution due to Rapid Changes in Pressure

temperature change in the solution during sampling is zero. As an aliquot of solution is discharged the pressure drops slightly and this will be accompanied by a small, isotropic fall in temperature throughout the reaction solution. Immediately after, as the pressure is restored to its original value, the temperature of the solution will rise an amount equal to the preceeding fall and so the net temperature change will be zero.

From Figure 6.2 it can be seen that the change in resistance, as the solution cooled in going from B to C, appeared to be a first order process. If this were so, that is, if the change in Q could be described by the rate law,

$$dQ/dt = k_T(Q_t - Q_\infty), \tag{6.2}$$

which on integrating gives

$$\log (Q_t - Q_\infty) = -(k_T t/2.303) + \text{const}, \tag{6.3}$$

then plots of log $(Q_t - Q_\infty)$ vs. time, t, should be linear. This was found to be so, as can be seen from Figure 6.3, where the data from the measurements at p = 345 bar have been plotted. Figure 6.3 is typical of the plots obtained for the data at the other pressures. The values of k_T, obtained from the slopes of these first order plots, are given in Table 6.1, together with the corresponding values of the pressure applied.

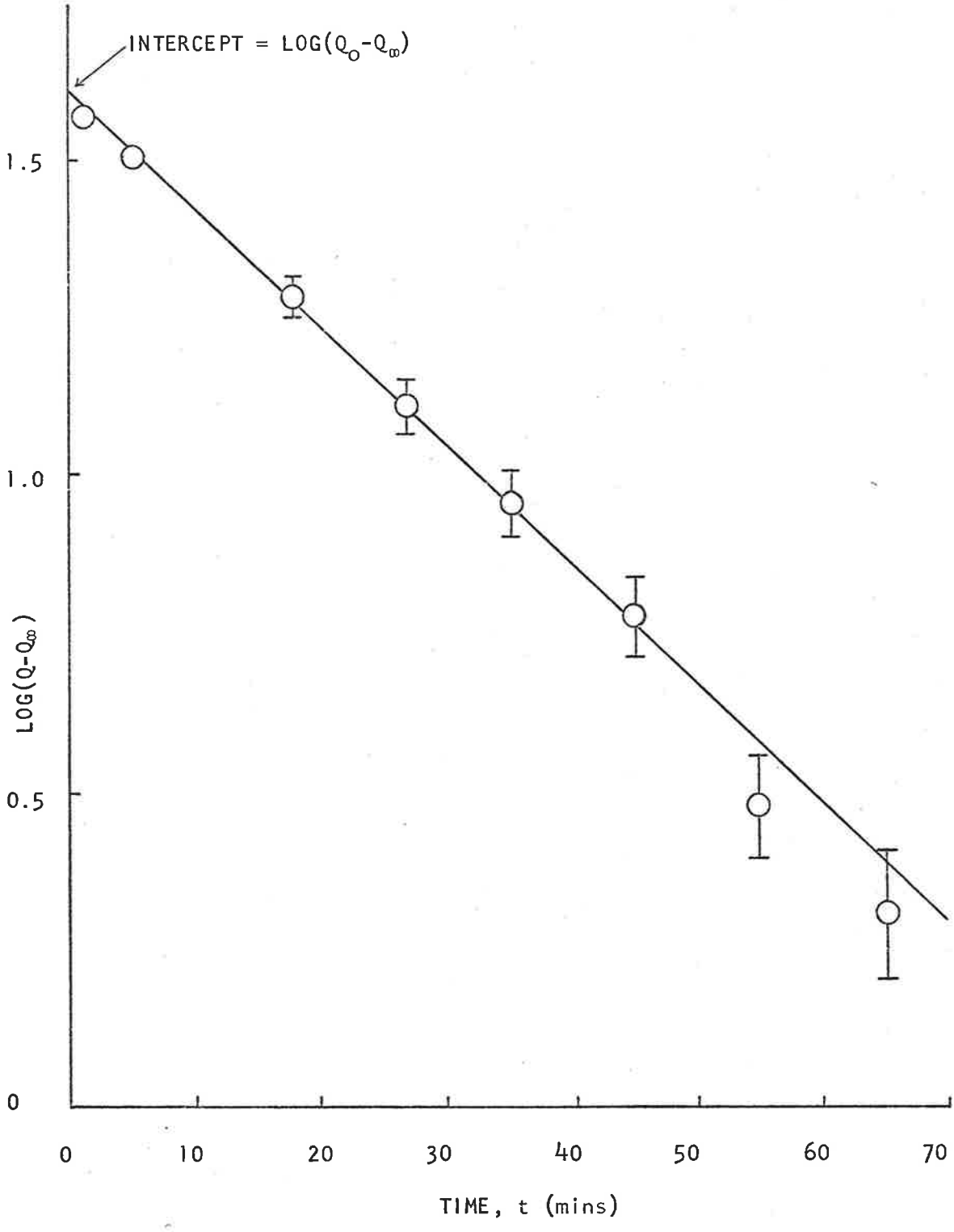

Figure 6.3 Typical First Order Plot of Change in Resistance, Q, with Time, during Temperature Equilibration after Rapid Change in Pressure (Pressure Change: 1 to 345 bar)

It can be seen that the values of k_T are essentially constant and independent of the pressure. The constant, k_T, could be described as a "coefficient of thermal conductivity" for that particular vessel, since it determines the rate at which thermal equilibrium can be established between the solution inside the reaction vessel and the surrounding medium. For the vessel used in these studies, then, it was found that $k_T = 0.020 \pm .001$ min.$^{-1}$.

Table 6.1

Values of Coefficient of Thermal Conductivity, k_T, at Different Pressur

p (bar)	k_T (min.$^{-1}$)
345	.019
689	.019
1034	.021
1379	.021
	(S.D. = $\pm$ .001)

Hence, the temperature, T, of a reaction solution at any given time, t, after the vessel had been pressurized to a given pressure, p, can be determined by equation (6.3), knowing the relation between Q and T and the value of the constant of integration.

The constant of integration is equal to log $(Q_o - Q_\infty)$, where Q_o and Q_∞ are the values of Q at times t = o and infinity respectively. Its value can be obtained at each of the pressures studied from the intercept of the log $(R - R_\infty)$ vs. time plots (cf. Figure 6.3). In

Figure 6.4 the values of $(Q_o - Q_\infty)$ obtained from these plots have been plotted as a function of pressure. Hence, the value of the constant of integration, $\log (Q_o - Q_\infty)$, can be obtained from this graph for any given pressure. The values at p = 689 bar and 1379 bar, obtained from Figure 6.4, are 2.074 and 2.472 respectively. Substituting in equation (6.3) gives the relations:

$$\text{for p = 689 bar:} \quad \log (Q - Q_\infty) = -0.020\ t + 2.074 \qquad (6.4)$$

$$\text{for p = 1379 bar:} \quad \log (Q - Q_\infty) = -0.020\ t + 2.472 \qquad (6.5)$$

The temperature coefficient of the thermistor, $\partial Q/\partial T$, was found to be 68 ohm. deg.$^{-1}$. Substituting and rearranging, equations (6.4) and (6.5) become:

$$\text{for p = 689 bar:} \quad T = (1/68)\exp(4.776 - 0.04606\ t) + 275 \qquad (6.6)$$

$$\text{for p = 1379 bar:} \quad T = (1/68)\exp(5.693 - 0.04606\ t) + 275 \qquad (6.7)$$

where T is the temperature of the reaction solution in degrees Kelvin at a time t minutes after pressurizing. Equations (6.6) and (6.7) were used to correct the observed rates of exchange to a constant temperature of 2.0°C, as described below in Section 6.3.2.

6.3.2 Evaluation of Rate Data for Exchange Runs

If we assume, initially, that the temperature of the solution remained constant throughout a run - as was the case for runs at

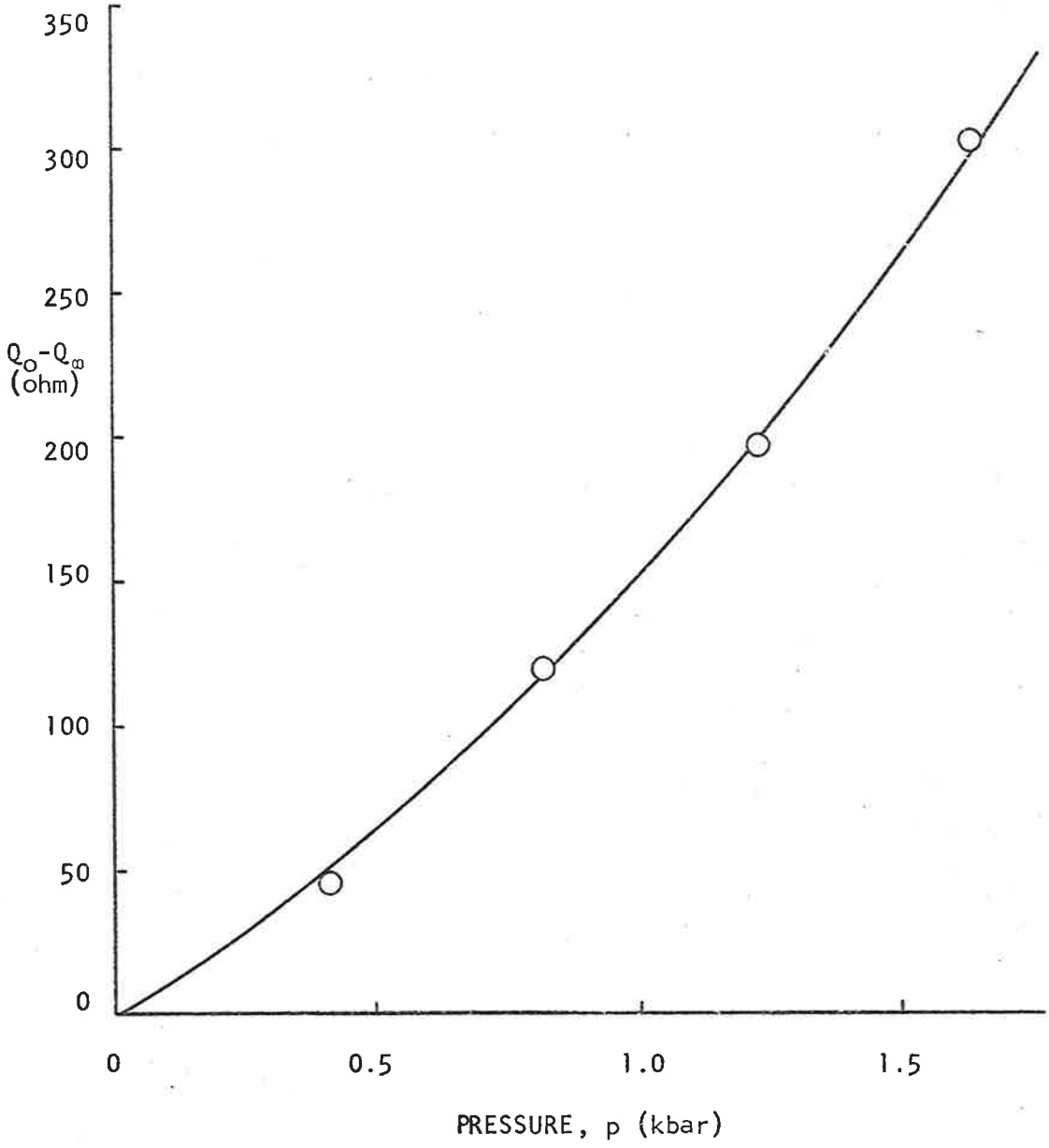

Figure 6.4 Variation of $(Q_o - Q_\infty)$ with Pressure

p = 1 bar, but not for the runs at higher pressures - then the rate of exchange can be obtained from the McKay equation (1.1), i.e. the rate of electron exchange, R, between Fe(II) and Fe(III) is given by:

$$R = -\frac{2.303}{t}\frac{[Fe^{II}][Fe^{III}]}{[Fe^{II}] + [Fe^{III}]}\log(1 - F) \qquad (6.8)$$

where $[Fe^{II}]$ and $[Fe^{III}]$ represent the total concentrations of Fe(II) a Fe(III) respectively, in all their forms. For this reaction, the fraction of exchange, F, given by equation (1.2), was evaluated using an experimental "infinite-time" value, determined after ten or more half-times had elapsed, when the distribution of the Fe-59 tracer between the Fe(II) and Fe(III) was essentially complete.

Since this reaction is described by second order kinetics, i.e.

$$R = k_{obs}[Fe^{II}][Fe^{III}], \qquad (6.9)$$

the observed rate constant, k_{obs}, can be found by plotting log (1 - F) against time and then using the half-time, $t_{1/2}$, thus obtained, in equation (1.3). Thus

$$k_{obs} = \frac{0.693}{t_{1/2}}\frac{1}{[Fe^{II}] + [Fe^{III}]} \qquad (6.10)$$

A typical exchange plot for p = 1 bar, where the temperature remained constant at 2.0°C throughout the run, is shown in Figure 6.5. It can be seen that for this plot, there was a zero-time exchange of about 10%. That this was due almost entirely, if not

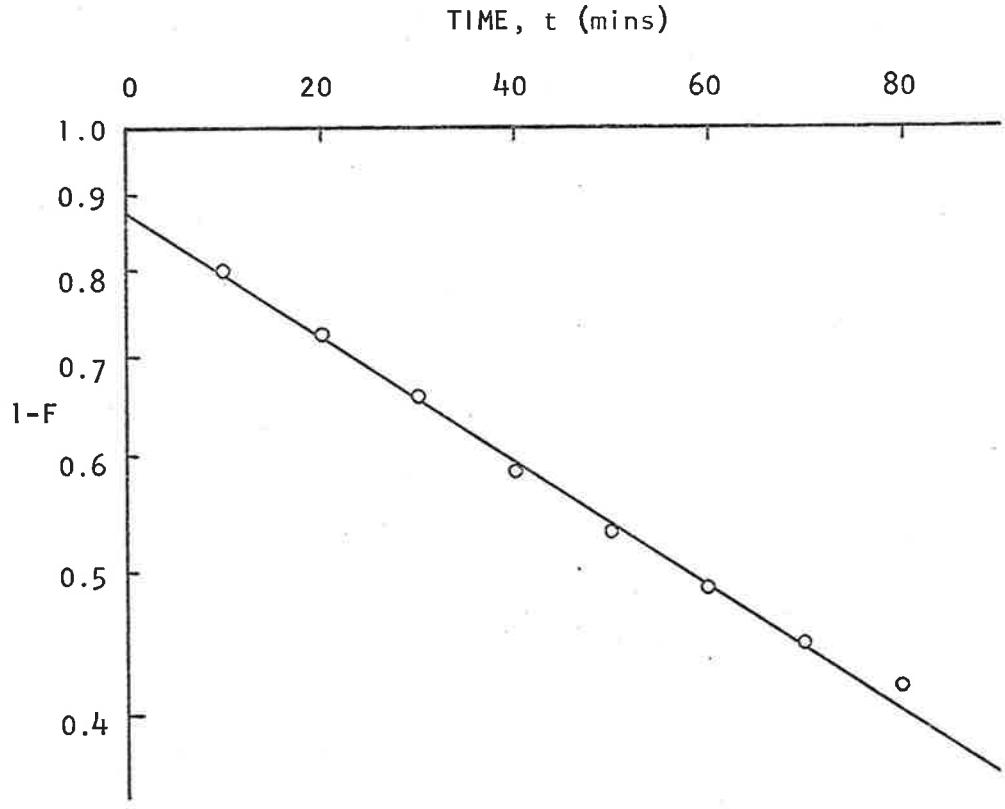

$[Fe^{II}] + [Fe^{III}] = 3.48 \times 10^{-5}$ M
$[H^+] = 0.117$ M
$\mu = 0.5$ M
T = 2.0°C
p = 1 bar

Figure 6.5 Typical Exchange Plot for p = 1 bar

completely, to the sampling and separation procedure was indicated by the observation that the zero-time exchange varied between 10% and 20%, depending on the rate of the particular run. Also, in some preliminary runs carried out in a stoppered glass vessel, where direct sampling from the reaction solution was possible, the zero-time exchange was only 3-4%. This may be compared to the value of 35% zero-time exchange reported originally by Silverman and Dodson.[93]

Because of this exchange induced by sampling and separation, it was important to perform all the operations associated with the sampling and separation procedures in an identical manner each time. In this way the amount of induced exchange remained constant for each sample and k_{obs} could still be obtained from the slope of the exchange plot, as indicated in Chapter 1.

6.3.3 Temperature Corrections to Observed Rate Constants

For the reactions conducted at high pressure, the temperature of the reaction solution at any given time after pressurizing was given by equation (6.6) or (6.7), depending on the pressure. Over a small time interval, the temperature of the reaction solution was effectively constant, and hence the observed rate constant at this temperature could be found using equations (6.8) and (6.9).

Thus the time for each exchange run was divided into eight equal parts, varying from 8 to 15 minutes depending on the run, and at the

end of each interval the solution was sampled. The rate constant was then calculated over this small time interval, for which the temperature was taken to be that calculated at the mid-point of the interval. The rate constant thus obtained was then corrected to 2.0°C, using the relation

$$\log (k_1/k_2) = - \frac{E}{2.303\ R} \left(\frac{1}{T_1} - \frac{1}{T_2}\right) \qquad (6.11)$$

where R is the universal gas constant and E the activation energy, which was taken to be 10.0 kcal. mole^{-1}.[93] For the runs at p = 689 bar, the correction to the rate constant, calculated over the first time interval, amounted to approximately 7%, and at p = 1379 bar, to approximately 14%. These corrections became smaller in the succeeding time intervals, as the temperature of the solution approached 2.0°C. Each exchange run thus yielded seven values for the observed rate constant, all corrected to 2.0°C. The rate constant for the run was then taken to be the mean of these values.

In order to make this method of temperature correction more precise, instead of using the experimental values of specific activity at times t_i and t_{i+1} for calculating the rate constant for that time interval, the values used were read from a graph of experimental specific activities plotted against time, through which a smooth curve was drawn. This procedure can be justified with reference to the runs carried out at p = 1 bar, where no temperature correction is

made. The values obtained for k_{obs}, by using either the experimental specific activities or the values read from a smooth curve through these values when plotted, can be compared with the rate constant estimated in the usual way by a "least squares" fit to all the data on the exchange plot. Table 6.2 contains typical data for a kinetic run at p = 1 bar.

Table 6.2

The Rate Constant for a Run at p = 1 bar, Evaluated by the Different Methods

	calculated using experimental values for specific activity	calculated using values of specific activity read from graph
Rate constant, k_i, for each time interval, t_i to t_{i+1}. (M^{-1} $min.^{-1}$)	114 132 106 133 149 162 106	133 129 127 129 130 135 140
Mean observed rate constant, k_{obs}. (M^{-1} $min.^{-1}$)	129 (S.D. = 22)	132 (S.D. = 5)
Observed rate constant, k_{obs}, determined from the slope of the exchange plot, using the least squares procedure = 136 $\pm$ 6 M^{-1} $min.^{-1}$.		

The mean value from each column can be compared with the value of the rate constant obtained from a McKay-type plot, using a least squares procedure to obtain the slope of the line of best fit through the experimental data. It is seen that the values of k_{obs} obtained by the different procedures are substantially the same.

However, the variation of values in the first column is seen to be much greater than in the second column. When a temperature correction is to be made to an individual value, k_i, the correction will be more accurate the closer the value of k_i is to its true value. Hence, the values of the second column would be more suitable.

For all the high pressure runs, then, where temperature corrections had to be made, the values of k_i were calculated using the values of specific activity read from a graph of the experimental values plotted against time.

Table 6.3 gives data for a similar comparison for a typical run at high pressure. The data have been corrected for temperature.

Table 6.3

The Rate Constant for a Run at 689 bar, Evaluated by the Different Methods

	calculated using experimental values for specific activity	calculated using values of specific activity read from graph
Rate constant, k_i, for each time interval, t_i to t_{i+1}, corrected to 2.0°C. (M^{-1} $min.^{-1}$)	177	178
	196	160
	151	159
	130	162
	169	158
	181	153
	109	154
Mean corrected rate constant, k_{obs}. (M^{-1} $min.^{-1}$)	159 (S.D. = 30)	161 (S.D. = 7)

Again it is seen that the variation in values is greater in the first column than in the second. Using the data from the second column has the further advantage that values which have an intolerable error can readily be seen, as for example the first value of k_i in column two. This is not evident from the first column. Values of k_i which differed by more than one standard deviation from the mean were neglected and the mean recalculated. Thus for the run illustrated in Table 6.3, the corrected rate constant, k_{obs}, was taken

to be 158 M^{-1} $min.^{-1}$, which was the mean of the second column, calculated after omitting the first value of k_i. The rate constants obtained in this way very rarely differed by more than a few percent from those calculated as the mean of the first column, but they were considered more accurate.

Calculations

A computer program was written to process the experimental data from the exchange runs. The input data consisted of the experimental conditions of pressure, $[H^+]$ and $[Fe^{II}] + [Fe^{III}]$, and the specific activities at times t and infinity for all runs. The program calculated the observed rate constants, corrected them for temperature changes due to pressurization and calculated the volume of activation for the hexaquo pathway for exchange from the $[H^+]$ and pressure dependence, as described in the following section.

6.3.4 The Effect of Pressure on the Electron Exchange Rate

Since a volume of activation refers to a single, elementary proces or pathway of reaction, the overall effect of pressure on a reaction must be interpreted in terms of the volumes of activation for each pathway or mechanism involved.

The Fe(II) - Fe(III) exchange has been shown[93] to be described by the rate law

$$R = k_{obs}[Fe^{II}][Fe^{III}]$$

$$= \{k_1 + k_2'/[H^+]\}\ [Fe^{II}][Fe^{III}] \qquad (6.12)$$

Hence, exchange is assumed to proceed by the following pathways consistent with this rate law:

$$Fe(H_2O)_6^{2+} + {}^{*}Fe(H_2O)_6^{3+} \underset{\leftarrow}{\overset{k_1}{\rightarrow}} Fe(H_2O)_6^{3+} + {}^{*}Fe(H_2O)_6^{2+} \qquad (A)$$

$$Fe(H_2O)_6^{2+} + {}^{*}Fe(H_2O)_5OH^{2+} \underset{\leftarrow}{\overset{k_2}{\rightarrow}} Fe(H_2O)_5OH^{2+} + {}^{*}Fe(H_2O)_6^{2+} \qquad (B)$$

k_1 is the rate constant for the acid-independent pathway, (A), and k_2 is the rate constant for the acid-dependent pathway, (B), and is given by

$$k_2 = k_2'/K_a \qquad (6.13)$$

where K_a is the acidity constant for the hydrolysis equilibrium

$$Fe(H_2O)_6^{3+} \underset{\leftarrow}{\rightarrow} Fe(H_2O)_5OH^{2+} + H^+ \qquad (6.14)$$

If the rate law given by equation (6.12) adequately describes the electron exchange process, then a plot of k_{obs} vs. $1/[H^+]$ should be linear, with an intercept k_1 and slope k_2'. The pressure dependence of k_1 and k_2' could then be determined by measuring the rate of exchange as a function of $[H^+]$ at several different pressures, to obtain values of k_1 and k_2' at these pressures.

The electron exchange was thus studied as a function of $[H^+]$ in the range $[H^+]$ = 0.464 M to 0.082 M, at pressures of 1, 689 and 1379 bar. The results are given in Table 6.4 where each value represents the mean of two or three runs.

Table 6.4

Variation of Observed Rate Constant, k_{obs}, with $[H^+]$ and Pressure

T = 2.0°C μ = 0.5 M $[Fe^{II}] + [Fe^{III}] = 3.48 \times 10^{-5}$ M

p (bar)	$[H^+]$ (M)	Mean Observed Rate Constant, k_{obs}. (M^{-1} $min.^{-1}$)
1	.464	137
	.188	187
	.117	271
	.082	369
689	.464	162
	.188	222
	.117	312
	.082	410
1379	.464	189
	.188	273
	.117	350
	.082	444

The values listed in Table 6.4 are plotted in Figure 6.6. In this plot, the line of best fit that has been drawn through the set of experimental data for each pressure has been drawn so as to best

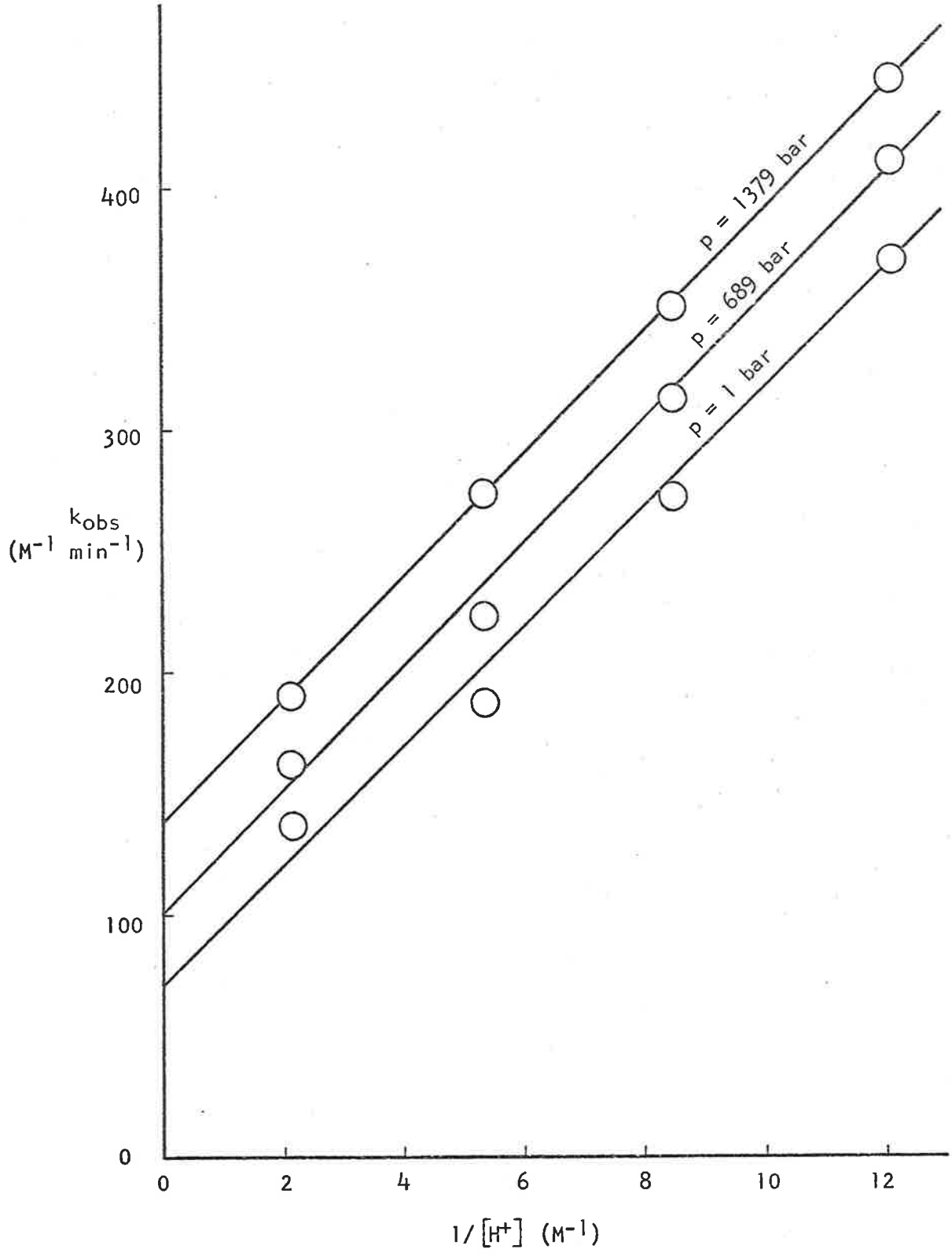

Figure 6.6 Dependence of Observed Rate Constant, k_{obs}, on Pressure, p, and $[H^+]$

satisfy two independent criteria. These are (i) that plots of k_{obs} vs. $1/[H^+]$ should be linear at constant pressure, and (ii) that plots of k_{obs} vs. pressure should be nearly linear at constant $[H^+]$ over a relatively small pressure range, such as used here.

The values of k_1 and k_2' at each pressure, obtained from the intercepts and slopes of these plots are given in Table 6.5.

Table 6.5

Variation of Rate Constants, k_1 and k_2', with Pressure

T = 2.0°C μ = 0.5 M $[Fe^{II}] + [Fe^{III}] = 3.48 \times 10^{-5}$ M

p (bar)	k_1 (M^{-1} $min.^{-1}$)	k_2' ($min.^{-1}$)
1	70 ± 10	24.6 ± .9
689	100 ± 8	25.4 ± .7
1379	137 ± 7	25.2 ± .6

The value of 70 ± 10 M^{-1} $min.^{-1}$ at 1 bar pressure for k_1, the rate constant for the acid-independent path, (A), is in excellent agreement with the value of 71 M^{-1} $min.^{-1}$, estimated from the data of Silverman and Dodson.[93] Similarly, the value of k_2 = (1.57 ± .10) x 10^3 M^{-1} $sec.^{-1}$ at p = 1 bar, calculated using the value K_a = 0.26 x 10^{-3} M for 0°C,[93] is in reasonable agreement with the value of 1.27 x 10^3 M^{-1} $sec.^{-1}$ estimated from Silverman and Dodson's data.

The values of k_1, given in Table 6.5, have been plotted in Figure 6.7 as log k_1 against pressure. From the slope of this plot,

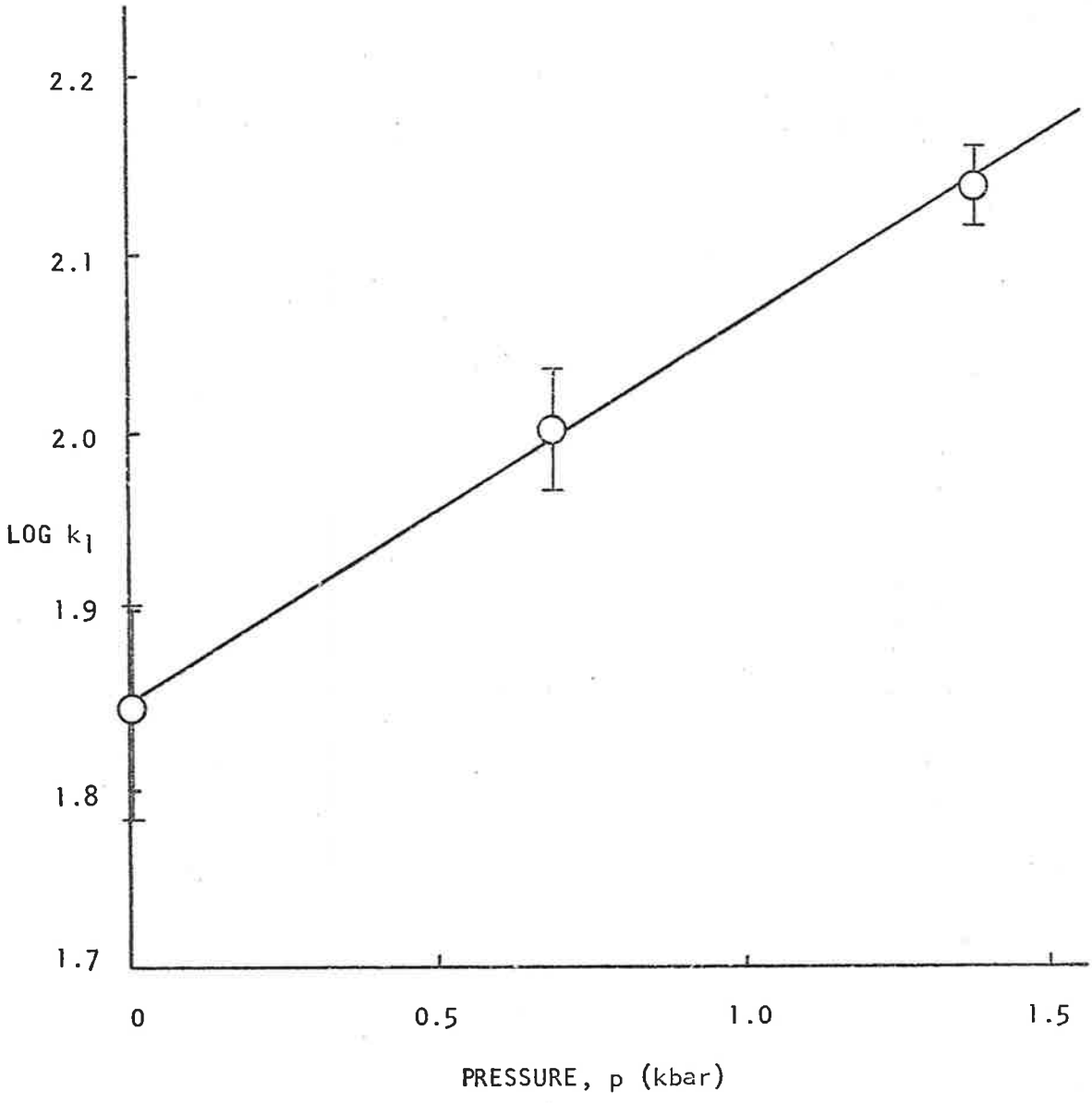

Figure 6.7 Pressure Dependence of Rate Constant, k_1

the volume of activation, corrected for the term RTβ (1.14 c.c. $mole^{-1}$), was found to be -12.2 ± 1.5 c.c. $mole^{-1}$. This value refers to the acid-independent pathway, represented by equation (A), for electron exchange between $Fe(H_2O)_6^{2+}$ and $Fe(H_2O)_6^{3+}$.

6.4 Discussion

6.4.1 Comparison of Observed and Predicted $\Delta V^{\ddagger}$ Values

The predicted value of $\Delta V^{\ddagger}$ for the electron exchange between the two hexaquo ions, $Fe(H_2O)_6^{2+}$ and $Fe(H_2O)_6^{3+}$, represented by equation (A), can be estimated as in the previous two chapters.

Taking the effective radius of $Fe(H_2O)_6^{2+}$ as 3.59 Å and that of $Fe(H_2O)_6^{3+}$ as 3.43 Å, the value of σ is then 7.02 Å. At 2.0°C, the dielectric constant of water has the value $\varepsilon = 87.22$. Again assuming the term $\partial\varepsilon/\partial p$ to be independent of temperature and to have the value 3.699×10^{-3} bar^{-1}, the term $\partial(1/\varepsilon)/\partial p$ can be estimated to be -0.4862×10^{-6} bar^{-1} at 2.0°C. The term $\{(\partial(1/\varepsilon_o)/\partial p)_T - (\partial(1/\varepsilon)/\partial p)_T\}$ is again evaluated from the values at 25°C. Hence, from equations (4.5) and (4.6), we obtain the following values for the contributions to $\Delta V^{\ddagger}$ predicted by the Marcus-Hush theory:

$$\Delta V^{\ddagger}_{\text{coulombic}} = -5.77 \text{ c.c. mole}^{-1}$$

$$\Delta V^{\ddagger}_{\text{solvent rearr.}} = -5.65 \text{ c.c. mole}^{-1}$$

The correction for finite ionic strength effects is obtained from equation (4.11), using the values $A = 0.4935\ M^{-1/2}\ \text{deg.}^{3/2}$, $B = 0.3251 \times 10^{8}\ \text{cm.}^{-1}\ M^{-1/2}\ \text{deg.}^{1/2}$ and $\beta = 4.98 \times 10^{-5}$ bar^{-1}, all at 2.0°C, and taking $\underline{a} = 3.5$ Å, $Z_1 = 2$, $Z_2 = 3$ and $\mu = 0.5$ M. This gives

$$\Delta V^{\ddagger}_{\text{D.H.}} = 3.51 \text{ c.c. mole}^{-1}.$$

The predicted volume of activation, for comparison with the measured value, is thus

$$\Delta V^{\ddagger}_{calc} = -5.77 - 5.65 - 3.51 = -14.93 \text{ c.c. mole}^{-1}$$

The measured volume of activation was found to be $\Delta V^{\ddagger}_{meas} = -12.2 \pm 1.5$ c.c. mole^{-1}. The two values are seen to be in reasonable agreement.

Again, if we consider the uncertainties in the predicted value of $\Delta V^{\ddagger}$, we find they arise from the uncertainties in the values of the various dielectric terms and from the values assigned to r_1, r_2 and σ.

If the uncertainties in r_1, r_2 and σ are 0.1 Å and 0.2 Å respectively, this leads to an uncertainty of 0.34 c.c. mole^{-1} in $\Delta V^{\ddagger}$. Also, if the compressibility of the ions is considered, the correction this introduces has been estimated[86] as approximately 0.5 c.c. mole^{-1}. Again the uncertainties in the dielectric terms cannot be estimated, because of lack of data, but they should not be too large.

When the uncertainties in the values of $\Delta V^{\ddagger}_{meas}$ and $\Delta V^{\ddagger}_{calc}$ are considered, it can be seen that there is quite reasonable agreement between the two values. Because the Marcus-Hush theory is based on the assumption of an outer-sphere activated complex, it would appear from the agreement between the calculated and measured

values of $\Delta V^{\ddagger}$ for the electron exchange between $Fe(H_2O)_6^{2+}$ and $Fe(H_2O)_6^{3+}$ that an outer-sphere activated complex is involved in the exchange between these two species.

6.4.2 Possible Alternative Mechanisms

Because of the lability of both partners in the $Fe(H_2O)_6^{2+}$ - $Fe(H_2O)_6^{3+}$ electron exchange, an inner-sphere mechanism is possible. If this were operative, the formation of the transition state would presumably involve the expulsion of a water molecule from the first coordination shell of one of the ions. This would be expected to contribute a value of close to +18 c.c. $mole^{-1}$ to $\Delta V^{\ddagger}$. If we assume that the electrostatic interaction terms are not significantly different for an inner-sphere and an outer-sphere activated complex, then these terms would be expected to contribute a value close to that for the outer-sphere case, i.e. -15 c.c. $mole^{-1}$. This would lead to an expected value of $\Delta V^{\ddagger}$ = +3 c.c. $mole^{-1}$. Because this value is not in accord with the observed value, it seems that an inner-sphere mechanism could not be consistent with the measured value of $\Delta V^{\ddagger}$.

It is just possible that a small percentage of the exchange proceeds by an inner-sphere path, and since this would contribute a small positive term to the observed $\Delta V^{\ddagger}$ value, the measured value of $\Delta V^{\ddagger}$ would then be slightly less negative than the predicted value.

An outer-sphere activated complex may, or may not, involve hydrogen bonds between the intact inner coordination spheres. Experimentally it is impossible to distinguish the two cases. Similarly it is not possible to distinguish whether hydrogen atom transfer occurs or whether direct electron migration through the two adjacent first coordination shells occurs. The net effect is the same. However, the possibility of net hydrogen atom transfer along an ordered array of water molecules between the two exchanging metal ions does not appear to be consistent with the measured value of $\Delta V^{\ddagger}$, since the coulombic term would then be close to zero and the solvent rearrangement term would be expected to be less negative than when the two ions are in close contact. Thus a value for $\Delta V^{\ddagger}$ considerably less negative than -15 c.c. mole^{-1} would be expected.

6.4.3 Interpretation of the Acid-Dependent Rate Constant, k_2'

The observed rate law, equation (6.12), for the Fe^{II} - Fe^{III} exchange can be interpreted as involving exchange between $Fe(H_2O)_6^{2+}$ and both $Fe(H_2O)_6^{3+}$ and $Fe(H_2O)_5OH^{2+}$. Hence, k_2' of equation (6.12) can be written as

$$k_2' = k_2 K_a \qquad (6.13)$$

where K_a refers to the equilibrium

$$Fe^{3+}_{aq} \rightleftarrows FeOH^{2+}_{aq} + H^{+}_{aq} \qquad (6.14)$$

and is given by

$$K_a = \frac{[FeOH^{2+}][H^+]}{[Fe^{3+}]} \qquad (6.15)$$

k_2 is the rate constant for the reaction:

$$Fe(H_2O)_6^{2+} + {}^{*}Fe(H_2O)_5OH^{2+} \rightleftarrows Fe(H_2O)_5OH^{2+} + {}^{*}Fe(H_2O)_6^{2+}$$

From (6.13) we obtain the relation

$$\frac{\partial RT \ln k_2'}{\partial p} = \frac{\partial RT \ln k_2}{\partial p} + \frac{\partial RT \ln K_a}{\partial p} \qquad (6.16)$$

$$= -\Delta V^{\ddagger}_{k_2} - RT\beta - \Delta\bar{V}_{K_a} + RT\beta \qquad (6.17)$$

$$\text{i.e. } \Delta V^{\ddagger}_{k_2} = -\partial RT \ln k_2'/\partial p - \Delta\bar{V}_{K_a} \qquad (6.18)$$

Hence, the pressure dependence of k_2 can be expressed in terms of the pressure dependence of k_2' and the partial molar volume change for reaction (6.14).

Now the partial molar volume change for reaction (6.14) is given by

$$\Delta\bar{V}_{K_a} = \bar{V}_{H^+} + \bar{V}_{FeOH^{2+}} - \bar{V}_{Fe^{3+}} \qquad (6.19)$$

Couture and Laidler[95] have proposed the following empirical relation fo the partial molal volume, $\bar{V}_+$, of a cation of charge Z_+ and radius r:

$$\bar{V}_+ = 16 + 4.9\ r^3 - 20\ Z_+ \qquad (6.20)$$

Assuming that the ionic radius, r, is the same for Fe(III) in both Fe^{3+}_{aq} and $FeOH^{2+}_{aq}$, it follows immediately from equation (6.20) that the quantity $(\bar{V}_{FeOH^{2+}} - \bar{V}_{Fe^{3+}})$ is equal to $-20(2-3) = +20$ c.c. mole^{-1}. It should be noted, however, that this assumes that the species $FeOH^{2+}$ can be treated as a spherical ion of charge +2. This assumption would tend to give a value for $(\bar{V}_{FeOH^{2+}} - \bar{V}_{Fe^{3+}})$ that is somewhat high. The value for $\bar{V}_{H^+}$ is taken, by convention, to be zero. Hence, from equation (6.19) we obtain $\Delta\bar{V}_{K_a} \simeq +20$ c.c. mole^{-1}.

Also, it is seen from Table 6.5 that, within experimental error, the variation of k' with pressure is zero. Hence, from equation (6.18) we obtain that $\Delta V^{\ddagger}_{k_2} \simeq -20$ c.c. mole^{-1}. Because of the assumptions made in arriving at this figure, the true value of $\Delta V^{\ddagger}_{k_2}$ would probably be somewhat less negative. Nevertheless, it is apparent that the value of $\Delta V^{\ddagger}_{k_2}$ will be distinctly negative. This implies that the electron exchange between Fe^{2+}_{aq} and $FeOH^{2+}_{aq}$ proceeds predominately, if not entirely, by an outer-sphere mechanism, since on the same reasoning as before, an inner-sphere mechanism would be expected to yield a positive value for $\Delta V^{\ddagger}_{k_2}$.

The uncertainty in the value of $\Delta V^{\ddagger}_{k_2}$ arises because the pressure dependence of K_a for the hydrolysis of Fe^{3+} has not been measured. When this data becomes available, a more accurate value for $\Delta V^{\ddagger}_{k_2}$ will be able to be obtained, and hence a more reliable interpretation in terms of the mechanism involved for the electron exchange between

$Fe(H_2O)_6^{2+}$ and $Fe(H_2O)_5OH^{2+}$.

6.4.4 Conclusion

The effect of pressure on the Fe^{II}_{aq} - Fe^{III}_{aq} electron exchange reaction has been measured, and the pressure dependence of the rate constant for the exchange between $Fe(H_2O)_6^{2+}$ and $Fe(H_2O)_6^{3+}$ has thus been obtained. The measured volume of activation for the exchange between these two species was found to be -12.2 ± 1.5 c.c. mole^{-1}. This has been compared to the value of -14.9 c.c. mole^{-1} predicted by the Marcus-Hush theory, which assumes an outer-sphere mechanism. Considering the uncertainties in both the measured and calculated values of $\Delta V^{\ddagger}$, the two values are in reasonable agreement. This agreement implies, then, that the electron exchange between $Fe(H_2O)_6^{2+}$ and $Fe(H_2O)_6^{3+}$ proceeds by an outer-sphere mechanism.

Because the pressure dependence of the hydrolysis equilibrium for Fe^{3+}_{aq} is not known, it was not possible to evaluate the pressure dependence of the exchange between $Fe(H_2O)_6^{2+}$ and $Fe(H_2O)_5OH^{2+}$, and thus the volume of activation for this reaction. An approximate estimate of this quantity has been made, and this estimate indicates that the electron exchange between the two species, $Fe(H_2O)_6^{2+}$ and $Fe(H_2O)_5OH^{2+}$, proceeds, at least predominately, by an outer-sphere mechanism also.

Conclusion

These studies of electron exchange reactions under pressure were undertaken with two main goals in view. These were to provide an alternative test to the Marcus-Hush theory of electron transfer reactions in solution, and to calibrate a method for determining the mechanism of a reaction by comparison of its measured $\Delta V^{\ddagger}$ value with those of known reactions.

The Marcus-Hush theory can be tested by the comparison of the measured and calculated values of k_{12}, the rate constant for the "cross-reaction" of two independent electron exchange reactions,[96] or by a comparison of the measured and calculated values of $\Delta H^{\ddagger}$ or $\Delta S^{\ddagger}$, which measures the temperature dependence of the basic equation. The comparison of the measured and calculated values of $\Delta V^{\ddagger}$ provides an alternative test to the theory, in that this evaluates the pressure dependence of the basic equation. The first two reactions studied, the electron exchange between $Co^{II}(EDTA)$ and $Co^{III}(EDTA)$ and between $Co(en)_3^{2+}$ and $Co(en)_3^{3+}$, are believed to be outer-sphere reactions. Inasmuch as this is true, these reactions could be used to test the electron transfer theory. It was found for both reactions that, within experimental error, the calculated and observed values of $\Delta V^{\ddagger}$ were in substantial agreement. Thus, these results confirm the correctness of the fundamental form of the theory. In particular, they show that the interaction of the reactants with the dielectric medium has been taken into account in an essentially correct manner. This point has

been one of principal concern in the development of the theory. Also, the equation derived for predicting $\Delta V^{\ddagger}$ values does not contain a term for the internal rearrangement of the ions. The way in which this should be accounted for, in the equation for $\Delta G^{\ddagger}$, has been an issue of considerable controversy. The equation for $\Delta H^{\ddagger}$ and $\Delta S^{\ddagger}$ must also involve this term.

The Fe^{II}_{aq} - Fe^{III}_{aq} electron exchange is one of unknown mechanism. The volume of activation for this reaction was measured with a view to determine its mechanism. Since the Marcus-Hush theory has been shown to predict correctly the volumes of activation for the two outer-sphere reactions studied first, then it should also predict the correct value for the Fe^{II}_{aq} - Fe^{III}_{aq} reaction, provided it proceeds by an outer-sphere mechanism. The substantial agreement between the measured and calculated values for the exchange between $Fe(H_2O)_6^{2+}$ and $Fe(H_2O)_6^{3+}$ has been taken to indicate, then, an outer-sphere mechanism. Although a precise value of $\Delta V^{\ddagger}$ for the reaction between $Fe(H_2O)_6^{2+}$ and $Fe(H_2O)_5OH^{2+}$ could not be obtained, it appeared likely on the estimate made, that this pathway of exchange involves an outer-sphere activated complex also.

It is interesting that for the Co(II)-Co(III) systems, the change in spin-multiplicity which is often invoked to help explain the relative slowness of these reactions, is not taken into account explicitly in the equation for the free energy of activation. A change in spin multiplicity would be expected to contribute a small entropic term, or perhaps a small enthalpy term, to $\Delta G^{\ddagger}$. This term

does not appear in the equation for $\Delta V^{\neq}$, and the results would indicate that this is not a significant term.

To increase the reliability of the method of using measured $\Delta V^{\neq}$ values for the determination of reaction mechanism, it would be desirable to calibrate the method further, especially by the measurement of some inner-sphere reactions. A suitable reaction would be the $Cr^{II}_{aq} - Cr^{III}_{aq}$ electron exchange[97], which proceeds at convenient rates and is believed to involve an inner-sphere transition state, since the rate of the Cr^{2+} catalyzed water exchange has been found to be the same as the rate of electron exchange.[98]

It would be of interest, also, to measure the volumes of activation of some outer-sphere reactions involving net electron transfer, when the overall free energy change is not zero. Candlin and Halpern[18] have reported briefly on the measurement of values of $\Delta V^{\neq}$ for the reduction of some $Co(NH_3)_5X^{2+}$ complexes with Fe^{2+}, but these are all believed to involve an inner-sphere transition state, and so the Marcus-Hush theory is not applicable.

In conclusion, it is evident from the results reported in this work, that the use of measured volumes of activation shows considerable promise for the determination of the mechanism of electron transfer reactions in solution.

BIBLIOGRAPHY

1. H. Le Chatelier, C.R. Acad. Sci. Paris, 99, 786 (1884).
2. W. Ostwald, J. prak. Chem., 18, 328 (1878).
3. W.C. Röntgen, Ann. Physik., 45, 98 (1892).
4. C.T. Burris and K.J. Laidler, Trans. Faraday Soc., 51, 1497 (1955)
5. R.J. Whithey, J.E. McAlduff and E. Whalley, Physics and Chemistry of High Pressures, 196 (Soc. Chem. Ind., London, 1962).
6. S.D. Hamann, "Physico-Chemical Effects of Pressure", Academic Press Inc., New York, 1957.
7. W.J. le Noble, Prog. Phys. Org. Chem., 5, 207 (1967).
8. J. Brady, F. Dachille and C.D. Schmulbach, Inorg. Chem., 2, 803 (1963).
9. C.D. Schmulbach, F. Dachille and M.E. Bunch, Inorg. Chem., 3, 808 (1964).
10. C.D. Schmulbach, J. Brady and F. Dachille, Inorg. Chem., 7, 287 (1968).
11. K.J. Laidler, Disc. Faraday Soc., 22, 88 (1956).
12. H.R. Hunt and H. Taube, J. Am. Chem. Soc., 80, 2642 (1958).
13. H.E. Brower, L. Hathaway and K.R. Brower, Inorg. Chem., 5, 1899 (1966).
14. W.J. le Noble and M. Duffy, J. Am. Chem. Soc., 86, 4512 (1964).
15. K.R. Brower, J. Am. Chem. Soc., 90, 5401 (1968).
16. W.E. Jones and T.W. Swaddle, Chem. Comm., 998, 1969 .
17. T. Taylor and L.R. Hathaway, Inorg. Chem., 8, 2135 (1969).
18. J.P. Candlin and J. Halpern, Inorg. Chem., 4, 1086 (1965).

19. a. M.G. Adamson and D.R. Stranks, Chem. Comm., 648, 1967 .

b. private communication.

20. H. Taube, Advan. Inorg. Chem. Radiochem., 1, 1 (1959).

21. J. Halpern, Quart. Rev. (London), 15, 207 (1961).

22. N. Sutin, Ann. Rev. Nucl. Sci., 12, 285 (1962).

23. W.L. Reynolds and R.W. Lumry, "Mechanisms of Electron Transfer", Ronald Press, New York, 1966.

24. F. Basolo and R.G. Pearson, Ch. 6 in "Mechanisms of Inorganic Reactions", John Wiley and Sons, Inc., New York, 1967, 2nd ed.

25. H.A.C. McKay, Nature, 142, 997 (1938).

26. A.A. Frost and R.G. Pearson, "Kinetics and Mechanism", John Wiley and Sons, Inc., New York, 1961, 2nd ed.

27. G.M. Harris, Trans. Faraday Soc., 47, 716 (1951).

28. R.J. Prestwood and A.C. Wahl, J. Am. Chem. Soc., 71, 3137 (1949).

29. H. Taube, H. Myers and R.C. Rich, J. Am. Chem. Soc., 75, 4118 (1953).

30. L.E. Orgel, Report 10th Solvay Conf., 329, 1956.

31. J. Weiss, Proc. Roy. Soc. (London), A222, 128 (1954).

32. R.J. Marcus, B.J. Zowlinski and H. Eyring, J. Phys. Chem., 58, 432 (1954).

33. K.J. Laidler, Canad. J. Chem., 37, 138 (1959).

34. K.J. Laidler and E. Sacher, Trans. Faraday Soc., 59, 396 (1963).

35. R.A. Marcus, J. Chem. Phys., 24, 966, 979 (1956), and 26, 867 (1957); Disc. Faraday Soc., 29, 129 (1960).

36. N.S. Hush, (a) Z. Electrochem., 61, 734 (1957); (b) J. Chem. Phys.,

28, 962 (1958); (c) Trans. Faraday Soc., 57, 557 (1961).

37. R.J. Campion, C.F. Deck, P. King and A.C. Wahl, Inorg. Chem., 6, 672 (1967).

38. R.J. Campion, T.J. Conocchiolo and N. Sutin, J. Am. Chem. Soc., 86, 4591 (1964).

39. T.J. Conocchiolo and N. Sutin, J. Am. Chem. Soc., 89, 282 (1967).

40. D.C. Walker, Quart. Rev., 21, 79 (1967).

41. R.A. Marcus, Ann. Rev. Phys. Chem., 15, 155 (1964).

42. E. Whalley, Advan. Phys. Org. Chem., 2, 93 (1964).

43. E. Whalley, Ann. Rev. Phys. Chem., 18, 205 (1967).

44. S.D. Hamann, Ann. Rev. Phys. Chem., 15, 349 (1964).

45. S.D. Hamann, in "High Pressure Physics and Chemistry", Vol. 2, Academic Press Inc., New York, 1963, ed. R.S. Bradley.

46. S.W. Benson and J.A. Berson, J. Am. Chem. Soc., 84, 152 (1962).

47. C. Walling and D.D. Tanner, J. Am. Chem. Soc., 85, 612 (1963).

48. J.B. Hyne, H.S. Golinkin and W.G. Laidlaw, J. Am. Chem. Soc., 88, 2104 (1966).

49. D.R. Stranks, private communication.

50. M.G. Evans and M. Polanyi, Trans. Faraday Soc., 31, 875 (1935).

51. T. Ri and H. Eyring, J. Chem. Phys., 8, 433 (1940).

52. M. Born, Z. Physik., 1, 45 (1920).

53. R.A. Robinson and R.H. Stokes, "Electrolyte Solutions", Butterworths London, 1959, 2nd ed.

54. J. Buchanan and S.D. Hamann, Trans. Faraday Soc., 49, 1425 (1953).

55. C.C. Bradley, "High Pressure Methods in Solid State Research", Butterworths, London, 1969.

56. R.S. Bradley and D.C. Munro, "High Pressure Chemistry", Pergamon Press, London, 1965.

57. W.R.D. Manning, Engineering, 159, 101, 183 (1945).

58. B. Crossland and J.A. Bones, Engineering, 179, 80, 114 (1955).

59. H. Leinss, Engineering, 180, 132 (1955).

60. H. Ll. Pugh, G. Hodgson and D.A. Gunn, J. Sci. Instr., 40, 221 (1963).

61. A.W. Adamson and K.S. Vorres, J. Inorg. Nucl. Chem., 3,.206 (1956).

62. Y.A. Im and D.H. Busch, J. Am. Chem. Soc., 83, 3357 (1961).

63. T.R. Bhat and M. Krishnamurthy, J. Inorg. Nucl. Chem., 25, 1147 (1963).

64. D.T. Sawyer and J.E. Tackett, J. Am. Chem. Soc., 85, 2390 (1963).

65. R.G. Wilkins and R. Yelin, J. Am. Chem. Soc., 89, 5496 (1967).

66. W.C.E. Higginson a. unpublished results, quoted in J. Am. Chem. Soc., 89, 5496 (1967).
b. J. Chem. Soc., 2761, 1962.

67. Stability Constants. J. Chem. Soc. Special Publication No. 17, London.

68. T.R. Bhat, D. Radhamma and J. Shankar, Inorg. Chem., 5, 1132 (1966)

69. Von H. Brintzinger, H. Thiele and U. Müller, Z. Anorg. Chem., 251, 285 (1943).

70. G. Schwarzenbach, Helv. Chim. Acta, 32, 839 (1949).

71. D.H. Busch and J.C. Bailar, J. Am. Chem. Soc., 75, 4574 (1953).

72. H.A. Weakliem and J.L. Hoard, J. Am. Chem. Soc., 81, 549 (1959).

73. R.D. Gillard and G. Wilkinson, J. Chem. Soc., 4271, 1963 .

74. M. Yasuda, Bull. Chem. Soc. Jap., 41, 139 (1968).

75. W.C.E. Higginson, a. J. Chem. Soc., 260, 1958 ;
b. J. Chem. Soc., 1998, 1960 .

76. "Handbook of Physics and Chemistry", The Chemical Rubber Co., Ohio, 1966, 47th edition.

77. F.P. Dwyer, E.C. Gyarfas and D.P. Mellor, J. Phys. Chem., 59, 296 (1955).

78. G. Schwarzenbach, Helv. Chim. Acta, 32, 839 (1949).

79. Von H. Brintzinger, H. Thiele and U. Müller, Z. Anorg. Chem., 251, 285 (1943).

80. Von W. Klemm, Z. Anorg. Chem., 252, 225 (1944).

81. D.H. Busch and J.C. Bailar, J. Am. Chem. Soc., 75, 4574 (1953).

82. B.B. Owen and S.R. Brinkley, Phys. Rev., 64, 32 (1943).

83. P.W. Bridgman, J. Chem. Phys., 3, 597 (1935).

84. T.W. Swaddle, unpublished results, private communication.

85. E.U. Franck, private communication.

86. D.R. Stranks, private communication.

87. J.A. Friend and E.K. Nunn, J. Chem. Soc., 1567, 1958 .

88. W.B. Lewis, C.D. Coryell and J.W. Irvine, J. Chem. Soc., S386, 1949 .

89. F.P. Dwyer and A.M. Sargeson, J. Phys. Chem., 65, 1892 (1961).

90. D.R. Stranks, in "Advances in the Chemistry of the Coordination Compounds", McMillan Co., New York, p. 571.

91. S.M. Hasany, private communication.

92. Adelaide University Computing Centre, Library Program LSQPOL.

93. J. Silverman and R.W. Dodson, J. Phys. Chem., 56, 846 (1952).

94. H. Taube, J. Chem. Educ., 45, 452 (1968).

95. A.M. Couture and K.J. Laidler, Canad. J. Chem., 34, 1209 (1956).

96. R.A. Marcus, J. Phys. Chem., 67, 853 (1963).

97. A. Anderson and N.A. Bonner, J. Am. Chem. Soc., 76, 3826 (1954).

98. J.P. Hunt and H. Taube, J. Chem. Phys., 19, 602 (1951).